Australian Government
Department of Defence
Defence Science and
Technology Organisation

France-Australia Technical Arrangement TA 1/99 – Work Package 1: Study of the Equivalence of Hot/Dry and Hot/Wet Testing

Paul J. Callus

Air Vehicles Division
Defence Science and Technology Organisation

DSTO-TR-1708

ABSTRACT

Substantial savings could be made in the airworthiness certification of composite aircraft structure if the strength of polymer matrix composites in the elevated temperature wet (ETW) condition could be predicted from parameters that are easier to measure such as strength in the elevated temperature dry (ETD) condition and the glass transition temperature (T_g). The feasibility of this approach was tested by measuring the strength of AS4/3501-6 unidirectional prepreg tape, T650/F584 plain weave prepreg fabric and T650/PR500 plain weave fabric consolidated by resin transfer moulding, in the dry and 70°C/85 % relative humidity equilibrated condition, from 25 to 120 °C using interlaminar shear, ±45° tension, open hole compression and compression after impact tests. Apart from a decrease in strength with increasing temperature and moisture content there was no consistent relation between ETD and ETW strength. It was therefore not possible to predict ETW strength for these materials and tests on the basis of ETD strength and T_g only.

Published by

Air Vehicles Division
DSTO Defence Science and Technology Organisation
506 Lorimer St
Fishermans Bend, Victoria 3207 Australia

Telephone: (03) 9626 7000
Fax: (03) 9626 7999

AR-013-374
April 2005

APPROVED FOR PUBLIC RELEASE

France-Australia Technical Arrangement TA 1/99 – Work Package 1: Study of the Equivalence of Hot/Dry and Hot/Wet Testing

Executive Summary

Aircraft structures are designed and certified on the basis of mechanical properties with the material in its most environmentally degraded condition in the worst anticipated service environment. For polymer matrix composites (PMCs), such as the carbon/epoxy used in the airframe of many modern aircraft, the critical properties are typically compression and shear strength in the elevated temperature wet (ETW) condition.

At present it is not possible to predict the ETW compression and shear properties of PMCs. Therefore material allowables and design data for airworthiness certification must be obtained by testing in the ETW condition. Specimens are first conditioned in a humidified chamber until the moisture content equilibrates. Even with accelerated conditioning this may take many weeks or months. After conditioning, the mechanical tests are conducted in a chamber where the air in the chamber is in either the ETW or the elevated temperature dry (ETD) condition. The former is relatively expensive but preferred because the moisture remains in the specimen throughout the test. The latter is cheaper but some of the moisture will be lost due to drying before the specimen fails and there is a risk that this may produce non-conservative test results. Regardless of the final testing technique, the entire process requires substantial equipment requirements and long conditioning times. These increase dramatically the cost of airworthiness certification for PMC aircraft structure.

The aim of the France/Australia Technical Arrangement (TA1/99) "New Certification Procedures for Composite Materials", Work Package 1, was to establish whether ETW compression and shear strength could be predicted on the basis of ETD strength and glass transition temperature (T_g). The properties of AS4/3501-6 unidirectional prepreg tape, T650/F584 plain weave prepreg fabric and T650/PR500 plain weave fabric consolidated by resin transfer moulding, in the dry and 70°C/85 % relative humidity equilibrated condition, were measured from 25 to 120 °C with interlaminar shear, ±45° tension, open hole compression and compression after impact tests.

Apart from a decrease in strength with increasing temperature and moisture content there was no consistent relation between ETD and ETW strength. This was similar to the observations made by the French using T300/914 and IM7/977-2. Thus for all the materials and tests evaluated in this program it was not possible to predict ETW strength on the basis of ETD strength and T_g only.

This paper represents the final report on the Australian component of France/Australia TA 1/99 Work Package 1. As with the equivalent French report, the experimental data showed clearly that the relation between ETD and ETW strength varied according to material and test. Substantial additional research will be required to establish the relation between them. The costs of such research should be balanced against the enormous savings to aircraft manufacturers and operators if much of the existing ETW testing were replaced by ETD testing.

Author

Paul J. Callus
Air Vehicles Division

Dr Paul Callus gained his PhD from Monash University in 1993. He worked with CSIRO for four years developing electrode coatings for ceramic fuel cells. He then spent two years at RMIT investigating failure processes in textile composites. He is currently a Senior Research Scientist in the Composites and Low Observables Functional Area of the Air Vehicles Division. He has worked on development of composite replacement panels and the certification of composite structure. His current focus is to apply this technology in the development of multifunctional aircraft structure.

Contents

1. Introduction

1.1 Airworthiness certification of composite aircraft structure

Aircraft structures are designed and certified on the basis of mechanical properties with the material in its most environmentally degraded condition in the worst anticipated service environment [1]. It is particularly important to account for environmental factors when using polymer matrix composites (PMCs) because the mechanical properties of polymer resin matrices are dependent on both temperature and moisture content.

Typically the mechanical properties of PMCs fall as temperature rises with the worst case being at the maximum operating temperature (also known as the material operational limit (MOL)). The rate of fall increases more significantly as the temperature approaches the glass transition temperature (T_g) of the matrix. Therefore most structures are designed so that the maximum operating temperature is well below T_g. Many polymers, including the epoxy resins used in aerospace grade composites, absorb small but significant quantities of moisture from the atmosphere. This moisture plasticises the resin and reduces its T_g. Moisture absorption commences from the time of manufacture and continues through the life of the aircraft. This is a diffusion process and the distribution of moisture through a structure will depend on the time and temperature history. The worst case is when the moisture is distributed uniformly through the material at the maximum that can be supported by the worst environment. This is conservatively called the end-of-life condition.

The mechanical properties of PMCs may be classified as fibre or resin dominated. Fibre dominated situations are those where the majority of applied loads are supported by the fibres, such as in-plane tension. Resin dominated situations are those where the applied loads are supported primarily by the resin matrix. For example in compression it is the resin that resists fibre buckling and in shear the resin resists relative movement between the fibres. The fibre dominated properties tend to be much higher than resin dominated properties in aerospace PMCs such as carbon/epoxy because the carbon fibres are much stiffer and stronger than the epoxy resin. Although aircraft designers aim to take advantage of the high fibre dominated properties, it is impossible for loading in complex structures such as airframes to achieve this. Therefore in most cases the critical mechanical properties are those related to the resin dominated compression and shear loading.

At present it is not possible to predict the resin dominated properties of environmentally degraded PMCs. Therefore design allowables must be obtained by testing in the degraded condition. For PMCs the critical case is usually the elevated temperature wet (ETW) condition. Specimens for ETW testing are first conditioned in a humidified chamber, typically at an elevated temperature and 85 % relative humidity (RH), until the moisture content equilibrates [2]. This approach has been accepted as providing a reasonable simulation of the end-of-life condition. Even with accelerated conditioning this may take many weeks or months, with large structures requiring up to one year. Conditioning cannot be accelerated further by, for example, immersing specimens in water because this is too aggressive, the equilibrium moisture content is higher than that obtained in service

and the failures are unrepresentative. After conditioning, the mechanical tests are conducted in a chamber (test box) where the air in the chamber is in either the elevated temperature wet (ETW) or the elevated temperature dry (ETD) condition. The former is relatively expensive but preferred because the moisture remains in the specimen throughout the test. The latter is cheaper but some of the moisture will be lost before the specimen fails and there is a concern that this may produce non-conservative test results. This problem is addressed by minimising the time that moisturised specimens are exposed to the ETD environment, although some loss is accepted because some time is required to raise the temperature at the centre of the specimen to the test temperature prior to failure. Regardless of the final testing technique, there are substantial equipment requirements and long conditioning times for the entire ETW testing process. These increase dramatically the cost of airworthiness certification for PMC materials.

1.2 Possible reduced testing requirements

It has been hypothesised that the same reduction in properties caused by the combined effect of temperature and moisture may be reproduced by elevating the test temperature on dry specimens [3], provided the mechanism of failure on both the microscopic and macroscopic scale is the same for both cases. Therefore, as indicated in Figure 1-1, the same design allowable may be obtained if an ETW test is replaced by the equivalent ETD test. If this approach could be validated then much of the expensive ETW conditioning equipment, test equipment and substantial time, required for airworthiness certification could be eliminated.

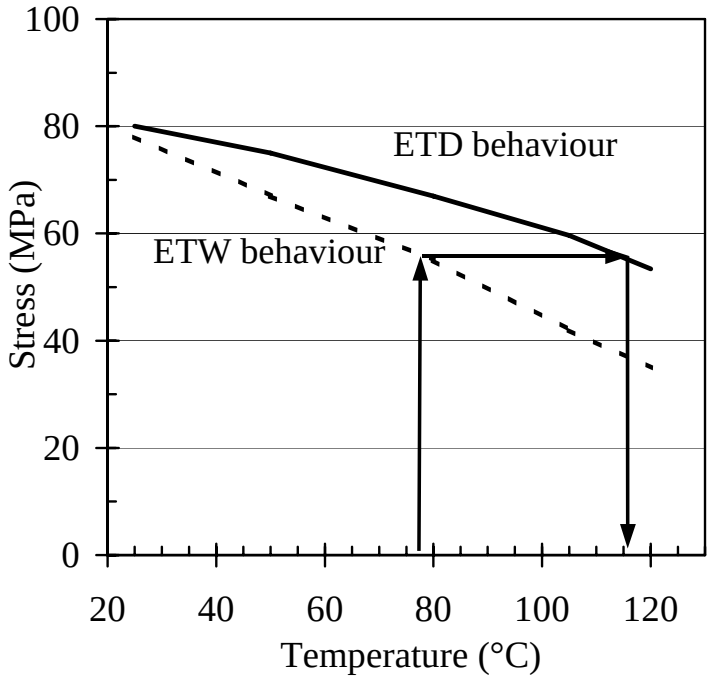

Figure 1-1: *Hypothetical plot demonstrating the equivalence ETW and ETD testing. In this case a 77 °C ETW test would be equivalent to a 116 °C ETD test*

1.3 Collaborative program

The aim of the work described in this report was to test the hypothesis presented in Section 1.2. This work was conducted as a collaborative program between the Defence Science and Technology Organisation (DSTO) (Australia) and Direction des systèmes d'armes (DGA) (France). It is defined in "Technical Arrangement 1/99, Work Package 1: Study of the equivalence of hot/dry and hot/wet testing" [4].

In this program DSTO has manufactured four types of coupon from three typical aerospace composite materials. Half of the coupons of each test type were environmentally conditioned to equilibrium moisture content (wet) while the other half were maintained in the dry condition. These coupons were tested at different temperatures. The glass transition temperatures of the dry and wet materials were also measured. The results were analysed to determine whether the ETW strength could be predicted on the basis of the ETD strength and T_g.

The French Centre d'Essais Aéronautique de Toulouse (CEAT) conducted the same tests on T300/914 and IM7/977-2 and reported the results [5].

2. Experimental Techniques

2.1 Materials

The materials used by DSTO in this program are those shown in Table 1.

2.2 Coupon manufacture and common test procedures

Large flat panels were laid up and cured under the conditions recommended by the manufacturer (Table 1). The lay-up of each panel type is shown in Table 2. Coupons were cut from the panels using a diamond saw with water lubricant.

Immediately following manufacture the coupons for ETD testing were placed in a vacuum oven at 70 °C. These coupons remained in the oven until the day they were tested. The only time they were removed was to apply strain gauges, where they would have been out of the oven for less than eight hours.

Coupons for ETW testing were placed in a Heraeus Vötsch HC 4055 environmental chamber set at 70 °C/85 % RH. The chamber was checked regularly to ensure that the set conditions were being maintained. Coupon weight was not recorded during conditioning however testing was not commenced until at least eight months after insertion. The typical conditioning time was two years with some batches being conditioned for five years. Given these long times it was assumed that the coupons had reached equilibrium moisture content prior to testing.

Table 1: Materials

Material	Description	Manufacturer	Cure	Manufacturer designation
AS4/ 3501-6	Prepreg, Unidirectional carbon fibre tape, Autoclave cure	Hercules	116 °C/1 h/568 kPa, 177 °C/1 h/689 kPa, 177 °C/1 h/vent	AS4/3601-6, 42% 150 gsm FAW, 48.5" MMS 549 Type 3 & 4
T650/ F584	Prepreg, Plain weave carbon fabric, Autoclave cure	Hexcel	177 °C/1 h/620 kPa, 177 °C/1 h/vent	W4G 282 -60 -F584 108:40%
T650/ PR500	Dry fibre, Plain weave carbon fabric, RTM consolidation	Fibre Hexcel Resin 3M	Degas 110 °C/15 min, Inject 145 °C/30 psi, Cure 180 °C/2 h	W4G 282 PR 500
T300J/ DA508	Prepreg, Unidirectional carbon fibre tape, Autoclave cure	Supplied by CEAT in cured form		

Table 2: Coupon lay-up

Test		Material		
Full name	Abbrev.	AS4/3501-6	T650/F584	T650/PR500
Glass Transition Temperature	T_g	16 ply	16 ply	16 ply
Interlaminar Shear	ILS	$[0]_{16}$	$[0/90]_{12}$	$[0/90]_{12}$
±45° Tension	±45° tension	$[45\ -45]_{4s}$	$[\pm45]_{12}$	$[\pm45]_{12}$
Open Hole Compression	OHC	$[45\ 0\ -45\ 90]_{2s}$	$[(\pm45)\ (0/90)]_{3s}$	$[(\pm45)\ (0/90)]_{3s}$
Compression After Impact	CAI	$[45\ 0\ -45\ 90]_{4s}$	$[(\pm45)\ (0/90)]_{6s}$	$[(\pm45)\ (0/90)]_{6s}$

As a check, small moisture content samples were cut from the ETW coupons within one day of completion of the test. These samples were weighed then placed in a vacuum oven at 70°C. The samples were weighed at regular intervals, with weighing continued until steady state weights were recorded. The moisture content of these samples was calculated and is recorded with the test results in the Appendices of this report.

All testing was conducted using fixtures that were enclosed in insulated test boxes. Air was blown into these boxes to preheat, then maintain, the environment and test fixtures at the test temperature. The RH of the air was not controlled nor measured. It was therefore expected to fall as test temperature rose, from ≈50 % RH at 25 °C to 0 % RH at 100 °C. This air would not alter the results of ETD tests because the coupons were already dry. However, on ETW coupons it was possible that the effects could be significant. Water began diffusing out of the wet coupons as soon as they were exposed to a humidity below the 85 % RH of the conditioning environment. The rate of diffusion rose by approximately one order of magnitude for every 10 °C rise in temperature. At 120 °C it was predicted that half of the outer ply would be dry within 10 minutes. Clearly the results of a test conducted under these conditions would reflect that of material that was not fully moisturised. Competing with this requirement to minimise the time that the coupon was

exposed to the dry air was the requirement to ensure sufficient time in the test box for the centre of the coupon to reach the test temperature.

The approach that was used to address these competing requirements was to preheat the test box and fixtures to the test temperature, open the door of the test box, minimise the time to install the coupon in the test fixture, close the door as soon as practicable and commence loading at a fixed time after the door was closed. The same fixed time was used for all coupons of a particular test type. This time was obtained from measurements of temperature versus time in dummy coupons that were installed into the test boxes preheated to the different test temperatures. The dummy coupons were of the same lay-up as the test coupons but with a thermocouple installed along their centre-plane. The insertion of the dummy coupons simulated, as closely as possible, the procedure for the actual tests (for example the dummy coupons were initially at room temperature, the test box preheated, the door opened, the dummy coupons installed into the test coupon location, the door held open for the same amount of time as would be required to load the test coupons, door closed and temperature in the test box restored using the same technique as would be used during testing). The time selected was the minimum time where the centre of the dummy coupon was within 2 °C of the test temperature for the 120 °C test case (this was the temperature that required the longest dwell to reach the test temperature). The fixed time varied between two and twelve minutes.

It was found that loading took from one to three minutes. During this time coupons continued to warm and lose moisture. Even if the centre of coupons were a few degrees below the test temperature at the commencement of loading, they would be very close to the test temperature at the time of failure. It was judged that extending the fixed time any further would result in excessive moisture losses and potentially unacceptable changes to the test results.

2.3 Glass transition temperature

For each material six 14 mm long x 9 mm wide coupons were cut from the glass transition temperature (T_g) panel. Three coupons were maintained in the dry condition (70 °C/vacuum) and three were conditioned at 70 °C/85 % RH to an equilibrium moisture content (wet).

Dynamic Mechanical Thermal Analysis (DMTA) tests were performed on each coupon in single point bending mode at a bending frequency of 1 Hz and a heating rate of 2 K min^{-1}. Plots of modulus and tan δ versus temperature were produced. There are a number of methods of calculating T_g from the DMTA results. In this work T_g was defined as the temperature at which tan δ was a maximum.

2.4 Interlaminar shear

For each material at least 50 14 mm long x 10 mm wide coupons were cut from the ILS panel. At least 25 coupons were maintained in the dry condition (70 °C/vacuum) and at least 25 were conditioned (70 °C/85 % RH) to an equilibrium moisture content (wet).

Coupons were tested in accordance with ASTM D2344 [8] using the three-point bend fixture shown in Figure 2-1 (a). The loading span was 10 mm, support rollers were 3.2 mm diameter and the load roller was 6.4 mm diameter. The fixture was enclosed in an insulated test box and installed in an Instron 1121 loading frame with a 10 kN load cell. As shown in Figure 2-1 (b), a hot air gun was inserted into the rear of the test box. Temperature was controlled manually. The thermocouple shown in Figure 2-1 (a) was monitored and the thermostat on the hot air gun adjusted to maintain the temperature in the test box at the nominal test temperature.

ILS tests were conducted in accordance with the following procedure:

1. Closed the front door of the test box.
2. Preheated and equilibrated the test box to the test temperature.
3. Turned off hot air gun then, as rapidly as possible, opened the front door, located the coupon on the support rollers, closed the front door and turned on the hot air gun to restore the test temperature.
4. Soaked for 4:00 min while maintaining the test temperature.
5. Loaded the coupon at 1 mm min^{-1} to failure. Recorded peak load.
6. Stopped crosshead and returned it to its initial position.
7. Opened test box and removed the failed coupon.
8. Repeated Steps 2 to 7 for the remaining coupons.
9. At the conclusion of testing, identified the failure location on the coupons and recorded any deviations from the valid failure mode.

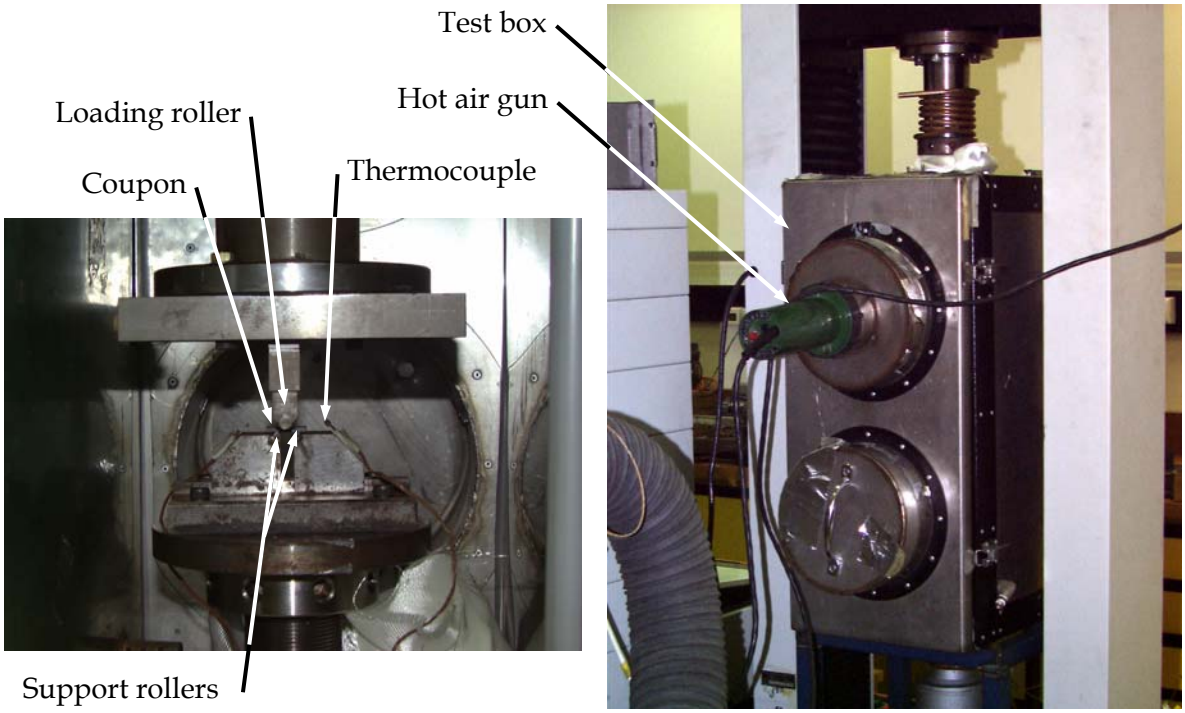

Figure 2-1: Photographs of the ILS test showing the (a) test fixture, coupon and thermocouple ends from the front of the test box, and (b) hot air gun fastened to the rear of the test box

2.5 ±45° tension

For each material at least 50 250 mm long x 25 mm wide coupons were cut from the ±45° tension panels. Strain gauges were bonded to three out of each batch of five specimens for the dry coupons in order to measure shear strain. For those coupons in which strain gauges were bonded, the bonding was conducted prior to drying. At least 25 coupons were maintained in the dry condition (70 °C/vacuum) and at least 25 were conditioned (70 °C/85 % RH) to an equilibrium moisture content (wet).

Coupons were tested in accordance with ASTM D3518 [9]. Testing was conducted in an Instron 1185 loading frame with a 100 kN load cell. Coupons were held with mechanical grips set to give a gauge length of 144 mm. The grips were enclosed in an insulated test box.

For tests on the ETD AS4/3501-6 and T650/F584 coupons the elevated temperatures were obtained using a hot air gun fastened to the rear of the test box. Temperature was controlled manually. A thermocouple in the test box was monitored and the thermostat of the hot air gun adjusted to maintain the nominal test temperature. Crosshead displacement was used to measure axial strain on all these coupons and, for those coupons with strain gauges installed, both longitudinal and transverse strain were measured.

For the remaining tests (ETW AS4/3501-6 and T650/F584, all T650/PR500) air was ducted into the test box from a Tabai model CR-10HL environmental generator. The generator was connected to the test box with two 100 mm diameter insulated aluminium ducts, a feed duct and a return duct. This system maintained temperature in the test box to within ±1 °C of the test temperature. In addition to crosshead displacement, strain in all of these coupons was measured using a MTS632.85F-05 biaxial extensometer.

±45° tension tests were conducted in accordance with the following procedure:

1. Closed the front door of the test box.
2. Preheated then equilibrated the test box to the test temperature.
3. If installed, connected strain gauge to data recorder.
4. Turned off the hot air source then, as rapidly as practicable, opened the front door and clamped the coupon in the grips. To prevent slippage between the coupons and grips a non-slip gripping interface was placed between the two. Metalite abrasive mesh was used for tests at 25, 50 and 80 °C, while 180 grit emery cloth was used for tests at 105 and 120 °C. A fresh piece of mesh/cloth was used for each coupon.
   The biaxial extensometer, if used, was installed on the coupon. Closed door of test box as soon as possible then turned on hot air source.
5. Waited for 2:00 min while maintaining the temperature inside the test box at the test temperature.
6. Loaded the coupon at 2 mm min^{-1}. Recorded crosshead displacement, load and, on coupons with strain gauges or an extensometer fitted, strain.
7. On coupons with the biaxial extensometer fitted the crosshead was stopped when the extensometer reached its limit of approximately 20,000 με. The door was opened, the extensometer removed from the coupon then the door closed. This step

was performed as quickly as practicable to minimise the time that the door was open. The crosshead was re-started and continued to coupon failure.
8. Stopped crosshead and returned it to its initial position.
9. Opened test box and removed the failed coupon.
10. Repeated Steps 3 to 9 for the remaining coupons.

ASTM D3518 states that the uniformity of the shear stress field in ±45° tension tests falls as axial strain increases because of fibre scissoring. Therefore the test ceases to produce valid shear stress-strain data for calculated shear strains in excess of 5 % (50,000 με). The maximum shear strains measured by the biaxial extensometer prior to it being removed from the coupons was approximately 35,000 με. It was therefore not possible to report the shear stress in accordance with the standard (the lesser of the shear strain at failure or the shear stress at 50,000 με shear strain). Thus the shear strengths reported in this work are the stresses at the failure (peak) test load.

2.6 Open hole compression

For each material at least 50 304.8 mm long x 38.1 mm wide coupons were cut from the OHC panel. A 6.35 mm diameter hole was drilled in the centre of each coupon using a "one-shot" drill.

Strain gauges were bonded to some specimens in order to measure axial compression strain. For those coupons in which strain gauges were bonded, the bonding was conducted prior to drying or environmental conditioning. At least 25 coupons were maintained in the dry condition (70 °C/vacuum) and at least 25 were conditioned (70 °C/85 % RH) to an equilibrium moisture content.

OHC tests were conducted in accordance with SACMA SRM 3R-94 [10]. The procedure used for the testing of these coupons is described in reference [11]. In order to provide the reader with an understanding of this test procedure, the remainder of this section is a summary of that reference.

The general arrangement of equipment is shown in Figure 2-2 and a close-up of the test fixture shown in Figure 2-3. Testing was conducted in an Instron 1185 loading frame with a 100 kN load cell. Coupons were loaded between compression platens. An alignment guide was fixed to both the upper and lower platen and the anti-buckling guides were clamped to these guides. The alignment guides ensured that coupons were parallel to the loading axis, did not kick over during testing and did not fail by end brooming. The platens were enclosed in an insulated test box. A Tabai model CR-10HL environmental generator was used to provide hot air for the test box. This air was transported into the test box through insulated ducts.

During testing the coupons were sandwiched between SACMA SRM 3R-94 anti-buckling guides. These prevented Euler buckling but permitted local buckling around the hole, end shortening of the coupon and the incorporation of bonded strain gauges. The anti-buckling guides acted as a heat sink and shielded the coupon from the air in the test box. Thus the

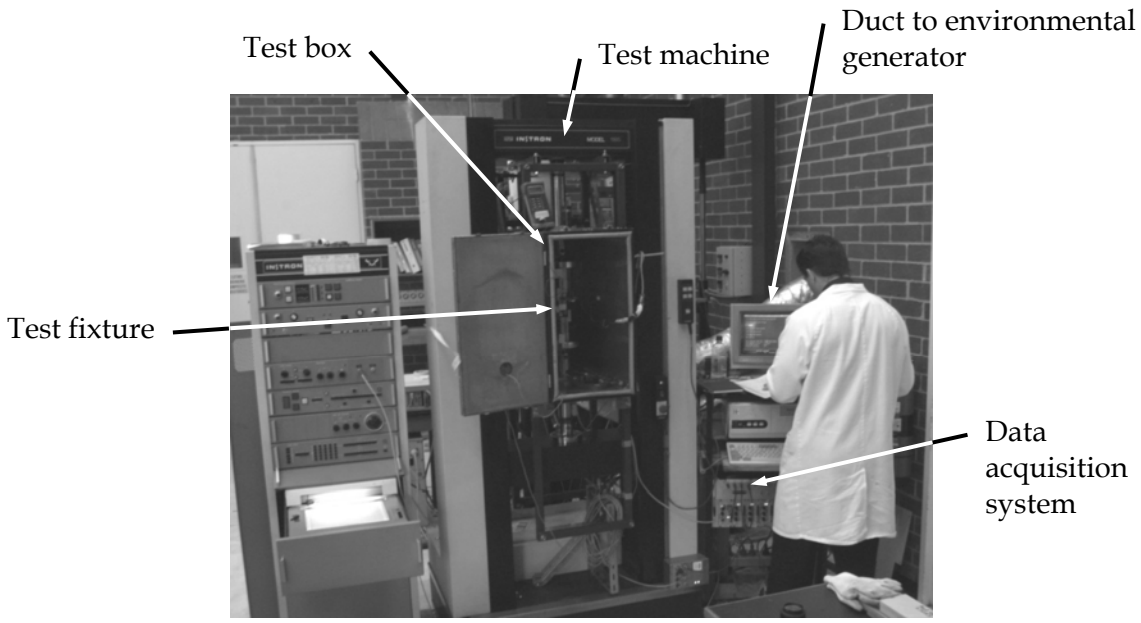

Figure 2-2: Overview of set-up for OHC testing

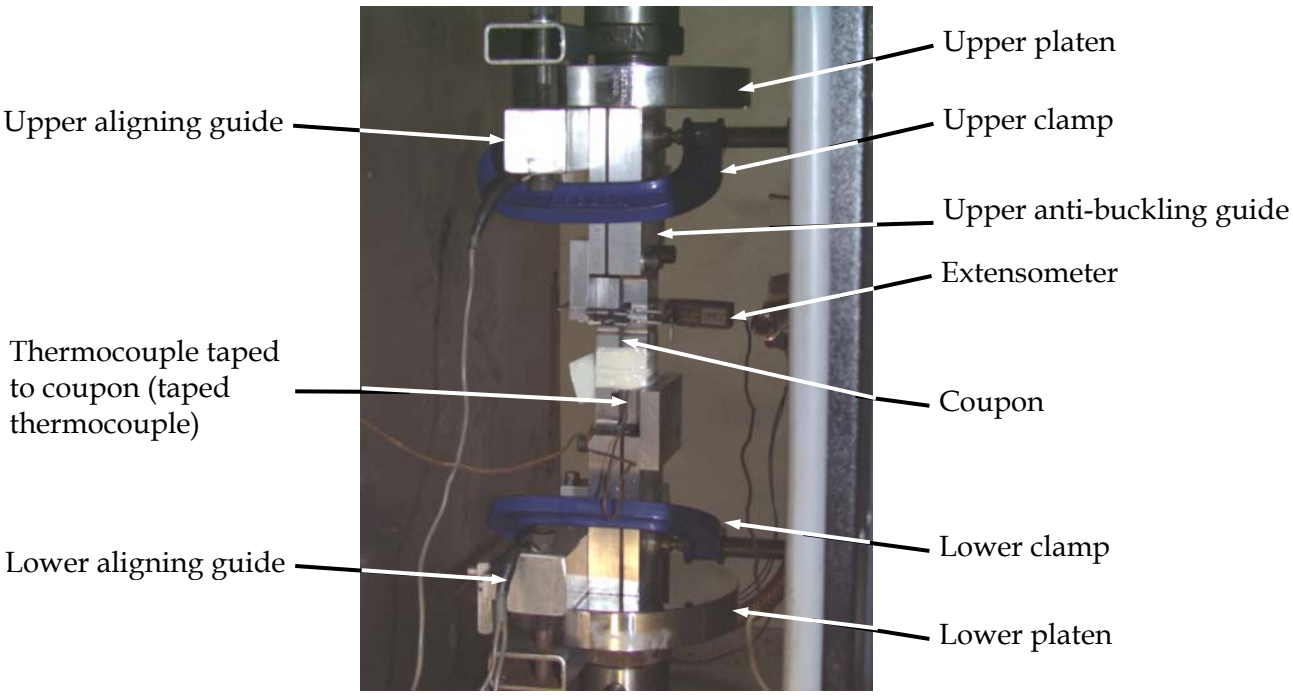

Figure 2-3: Final OHC test setup with anti-buckling guides clamped against alignment guides

time required to heat a coupon mounted in anti-buckling guides was substantial. For example, it was found that for a coupon/anti-buckling fixture at 20 °C introduced into the test box at 80 °C, the coupon would equilibrate at ≈78 °C after ≈1 h 25 minutes. To address this problem the following approaches were used:

(i) preheated the anti-buckling guides,
(ii) minimised the time that the guides were out of the test environment, and
(iii) ran the test box temperature hotter than the nominal test temperature.

A K-type thermocouple was taped to the coupon (taped thermocouple) and used as feedback to control the temperature of the environmental generator. The taped thermocouple temperature was considered representative of the actual coupon temperature. Separate trials were conducted and the difference between these two was found to be less than 5 °C.

An extensometer provided a more robust alternative to strain gauges for high temperature testing of moisturised specimens. Knife-edges were designed for an MTS632.26C-20 extensometer. These knife-edges fitted through the strain gauge window. The extensometer was calibrated with these knife-edges installed in the test environment. All tests were conducted with the extensometer installed.

The following is a summary of the testing procedure:

1. Test fixtures were placed in the test box and the front door closed. The test box was preheated to the temperature shown in column two of Table 3 and equilibrated at this temperature.
2. Removed coupons from the conditioning environment (vacuum oven or environmental chamber). Measured and recorded dimensions.
3. Opened the test box door and removed the anti-buckling guides. Closed door.
4. Assembled the coupon in the anti-buckling guides allowing for strain gauge leads if strain gauges were attached.
5. Located a thermocouple on the side of the coupon, covered it with air-weave breather cloth and fastened it in place using high temperature tape. The air-weave insulated the thermocouple from the environment and ensured the temperature of the coupon was monitored.

Table 3: Environmental generator set points required for the indicated test temperatures

Nominal test T (°C)	Tabai set point when coupon first loaded (°C)	Tabai set point when taped thermocouple reached test T (°C)
25	25	25
50	60	50
80	100	80
105	135	115
120	155	125

6. Positioned the knife-edges of the extensometer on the coupon and secured the extensometer using O-rings.
7. Opened the front door of the test box then, as rapidly as practicable, located the anti-buckling guides against the alignment guides and clamped them in position. Connected the extensometer to the data acquisition system, checked the readout then removed the retaining pin. The final configuration is shown in Figure 2-3. Closed the door within six minutes of opening it.
8. With the Tabai set point at the temperatures shown in Table 3 the taped thermocouple would typically reach the test temperature within five minutes of the test box door closing. When the taped thermocouple temperature reached the nominal test temperature, regardless of whether this occurred in the five minutes prior to starting the test or during loading, then the Tabai set point was lowered to the value shown in the third column Table 3.
9. Testing was commenced 5:00 minutes after the door was closed. The coupon was loaded at 1 mm min^{-1} to failure. The crosshead displacement, load, extensometer strain and, on coupons with strain gauge fitted, strain gauge strain were recorded.
10. Upon failure the crosshead direction was reversed before 3 sec had elapsed. The crosshead was stopped when load returned to zero.
11. The Tabai set point was raised to the temperature shown in column two of Table 3 in preparation for the next test.
12. The test box door was opened and, as quickly as practicable, the extensometer pin installed and the coupon/anti-buckling guide removed. The crosshead was lowered by 2-3 mm and the door closed in preparation for the next coupon.
13. The failed coupon was removed from the anti-buckling guides and instrumentation.
14. Repeated Steps 4 to 13 for the remaining coupons.

2.7 Compression after impact

For each material at least 50 150 mm long x 100 mm wide coupons were cut from the CAI panel. At least 25 coupons were maintained in the dry condition (70 °C/vacuum) and at least 25 were conditioned (70 °C/85 % RH) to equilibrium moisture content. CAI tests were conducted in accordance with SACMA SRM 2R-94 [12].

2.7.1 Impacting

All coupons were C-scanned after they had reached an equilibrium moisture content. The scans revealed that the specimens were free of any manufacturing defects. Coupons were then impacted. The procedure for performing the impacting was described in reference [13]. The following two paragraphs are a summary of the important features of the impacting.

Impacting was conducted on the drop-weight impact machine shown in Figure 2-4. This consisted of a 5.60 kg impactor, with a 15.75 mm diameter hemispherical steel tup, mounted on a vertical rail. The impactor slid freely up and down the rail. A carriage and release assembly was also mounted on the rail. The carriage was attached to a winch that

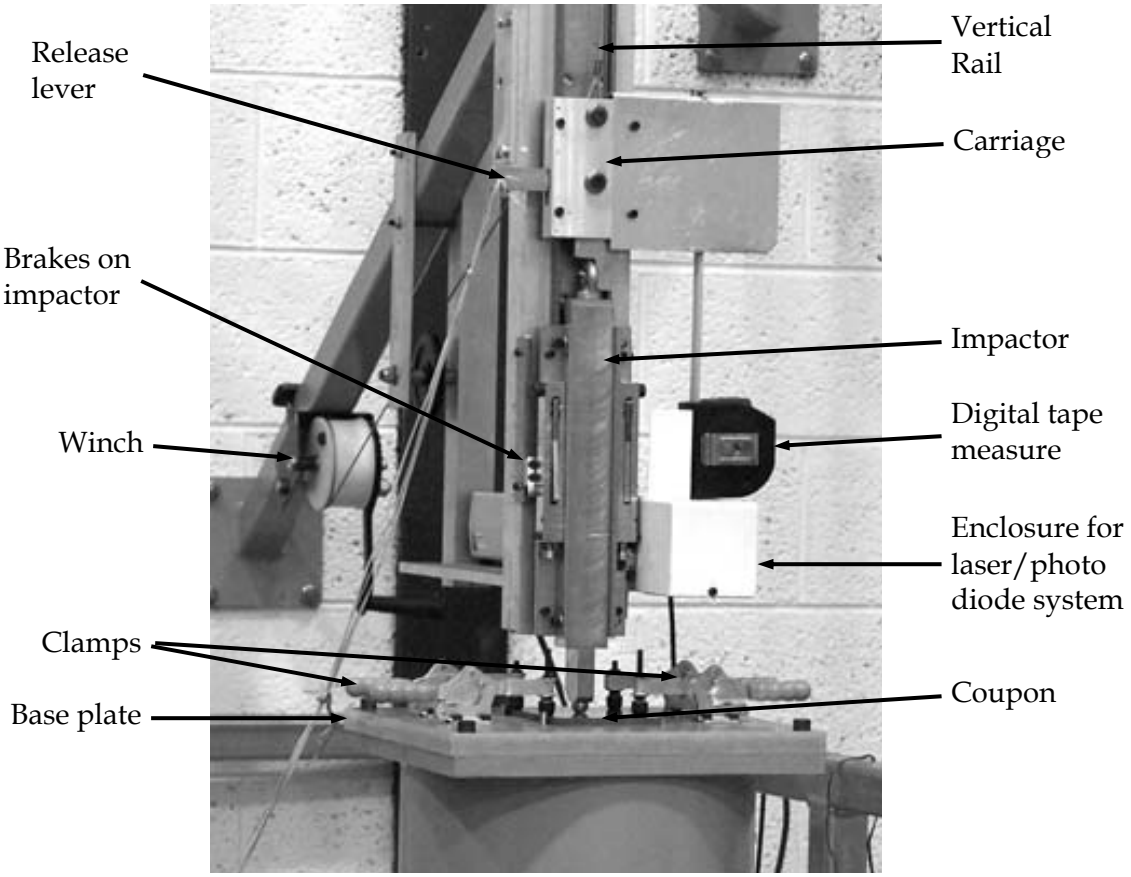

Figure 2-4: The drop-weight impact machine

was used to set the height of the impactor. A digital tape measure was fixed to the carriage so that drop height could be measured. A base plate was located under the rail. It contained a central 76.2 mm x 127.0 mm cut-out and was positioned so that the impactor tup was aligned with the centre of the cut-out. Locating pins were installed on the base plate to locate coupons centrally over the cut-out. Four clamps were mounted around the cut-out to hold coupons to the base plate. Brakes on the impactor were activated when the impactor struck the coupon. These allowed the impactor to rebound but prevented it from restriking the coupon.

Incident and rebound velocity was measured using a laser/photo-diode system and a flag on the impactor. The time that the flag, of known width, broke the laser beam immediately prior to, and after, impact was recorded and velocity calculated. The voltage output from the photo-diode, 3.5 V when the laser illuminated it and 0.0 V when the flag blocked the laser, was recorded on a storage oscilloscope then downloaded to an Excel spreadsheet for analysis. It was found that the velocity of the impactor was fractionally below that predicted by a perfect conversion of potential to kinetic energy. This loss was caused by friction between the impactor and vertical rail. Increasing the drop height compensated for

this loss. Thus the SACMA SRM 2R-94 target energy of 6.7 J mm^{-1} of coupon thickness was achieved.

The following is a summary of the impacting procedure:

1. Measured coupon thickness. Calculated target incident energy and drop height (including compensation for losses).
2. Located coupon against aligning pins and clamped it to the base plate.
3. Gently rested the impactor on the coupon and armed the brakes. Zeroed the digital tape measure and raised the impactor to the calculated drop height.
4. Armed the data acquisition system.
5. Released the impactor. Allowed it to strike coupon and rebound. The brakes prevented it from re-striking the coupon.
6. Released the clamps and removed the coupon from the base plate.
7. Downloaded data and recorded incident/rebound velocities and energy.
8. Disarmed brakes.
9. Repeated Steps 1 to 8 for the remaining coupons.

The impacted coupons were C-scanned and damage area measured and recorded.

2.7.2 CAI testing

2.7.2.1 General

In preparation for CAI testing, strain gauges were bonded to some specimens in order to measure compression strain.

The procedure used for the testing of these coupons is described in reference [6]. In order to provide the reader with an understanding of this test procedure, the remainder of this section is a summary of that reference.

The general and detailed arrangements of test equipment are shown in Figure 2-5 and Figure 2-6 respectively. Testing was conducted in an Instron 1343 loading frame with a 250 kN load cell. A SACMA SRM 2R CAI test fixture was bolted to tongues that were clamped into the hydraulic grips of the test machine. This test fixture clamped, introduced end loading and prevented Euler (global) buckling of the coupon. It was enclosed in an insulated test box. A DSTO constructed environmental generator was used to provide hot air for the test box. This air was transported into the test box through insulated ducts.

2.7.2.2 Alignment

The test fixture was aligned in the test machine and checked using an alignment check coupon. This was a coupon that contained two sets of back-to-back strain gauges. Considerable effort was required to ensure a satisfactory alignment, particularly to account for bending about the coupon normal (z-axis). This was important because the parallelism of each coupon could not be guaranteed nor accounted for using fixed grips. A self aligning upper platen (rocker) between the upper platen (tongue) and upper coupon clamp, was found to decrease substantially the strain gradient across the width of the alignment check coupon.

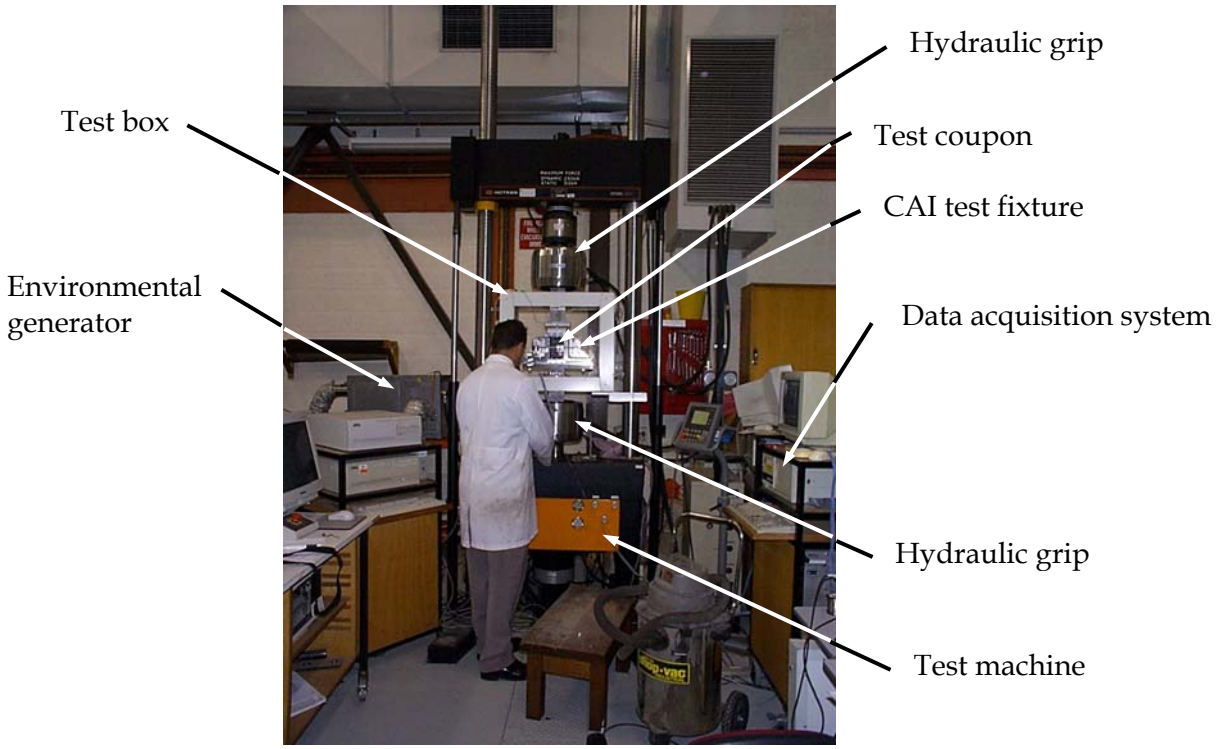

Figure 2-5: Overview of set-up for CAI testing

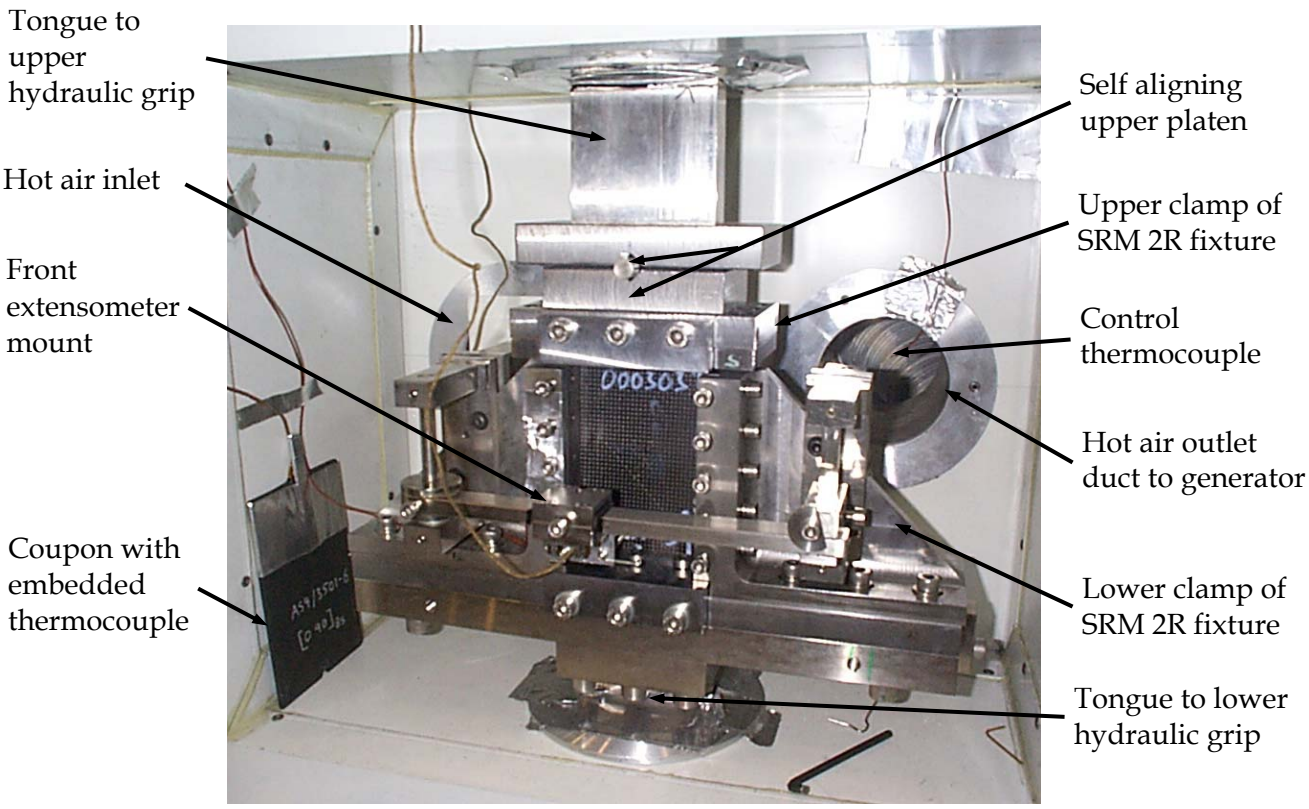

Figure 2-6: The CAI test set-up immediately prior to closing the front door of the test box

2.7.2.3 Strain measurement

SACMA SRM 2R-94 mandates that four bonded foil strain gauges, as two sets of back-to-back gauges, are to be installed on every test coupon. It was prohibitively expensive and time consuming to do this for all 150 coupons tested in this program. In particular it was not possible to reliably bond strain gauges onto coupons that had previously been moisturised to equilibrium without firstly drying the coupon. Therefore only approximately 30% of the coupons were strain gauged.

Extensometers provided an alternative to strain gauges and were particularly convenient for high temperature testing. The time required to mount an extensometer to the face of a coupon at the time of testing was far shorter than that required to bond and protect strain gauges prior to environmental conditioning.

Mounts were designed and manufactured. They were fastened to the SACMA SRM 2R 94 test fixture and supported a MTS 632.26C-20 extensometer at the front and a MTS 632.13C-20 extensometer at the rear. The mounts were hinged to allow for easy coupon removal and spring loaded so that the extensometers were pressed against the face of the coupon but still accommodated movement of the coupon during the test. The extensometers were fitted with three point knife-edges. The points on these knife-edges located more positively on the composite coupons than the traditional blade knife-edges.

This extensometer arrangement was calibrated against the strains measured on the alignment check coupon for each of the test environments and used for all tests.

2.7.2.4 Test environment

In contrast to the OHC testing, the CAI test fixture did not shield significantly the coupons from the chamber environment. Thus the temperature of coupons installed in the CAI fixture rose at approximately the same rate as fully exposed coupons in the same environment. However CAI coupons were approximately double the thickness of coupons from the other tests and so took substantially longer to heat.

A thermocouple located in front of the outlet duct immediately inside the test box was used to provide input to the controller of the hot blower. The set point on the blower was that required for the embedded thermocouple coupon (150 mm x 100 mm, $[45\ 0\ {-45}\ 90]_{4s}$ lay-up, AS4/3501-6 tape, with a thermocouple embedded in the midplane of the laminate at the centre of the specimen) to be 5 °C above the test temperature after a soak time of 12 min. The reason for this additional 5 °C was that, as shown in Figure 2-6, the embedded thermocouple coupon was located at lower left hand corner of the test box, near the hot air inlet. This location was 5 °C hotter than the temperature that would be indicated if it were in the position of the test coupon during testing.

2.7.2.5 Test procedure

The following is a summary of the testing procedure:

1. Installed all parts of the test fixture in the test box and closed the front door. Preheated and equilibrated the test box to the test temperature.

2. Removed coupons from the conditioning environment (vacuum oven or environmental chamber). Measured and recorded dimensions.
3. Installed/soldered strain gauge lead wires if fitted.
4. Turned generator off, opened test box door, removed previous coupon, mounted current coupon, set-up fixture, set-up extensometers, closed door. This step was completed within four minutes.
5. Soaked coupon for 12:00 min. At the end of this time the rate of temperature change in the embedded thermocouple coupon was less than 0.5 °C min^{-1}.
6. Immediately upon completion of the soak time, activated the data acquisition system and loaded the coupon at 0.5 mm min^{-1} to failure. Recorded any observations, particularly the load at which acoustic emissions were detected.
7. Upon failure stopped the actuator and data acquisition system within 5 s. Returned the actuator to the starting position.
8. Left the hot air blower on and coupon in the test box in preparation for the next test.
9. Repeated Steps 2 to 8 for the remaining coupons.

3. Results

3.1 Fibre volume fraction

Fibre volume fraction was calculated using Equation 1. The values for each coupon are reported in Appendices C to F while the averages for each material and test type are shown in Table 4.

$$V_f = \frac{100\, A_w n}{t\rho} \tag{1}$$

Where:

V_f = volume fraction (%)
A_w = areal weight of fibres (g m^{-2})
n = number of fibre layers
t = thickness of panel (m)
ρ = density of fibres (g m^{-3})

3.2 Glass transition temperature

A representative plot of E and tan δ versus temperature for each of the materials/conditions is shown in Figure 3-1. The values of T_g (max tan δ) for each of the specimens is shown in Appendix A. The average T_g, together with the average moisture contents of the 25 °C OHC and CAI coupons, are shown in Table 5.

Table 4: Average volume fraction of coupons

Material	Volume fraction (volume %)				
	ILS	±45° tension	OHC	CAI	Average
AS4/3501-6	55.3	55.4	57.5	57.4	56.4
T650/F584	52.0	49.7	49.2	49.5	50.1
T650/PR500	52.8	53.1	55.1	48.9	52.5

Table 5: Average T_g and moisture content for the tested coupons

Material	Average T_g (°C)		Tg drop		Moisture content (wt %)
	Dry	Wet	(°C)	(%)	
AS4/3501-6	209	156	53	25	1.44
T650/F584	183	152	31	17	1.20
T650/PR500	197	191	6	3	0.63

3.3 Interlaminar shear

Interlaminar shear strength (ILSS) was calculated using the coupon dimension and peak loads shown in Appendix B. The absolute strengths for each coupon were normalised relative to the average 25 °C dry ILSS for that material. The average absolute and normalised ILSS data is shown in Appendix B and plotted in Figure 3-2.

The failed coupons were examined visually and photographed. As there was no difference in the appearance of coupons for each material only the T650/PR500 coupons are shown in Figure 3.3. There was very little difference between the coupons prior to, and after, failure at all temperatures, although the 120 °C coupons exhibited a slight bend.

3.4 ±45° tension

The shear stress-shear strain (τ–γ) behaviour of each coupon that was fitted with a biaxial strain gauge or biaxial extensometer was plotted. The τ-γ behaviour was very similar for all materials and conditions, a typical example being shown in Figure 3-4. There was an initial linear response followed by a gradual softening to failure. The γ at the transition from linear to non-linear behaviour varied widely with final failure typically occurred at axial strains in excess of 70,000 με, well beyond the range of validity (γ = 50,000 με) for the ±45° tension test.

Summaries of the ±45° tension test and reduced data are shown in Appendix C. The absolute ±45° tension strength for each coupon was normalised relative to the average 25°C dry ±45° tension strength for that material. This data is plotted in
Figure 3-5.

Representative failed coupons were photographed and are shown in Figure 3-6 to Figure 3-8. Figure 3-6 shows that the appearance of the AS4/3501-6 was similar at all

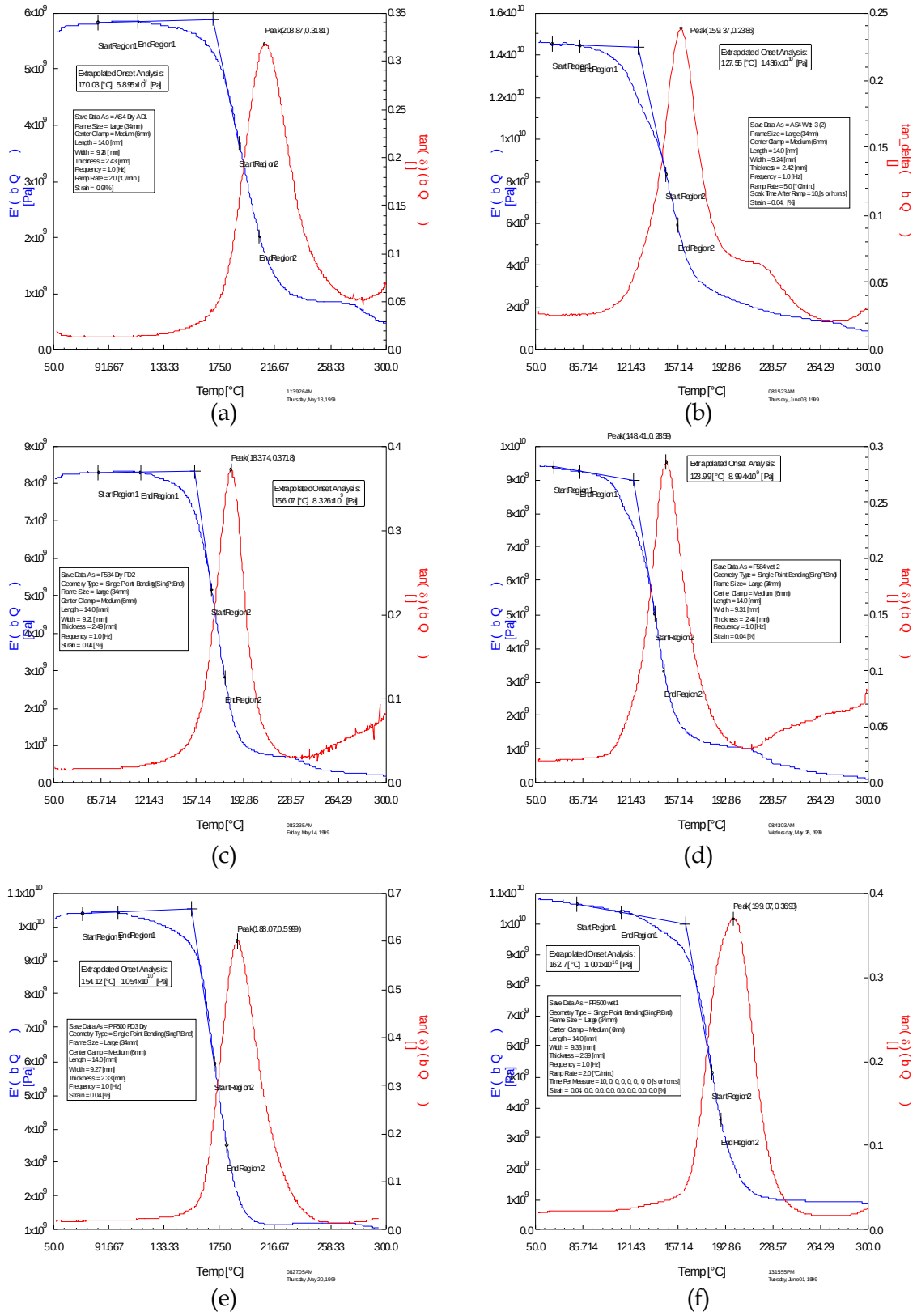

Figure 3-1: DMTA results for AS4/3501-6 (a) dry and (b) wet, T650/F584 (c) dry and (d) wet, and T650/PR500 (e) dry and (f) wet

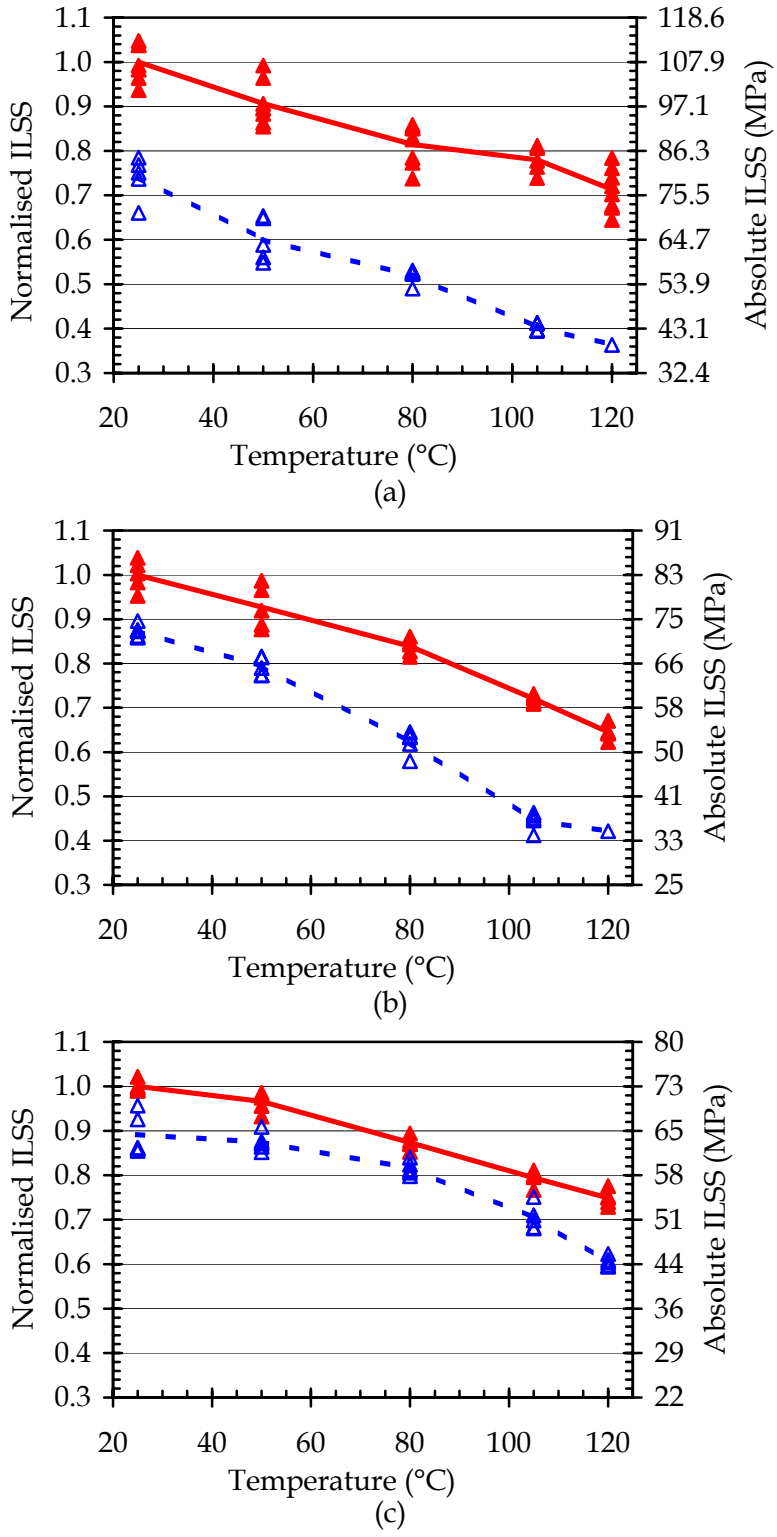

Figure 3-2: Normalised and absolute ILSS for (a) AS4/3501-6, (b) T650/F584 and (c) T650/PR500. ETD data is shown as solid markers and lines, ETW data is shown as open markers and dotted lines

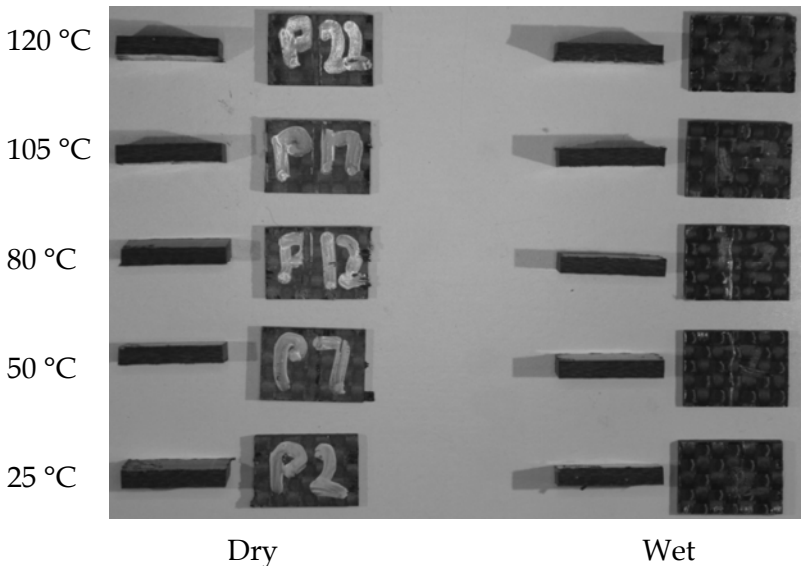

Figure 3-3: Representative failed T650/PR500 ILS coupons

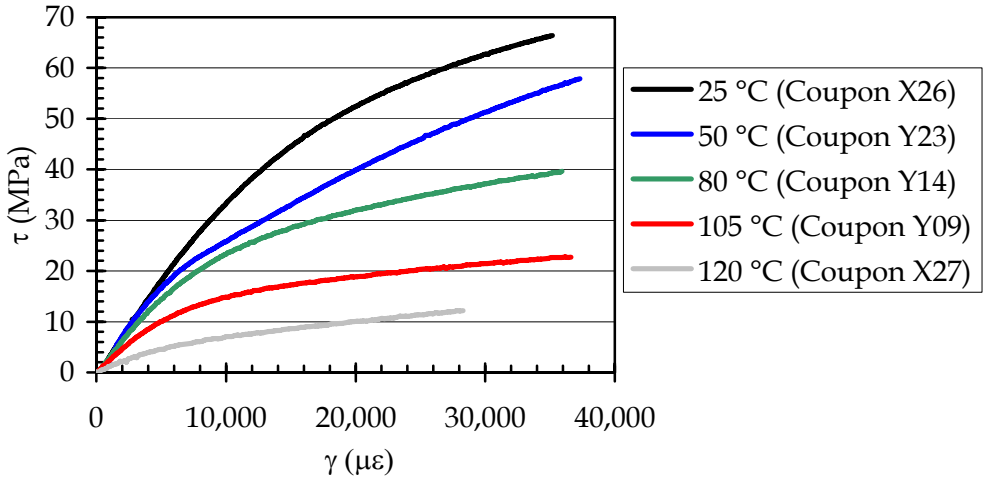

Figure 3-4: Shear behaviour of wet T650/F584 ±45° tension coupons over the range of the biaxial extensometer. Both temperature and coupon number are indicated

temperatures and conditions. Failure occurred within the gauge and consisted of ply splitting with long fibre pull-out. Slitting of the surface plies was observed along the entire gauge length but very little apparent necking.

In contrast, Figure 3-7 shows the dry T650/F584 to have more localised damage with distinct necking at 105 and 120 °C. Wet coupons showed localised necking at 50 and 80 °C then narrowing of the entire coupon at 105 and 120 °C. The fibre pull-out on all failure faces was much shorter than for the AS4/3501-6.

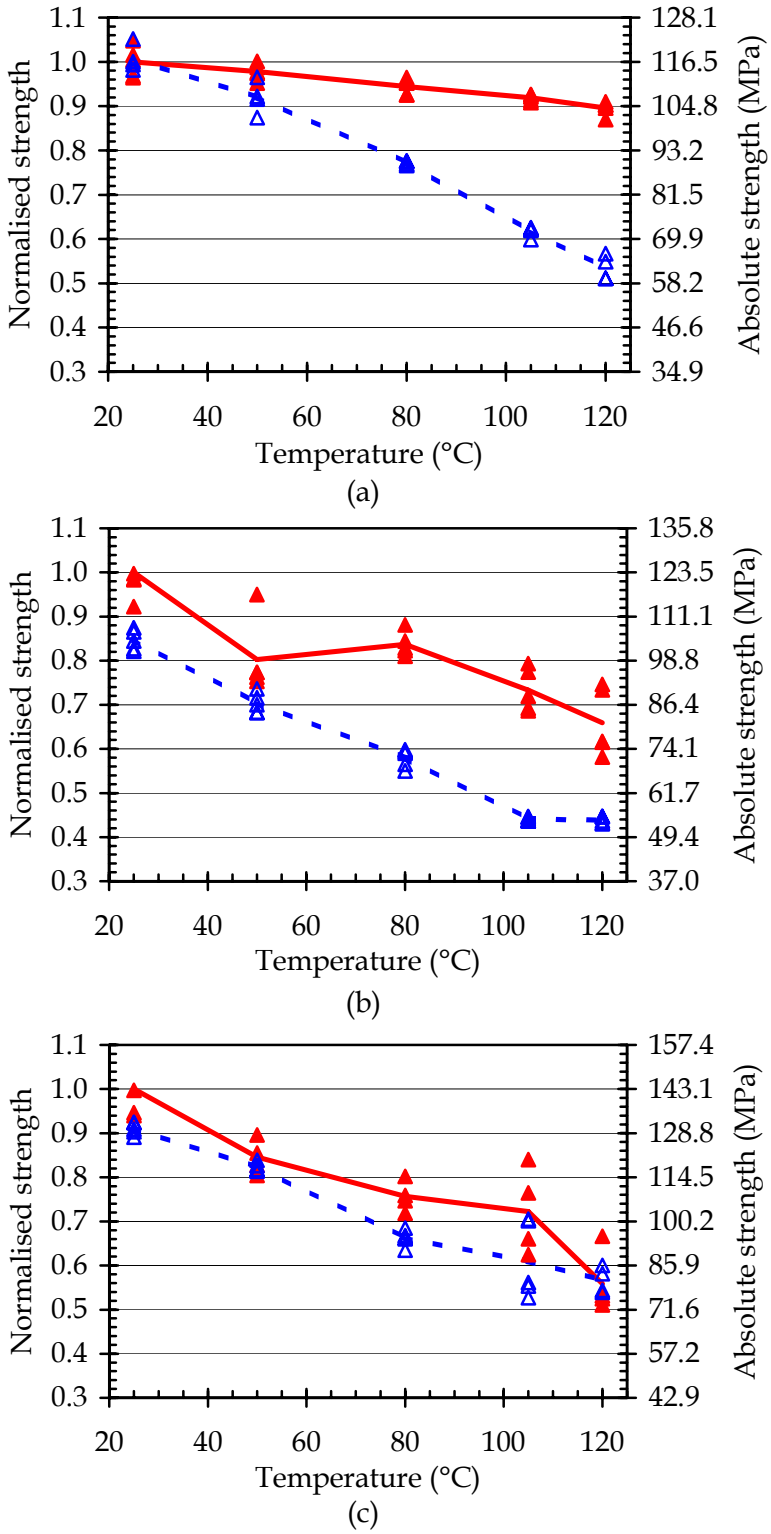

Figure 3-5: Normalised and absolute ±45° tension strength for (a) AS4/3501-6, (b) T650/F584, and (c) T650/PR500. ETD data is shown as solid markers and lines, ETW data is shown as open markers and dotted lines

(a)

(b)

Figure 3-6: Representative failed (a) dry and (b) moisturised AS4/3501-6 ±45° tension coupons. The test temperature is indicated on each coupon

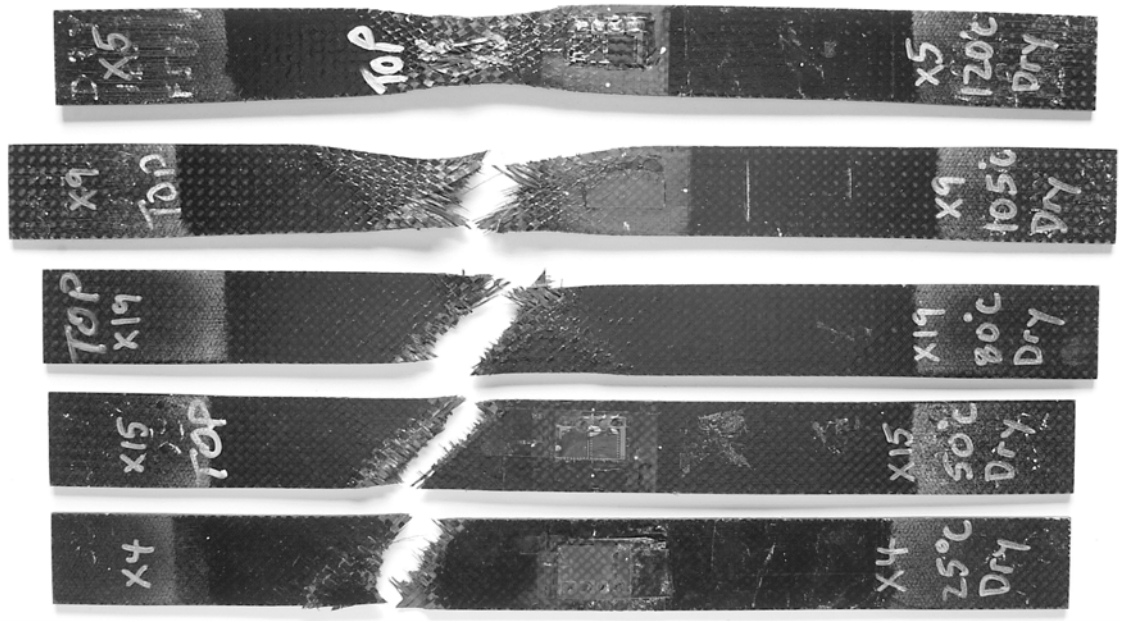

(a)

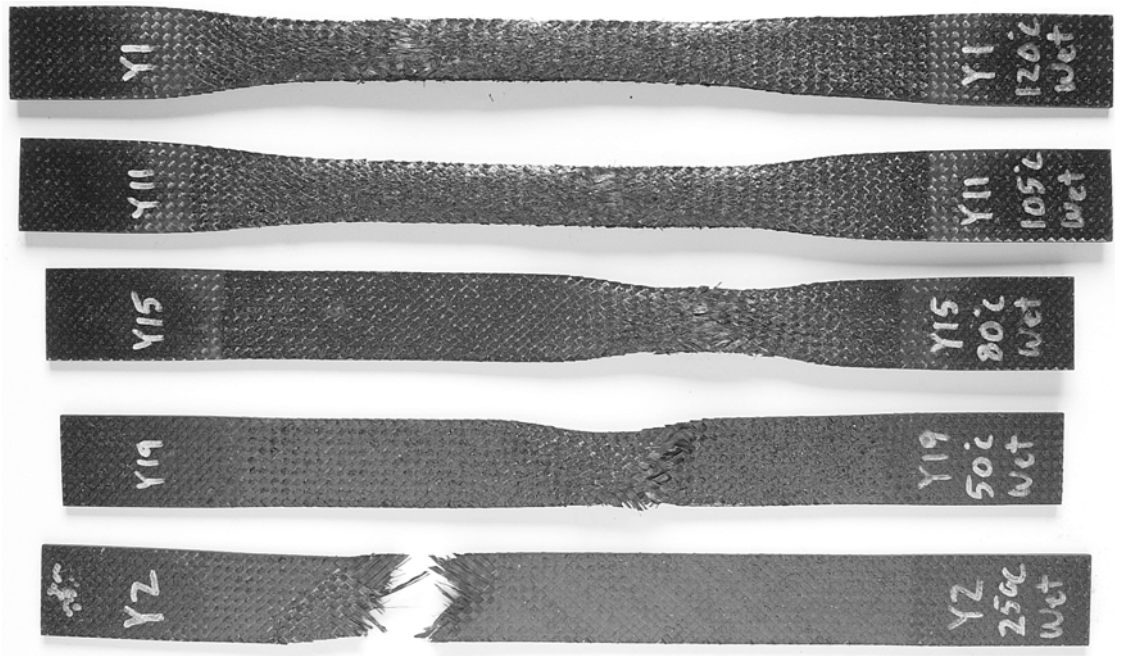

(b)

Figure 3-7: Representative failed (a) dry and (b) moisturised T650/F584 ±45° tension coupons. The test temperature is indicated on each coupon

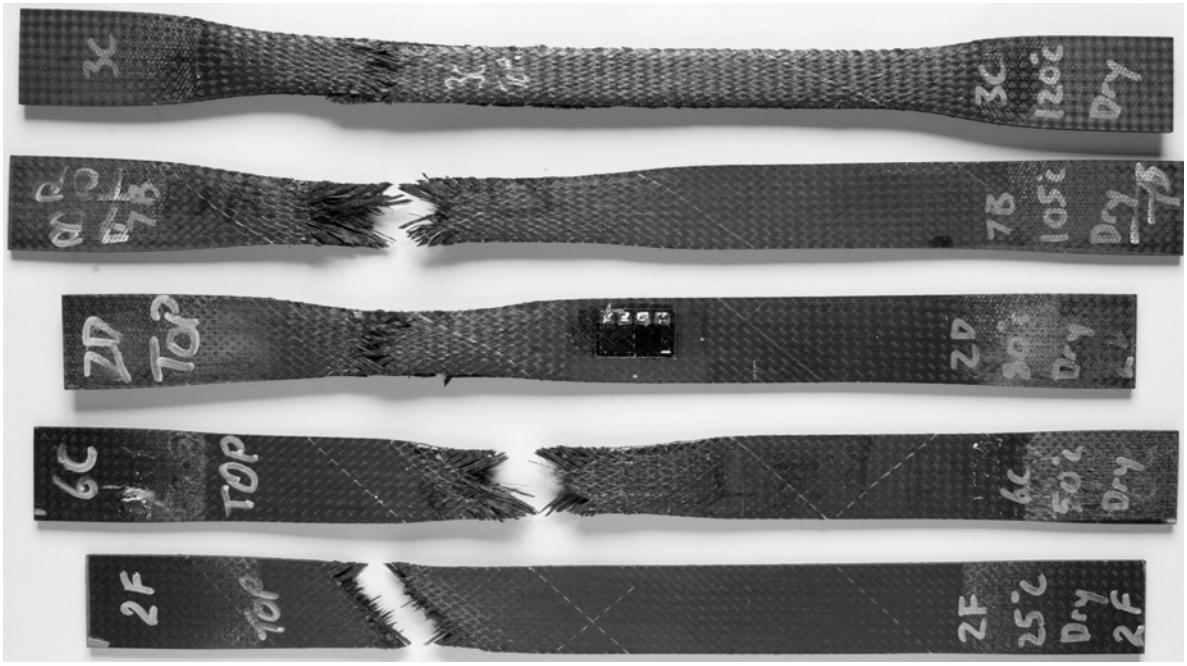

(a)

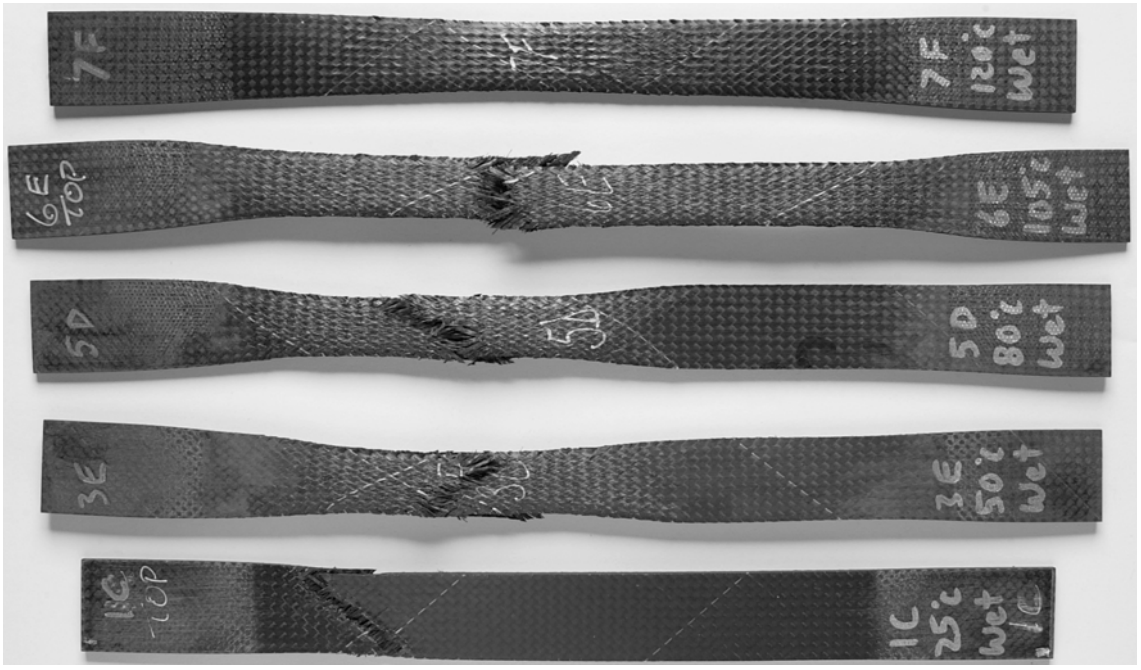

(b)

Figure 3-8: Representative failed (a) dry and (b) moisturised T650/PR500 ±45° tension coupons. The test temperature is indicated on each coupon

Figure 3-8 shows the fibre pull-out zone of all T650/PR500 coupons to be between that of the AS4/3501-6 and T650/F584. The dry coupons showed a distinct, broad neck, that increased in length as temperature increased. At 120 °C the neck had extended to become a narrowing of the entire gauge length. The wet coupons were similar to the dry coupons except that the neck was longer at each temperature, so for example the neck in the wet 105 °C coupon extended the full gauge length.

3.5 Open hole compression

The stress-strain (σ–ε) behaviour of each coupon was very similar for all materials in both the dry and wet condition. Figure 3-9 shows a typical response. The only difference in the essentially linear response for all materials was a reduction in failure strain as temperature increased.

Summaries of the OHC test and reduced data are shown in Appendix D. The absolute OHC strength of each coupon was normalised relative to the average 25 °C dry OHC strength for that material. The modulus and strain to failure are plotted in Figure 3-10 and the OHC strength in Figure 3-11. The moisture content of the traveller coupons was calculated and is plotted in Figure 3-12.

Ten additional OHC coupons were tested. These were manufactured from T300J/DA508 prepreg tape by CEAT and sent to Australia. The data is tabulated in Appendix D and plotted in Figure 3-13.

The failed OHC coupons were photographed with representative examples being shown in Figure 3-14 to Figure 3-16.

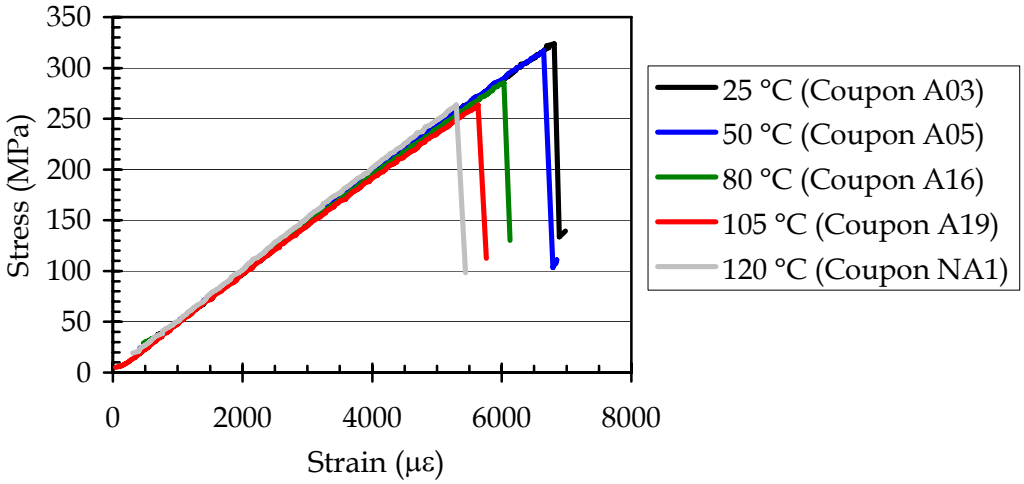

Figure 3-9: OHC behaviour of dry AS4/3501-6

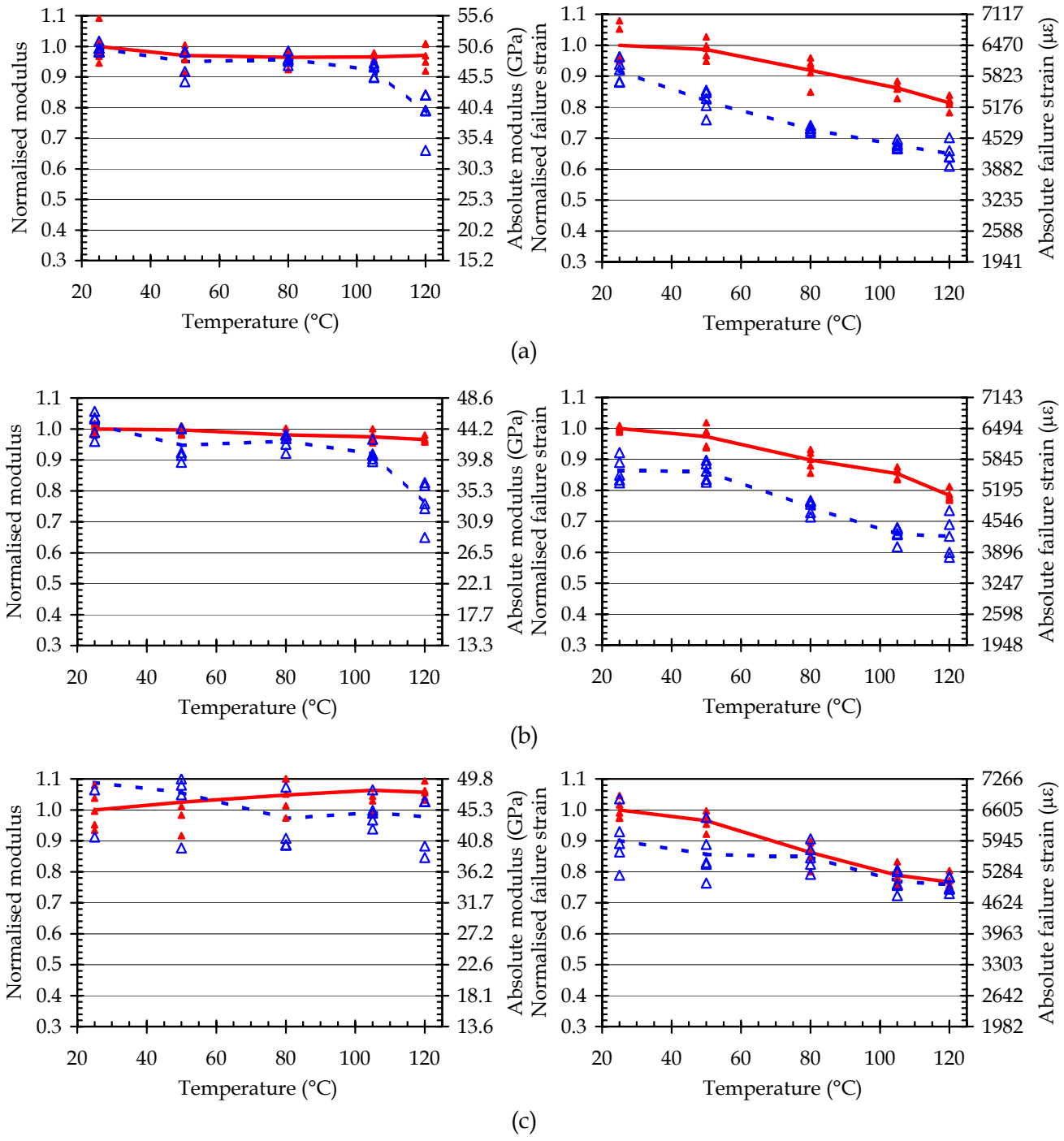

Figure 3-10: Normalised and absolute OHC modulus and strain to failure for (a) AS4/3501-6, (b) T650/F584, and (c) T650/PR500. Solid markers and line are ETD data. Open markers and dotted lines are ETW data

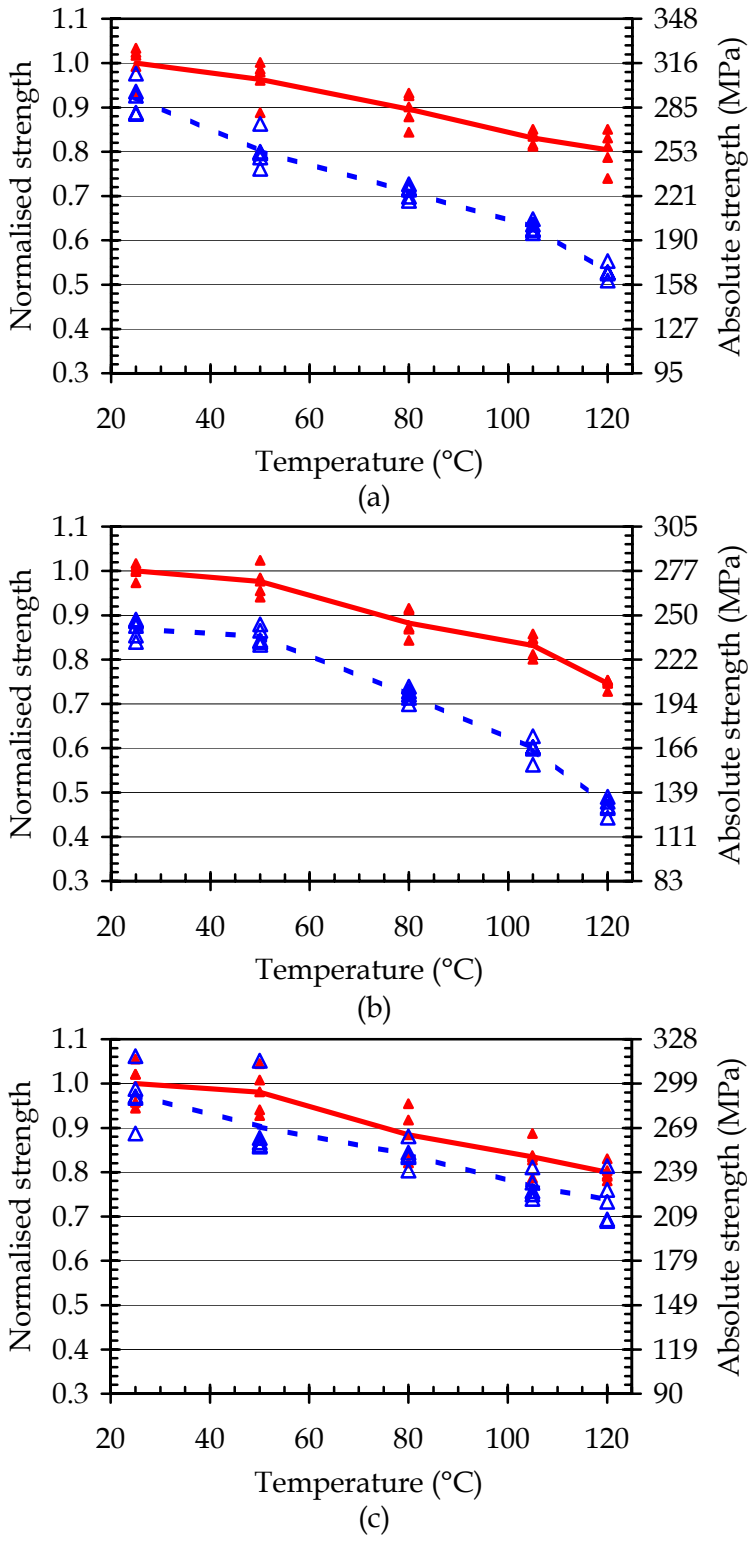

Figure 3-11: Normalised and absolute OHC strength for (a) AS4/3501-6, (b) T650/F584, and (c) T650/PR500. ETD data is shown as solid markers and lines, ETW data is shown as open markers and dotted lines

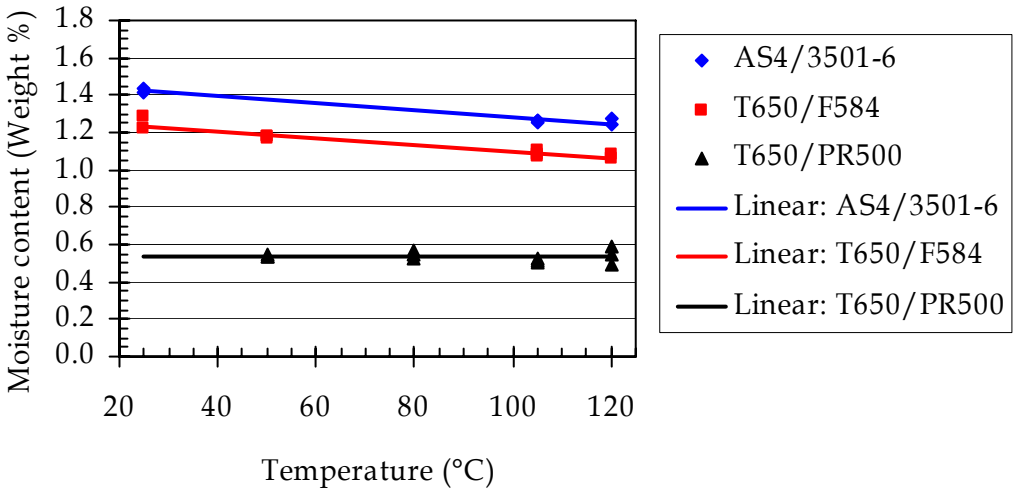

Figure 3-12: Equilibrium moisture content of samples cut from OHC test coupons immediately after testing

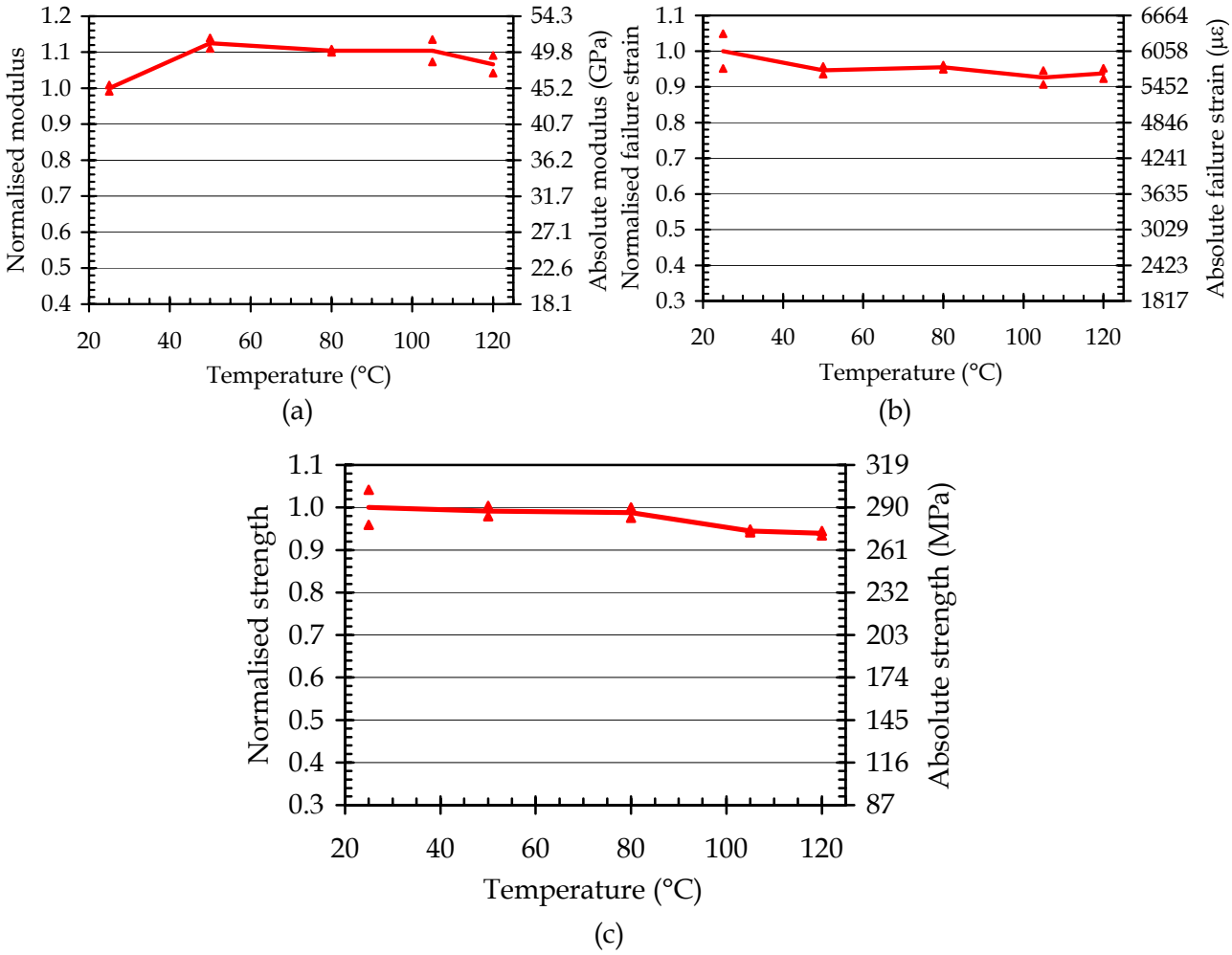

Figure 3-13: Normalised and absolute OHC (a) modulus, (b) strain-to-failure, and (c) strength of dry T300J/DA508

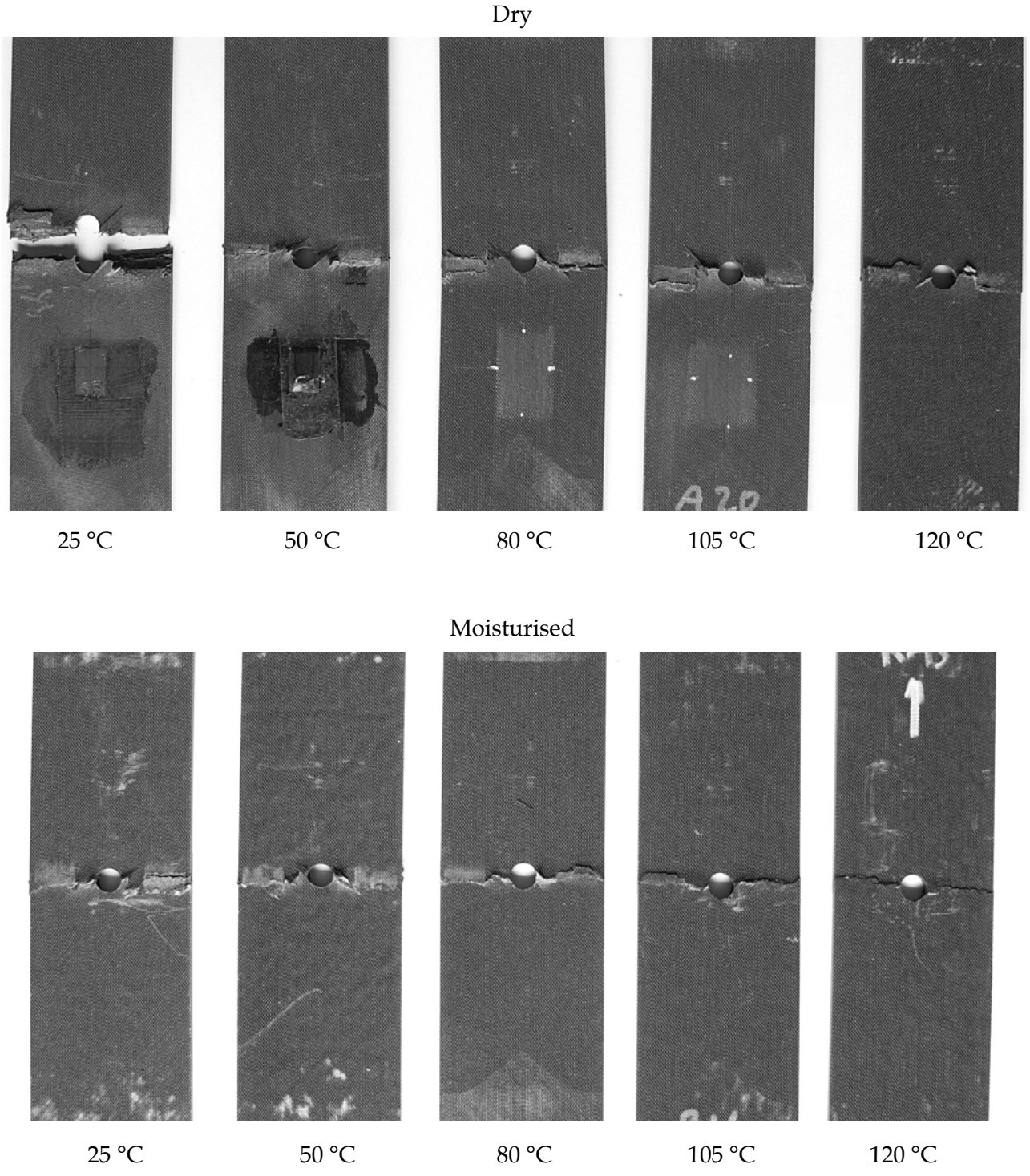

Figure 3-14: Representative failed AS4/3501-6 OHC coupons

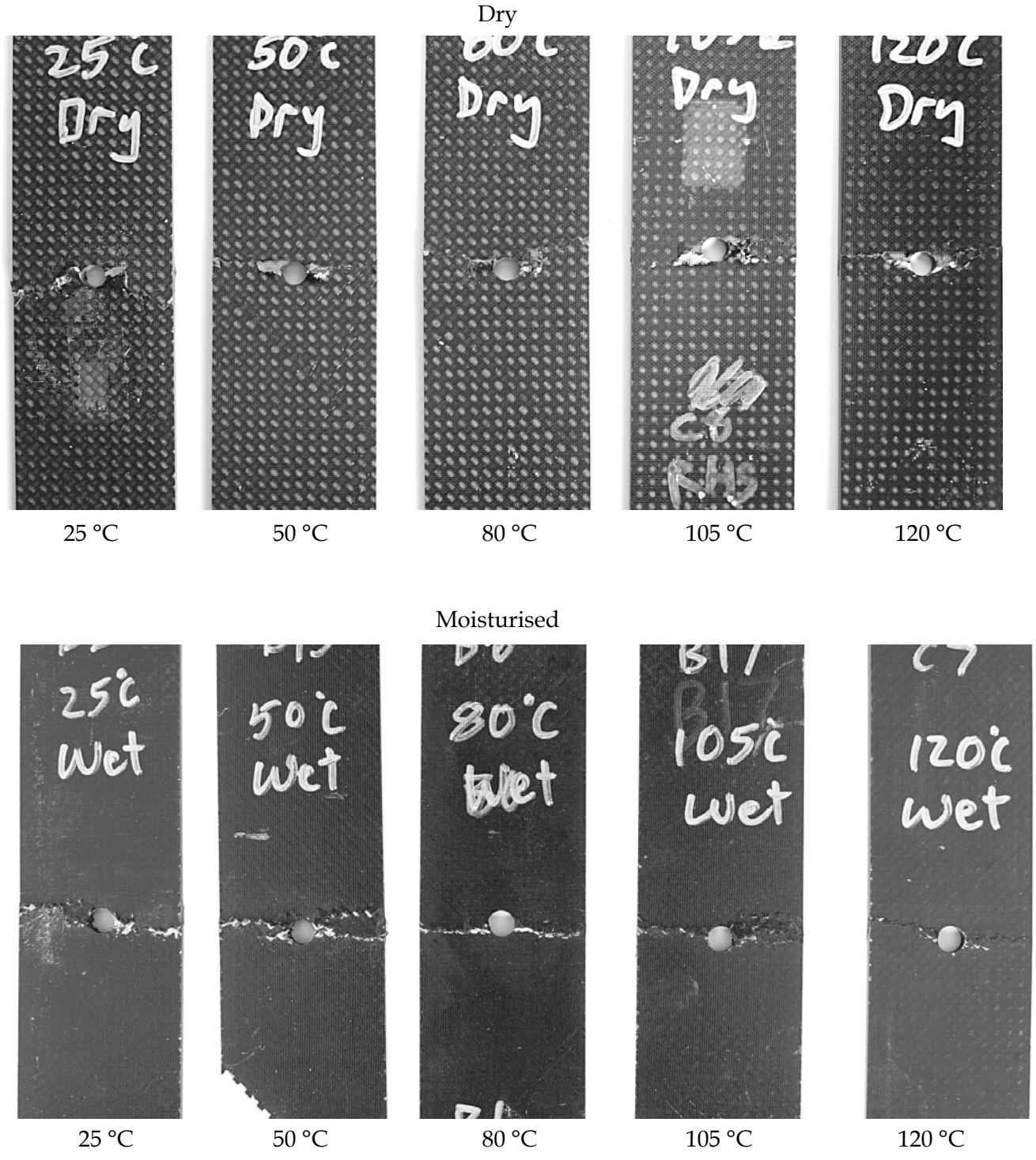

Figure 3-15: Representative failed T650/F584 OHC coupons

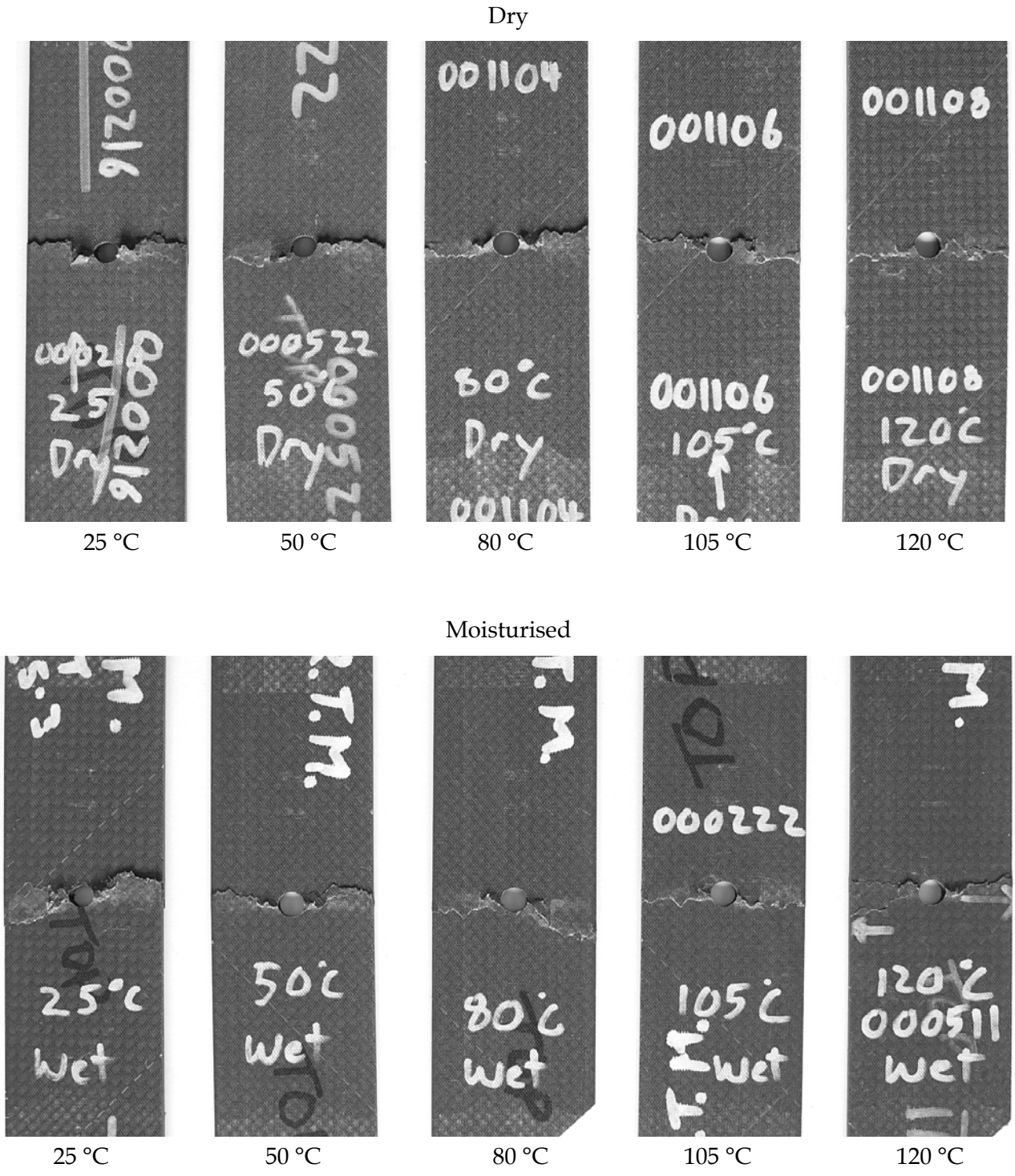

Figure 3-16: Representative failed T650/PR500 OHC coupons

3.6 Compression after impact

There was considerable variation in the C-scans of the impacted AS4/3501-6. As shown in Figure 3-17 the dry coupons showed either an approximately circular central region (Figure 3-17 (a)) or the same heavily damaged central region coupled with a broad, but less heavily damaged, outer region (Figure 3-17 (b)). The wet coupons showed both of these features (Figure 3-17 (c) and (d)) and the classic dumbbell shaped damage as reported in the literature (Figure 3-17 (e). In contrast, as shown in Figure 3-18, the shape and size of impact damage in each of the other two materials was consistent. The impact damage area was calculated and is tabulated in Appendix E and plotted in Figure 3-19.

The stress-strain (σ–ε) behaviour of each coupon was very similar for all materials in both the dry and wet condition. Figure 3-20 shows the response for wet T650/F584. The only difference in the essentially linear to failure response for all materials was being a reduction in failure strain as temperature increased.

Summaries of the CAI test and reduced data are shown in Appendix E. The absolute CAI properties for each coupon were normalised relative to the average 25 °C dry CAI property for that material. The mechanical properties are plotted in Figure 3-21 and Figure 3-22 and the moisture content is plotted in Figure 3-23.

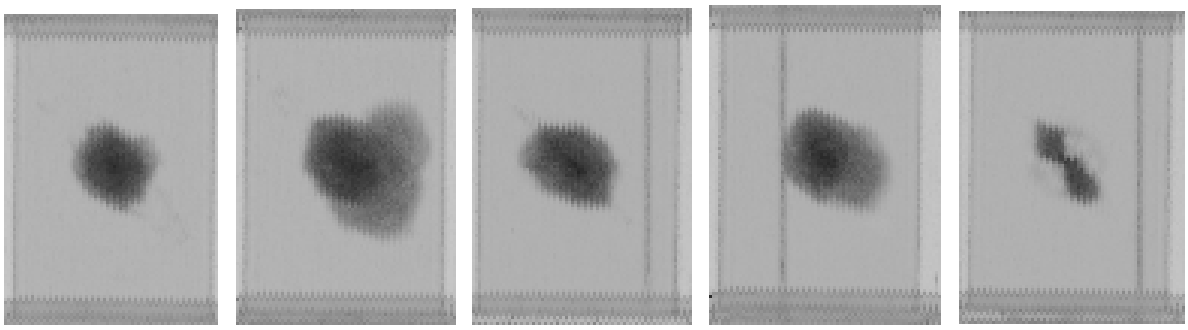

(a) (b) (c) (d) (e)

Figure 3-17: Typical C-Scan images from dry (a) B12, (b) B15 and wet (c) A7, (d) A15, (e) A3 AS4/3501-6

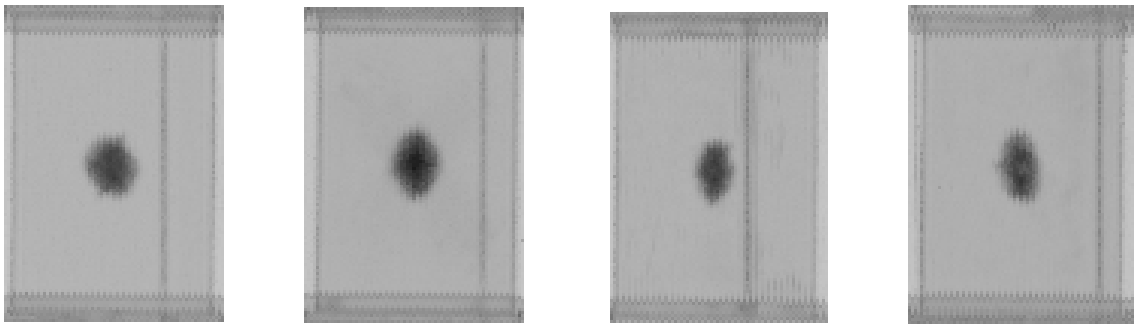

(a) (b) (c) (d)

Figure 3-18: Typical C-scan images from (a) dry (A12) and (b) wet (B14) T650/F584 and (c) dry (000407) and (d) wet (000308) T650/PR500

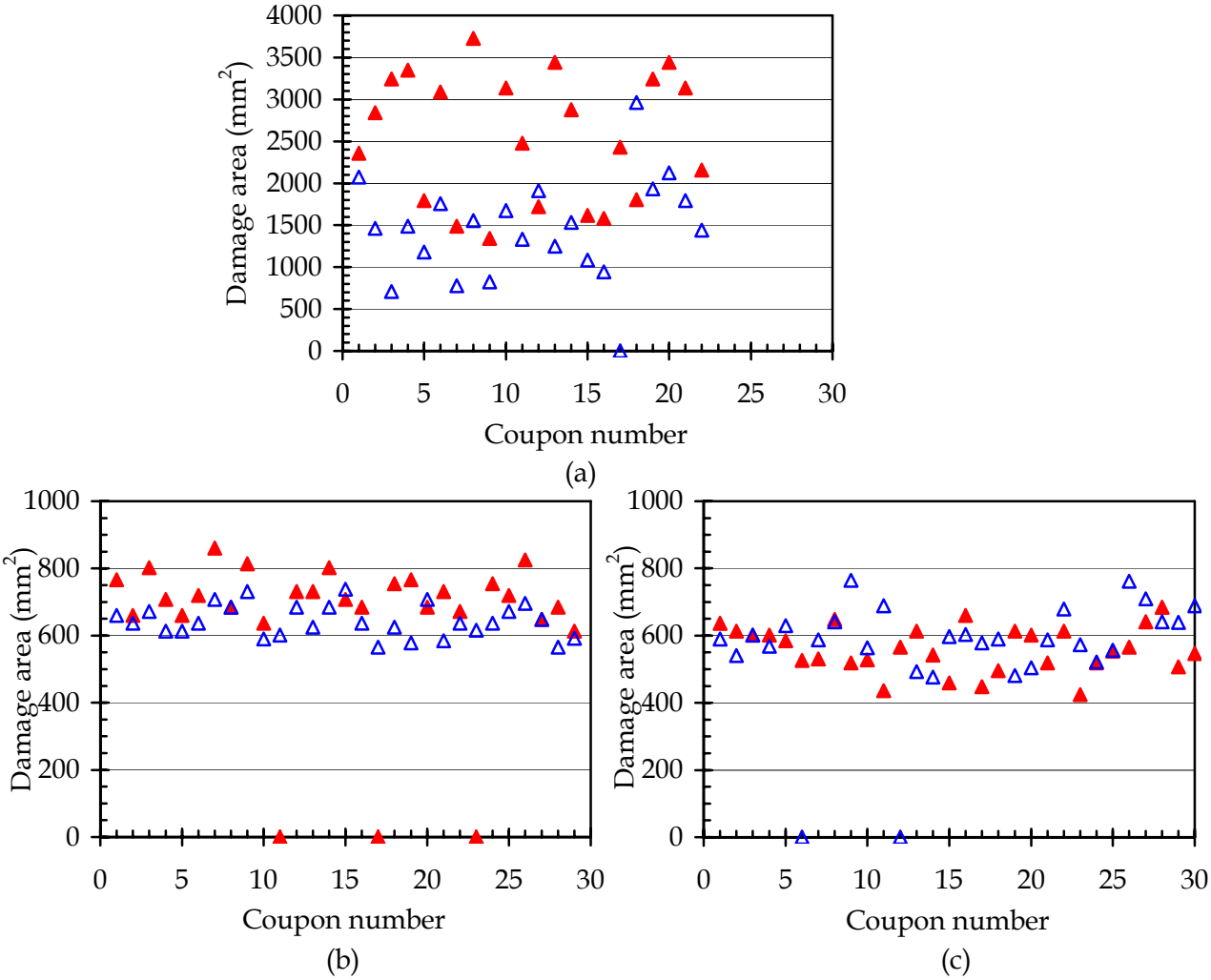

Figure 3-19: Damage areas on the (a) AS4/3501-6, (b) T650/F584 and (c) T650/PR500 coupons. Solid and open markers represent the dry and wet coupons respectively

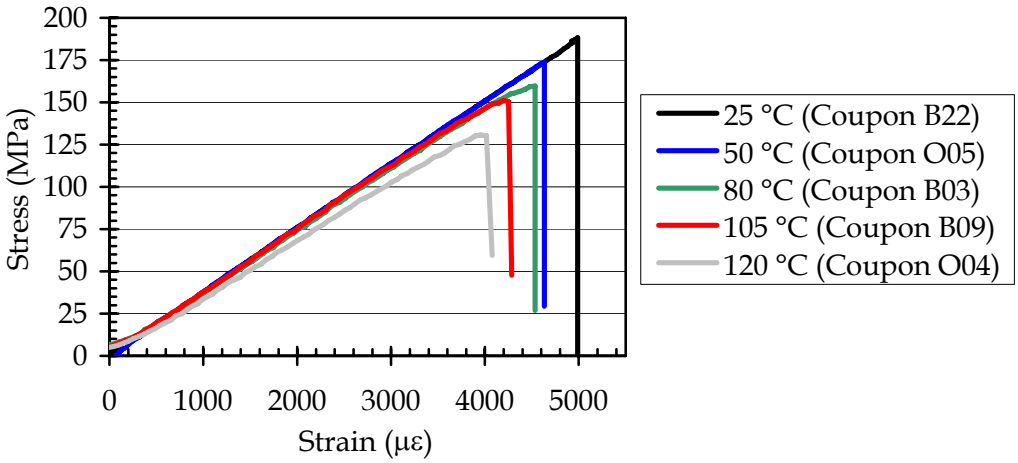

Figure 3-20: CAI behaviour of moisturised T650/F584

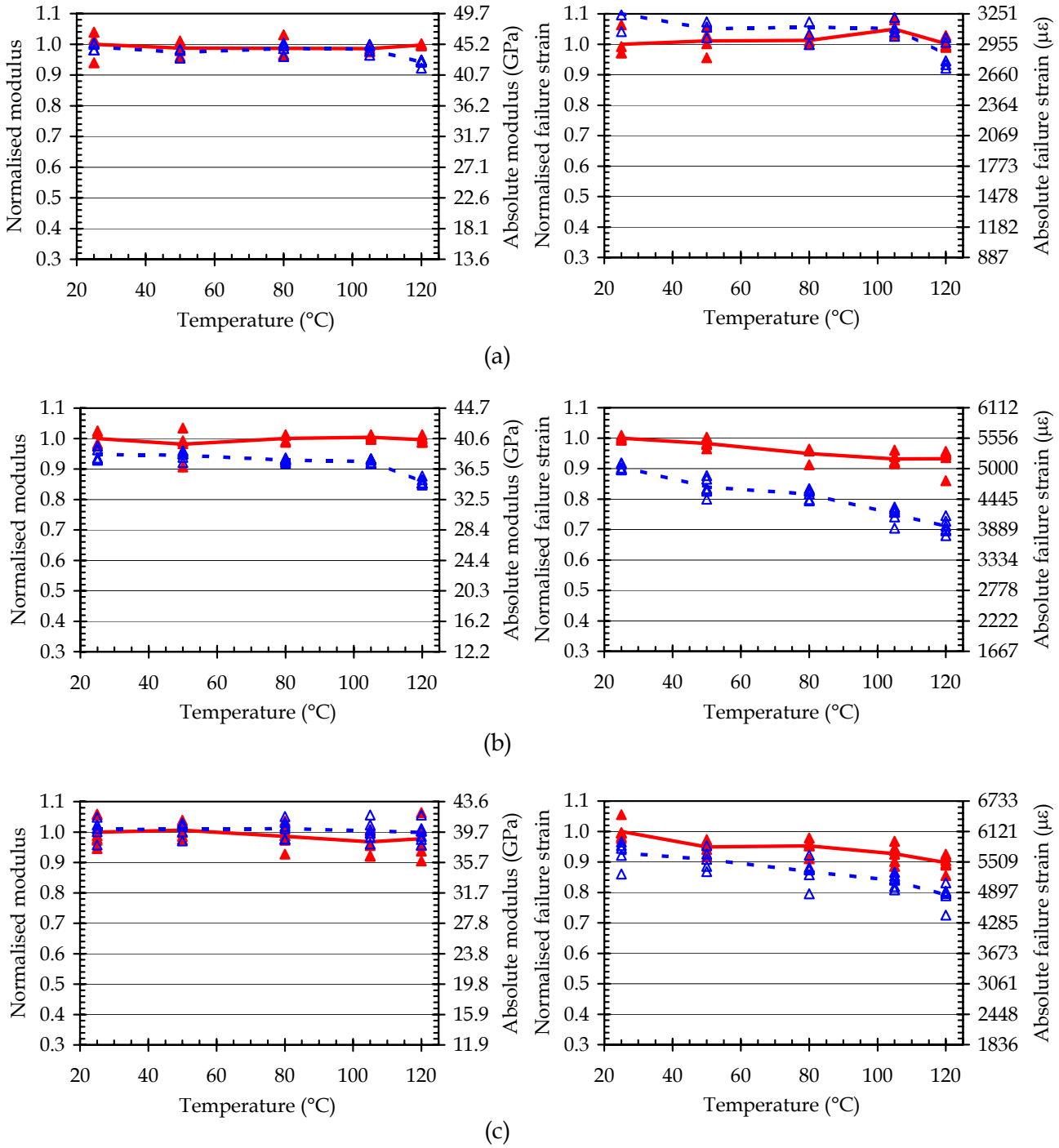

Figure 3-21: Normalised and absolute CAI modulus and strain to failure for (a) AS4/3501-6, (b) T650/F584, and (c) T650/PR500. Solid markers and line are ETD data. Open markers and dotted lines are ETW data

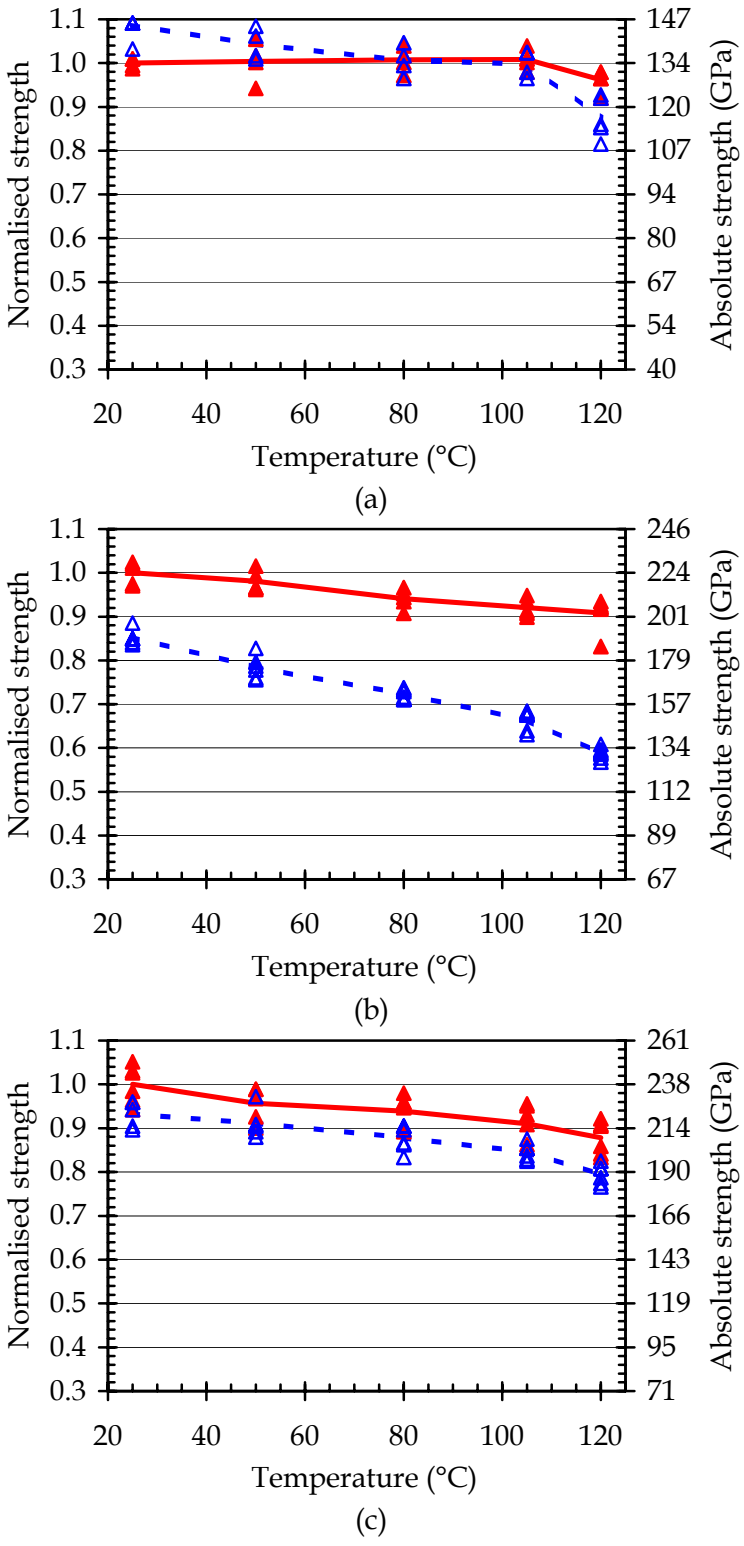

Figure 3-22: Normalised and absolute CAI strength for (a) AS4/3501-6, (b) T650/F584, and (c) T650/PR500. ETD data is shown as solid markers and lines, ETW data is shown as open markers and dotted lines

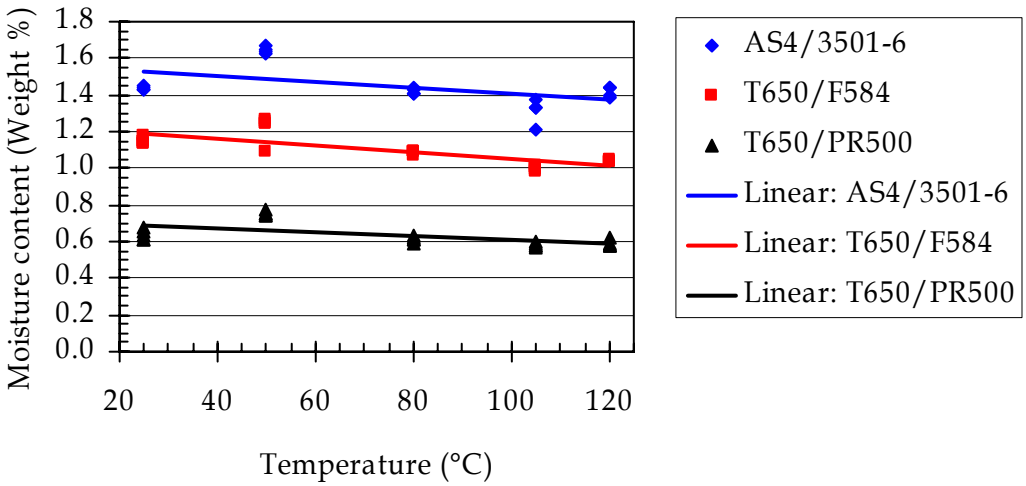

Figure 3-23: Equilibrium moisture content of samples cut from CAI test coupons immediately after testing

Failure in the CAI coupons originated at the impact site and propagated laterally to the edge of the coupon. The central 40 mm (20 mm each side of the failure) was cut from one coupon of each test condition and photographed.

There was little visible sign of failure in the AS4/3501-6 coupons (Figure 3-24), and little change between the specimens. At most the microbuckle line may have been slightly more pronounced as temperature increased, however this difference was subtle.

This contrasts with the T650/F584 shown in Figure 3-25. There was an obvious bulge, containing the microbuckled material, across the width of each coupon. The size and shape of the bulge was reasonably consistent for each condition (dry or wet) as temperature increased. However the appearance of the dry and wet coupons was clearly different. The dry coupons had an as-manufactured smooth and shiny appearance. The wet coupons appeared roughened and dull and the surface had a slight powdery feel. When these coupons were cut the fibres protruded from the face by up to a few millimetres.

The appearance of the T650/PR500 failures in Figure 3-26 was similar to the dry T650/F584. An obvious bulge across the full width of the specimen. In contrast with the T650/F584, the surface of both dry and wet coupons was very similar, smooth and shiny.

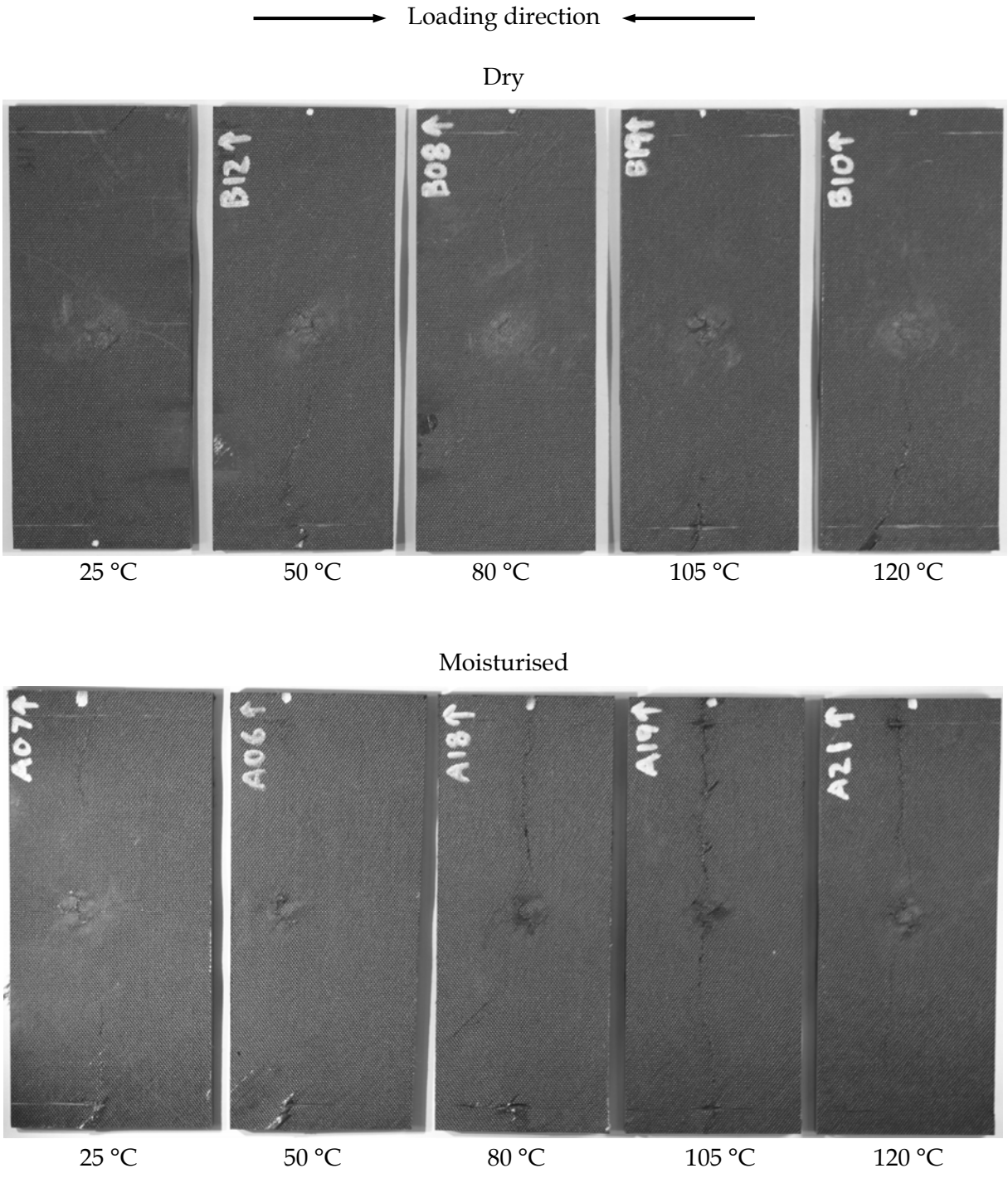

Figure 3-24: Representative failure regions on AS4/3501-6 CAI coupons

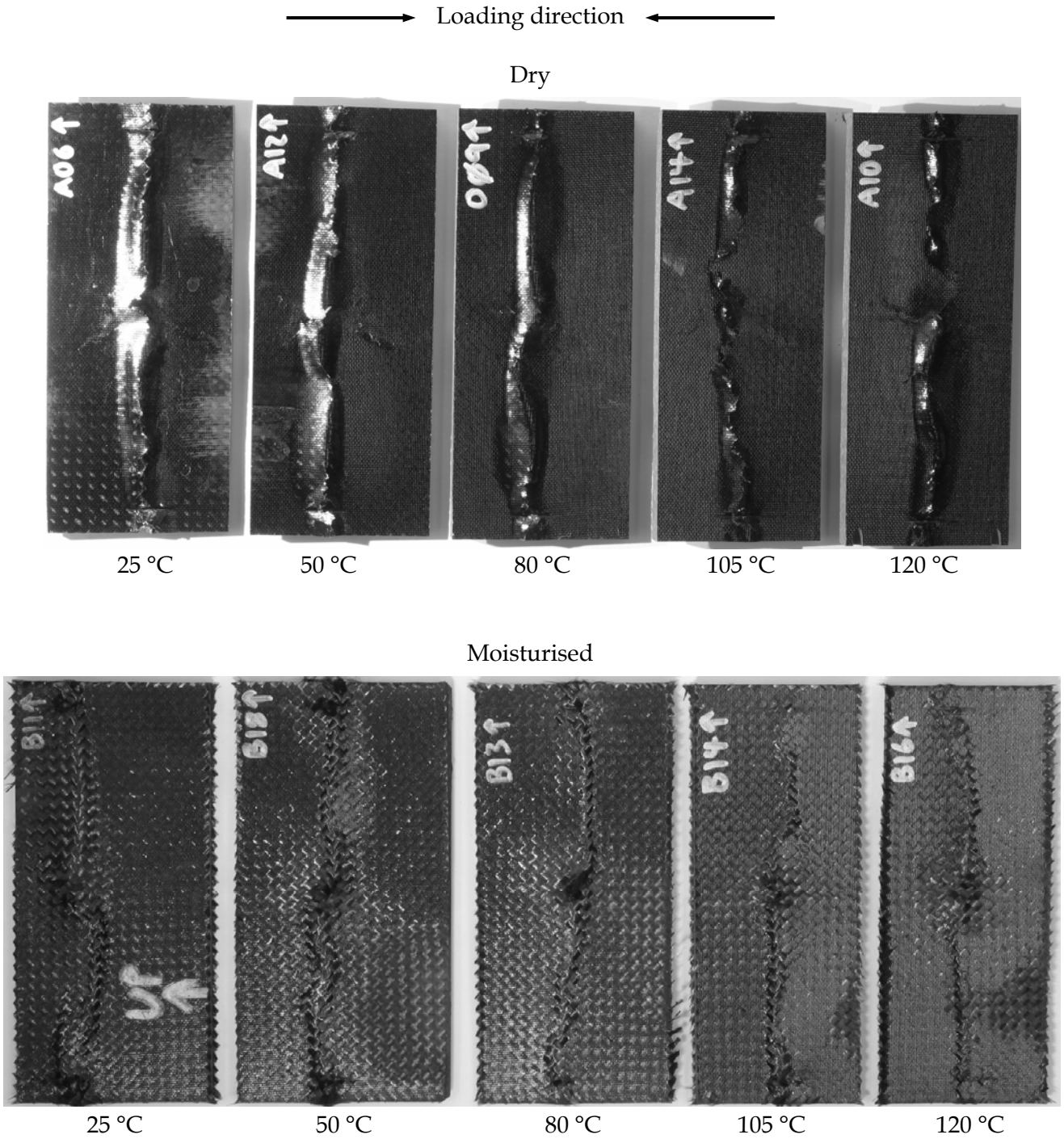

Figure 3-25: Representative failure regions on T650/F584 CAI coupons

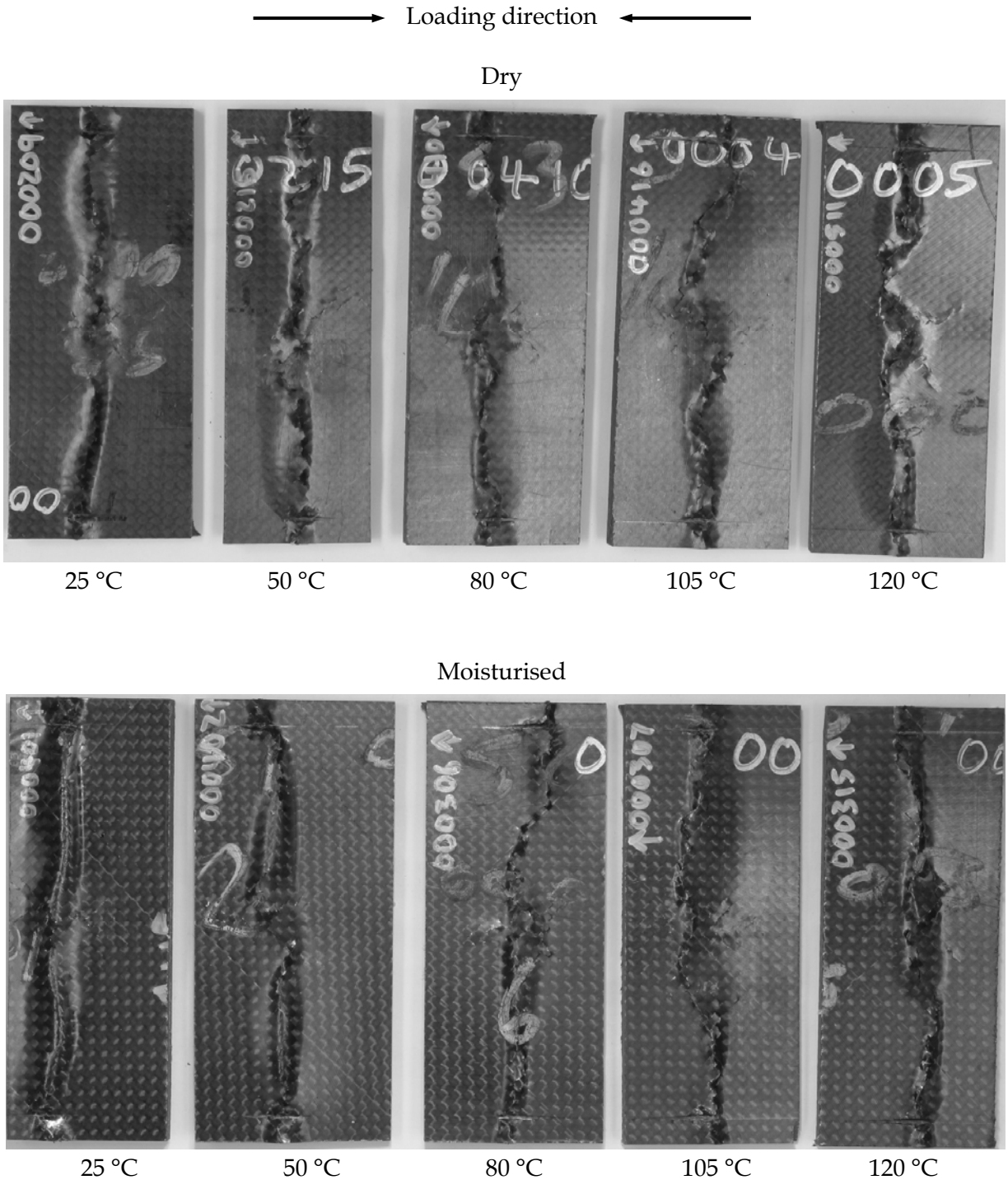

Figure 3-26: Representative failure regions on T650/PR500 CAI coupons

4. Discussion

4.1 Fibre volume fraction

The V_f for each of the AS4/3501-6 and T650/F584 prepregs was within 1 % of the average because the curing pressure (under vacuum bag in autoclave) was the same for all panels of each material.

There was a moderate difference in the V_f of the T650/PR500 coupons, from 48.9 vol. % for CAI up to 55.1 vol. % for OHC. This material was manufactured in a closed mould by RTM. Variability arose because the panels for each coupon type were made using different moulds. Only two or three panels were manufactured from each mould so the processing parameters, particularly the pressure of the press that closed the mould, were not optimised to obtain an exact V_f. More importantly, the conditions for each coupon type were the same, as was reflected by the small variation of V_f for coupons of each test type. The test results were not normalised to a standard V_f because the variability will not affect adversely the comparison of properties as the comparisons were performed separately for each test.

4.2 Glass transition temperature

The T_g quoted in Table 5 for the dry coupons were regarded as accurate. The T_g of the wet coupons would be lower than that reported because some drying of these coupons would have occurred during the DMTA run. This problem is inherent to T_g measurement in coupons containing absorbed moisture. Heating is required to determine the T_g, however this dries the coupon, artificially increasing T_g. The usual approach, and that used for these tests, was to use the same heating rate so that although the extent of the drying was not controlled all coupons were treated equally. This error may be a problem if equations relating ETD and ETW properties required an accurate measure of T_g.

Clearly the effect of moisture was substantial on the early generation 3501-6 resin system. The 53 °C fall brought wet T_g down to approximately the same level as the wet T_g of the second generation F584 resin, although the dry T_g of the latter was 26 °C lower. This difference can be partially explained by the difference in moisture absorption between the two systems. The T_g of AS4/3501-6 fell by 37 °C for every 1 wt % of absorbed moisture while the T_g of T650/F584 fell by 26 °C for every 1 wt % of moisture absorbed. The AS4/3501-6 absorbed 20 % more moisture than the T650/F584 and so the drop in T_g was correspondingly larger.

The more recently developed T650/PR500 was formulated for good retention of hot/wet properties [14]. It certainly absorbed substantially less moisture than the two other systems however this alone does not explain the much lower fall in T_g. Table 5 shows that T_g for this material fell by slightly less than 10 °C for every 1 wt % of moisture. The resin chemistry has been modified to both reduce moisture absorption and give an approximately three-fold increase in resistance to the plasticising effects of absorbed water when compared to previous generation epoxy resins.

4.3 Interlaminar shear

The shapes of the strength versus temperature plots for AS4/3501-6 and T650/PR500 in Figure 3-2 were not dissimilar. It is conceivable that ETW ILSS may be approximated from ETD ILSS on the basis of a fixed temperature difference. This is much more feasible for T650/PR500 than AS4/3501-6. The ETW knockdown (ETW strength/ETD strength at a particular temperature) for AS4/3501-6 ILSS at each test temperature was large. For example, assuming the data is linear then an ETW test at 77 °C would be simulated by an ETD test at 187 °C. Although this is still 22 °C below the T_g for dry AS4/3501-6, further testing would be required to verify that the ILSS behaviour remained linear at temperatures above 120 °C. Such tests were beyond the scope of this program.

There was a moderate divergence of the ETW and ETD curves for T650/F584 that would make such predictions prone to larger, but possibly not unacceptable, errors.

The similarity in appearance of the failed coupons supports the possibility of substituting ETW tests with ETD tests. However, as indicated previously, additional ETD tests would need to be conducted at temperatures up to 190 °C to verify that this remained the case.

In contrast with the hypothetical relation shown in Figure 1-1, Figure 3-2 showed that the ILSS knockdown at 25 °C for each material was 10 to 25 %. This behaviour has been reported previously [15]. It is possible that the difference in ETD and ETW strength may diminished at sub-ambient temperatures, however it appears that the effect of moisture on the composites is more complex than merely reducing T_g and bringing any test temperature closer to the resin T_g. The moisture may preferentially migrate to the fibre/resin interface and modify the fibre/resin bonding and/or fibre/resin interphase. Further work is required to establish the cause of this drop in properties.

Figure 3-2 was compared with the equivalent figure in reference [5]. The T300/914 and IM7/977-2 materials showed the same approximately linear behaviour, at approximately the same absolute ILSS, as the AS4/3501-6, T650/F584 and T650/PR500. The ETW knockdown for the T300/914 and IM7/977-2 was very low. This was attributed to a long delay between conditioning and testing and the conclusion that the moisture content in these ETW coupons was low.

4.4 ±45° tension

The τ-γ behaviour shown on Figure 3-4 is the classic behaviour for PMCs, an initially linear response followed by gradual softening to final failure. In the ±45° tension test the applied load is supported largely by the resin and the mechanical response of the composite will closely follow that of the resin. The shear stiffness and shear strength of the resin decreased with increasing temperature because of increased epoxy polymer chain mobility.

The effect of temperature and moisture content on ±45° tension strength is shown in Figure 3-5. There was a substantial difference between the materials. The relations for

T650/F584 and T650/PR500 were much closer to the parallel ILSS curves. The temperature knockdown was approximately 70 °C for T650/F584 and 15 °C for T650/PR500. These were similar to the behaviour of IM7/977-2, which had a temperature knockdown of 25 °C [5].

The data for AS4/3501-6 matched the classic plot that was illustrated in Figure 1-1. As shown in Figure 4-1 the ETW data was an excellent match for the model proposed by Chamis [16] and shown as Equation 2. However this was the only data from the present work that fitted this model. It is possible that, for the reasons described in the sixth paragraph of Section 4.6, the model may also fit reasonably the AS4/3501-6 CAI data. The very limited predictive capability of Equation 2 is not surprising given that it was an empirical curve fit of some properties of first generation epoxy composites reported in the mid 1970's. It is clear that factors in addition to the temperature difference between the test and T_g must be considered when predicting hygrothermal composite properties.

$$\frac{P_{ETW}}{P_{RTD}} \approx \sqrt{\frac{T_{gw} - T}{T_{gw} - T_{RT}}} \tag{2}$$

Where:

P_{ETW} = Resin mechanical property in the ETW condition
P_{RTD} = Resin mechanical property in the room temperature dry (RTD) condition
T_{gw} = T_g of the wet material (K)
T = Test temperature (K)
T_{RT} = 298 K

Fractography showed splits in the surface plies along the full gauge length of AS4/3501-6 coupons tested at low temperature. These became less visible and more confined to the

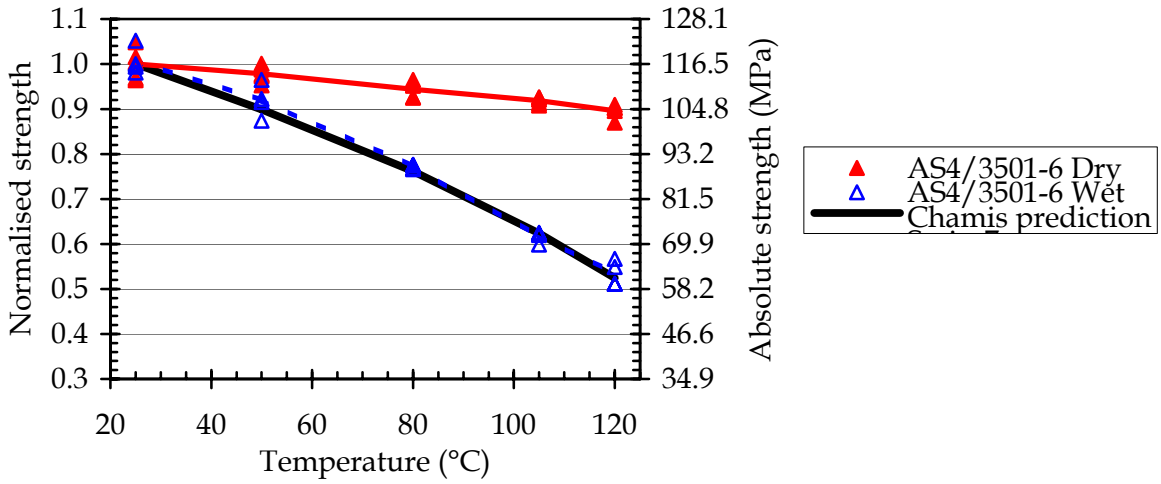

Figure 4-1: Normalised and absolute ILSS for AS4/3501-6 with predicted ETW from Equation 2

final failure region as test temperature and moisture content rose. The presence of, and variations in, splitting occurred because the coupons were manufactured from unidirectional tape. At low temperature the resin had sufficient strength to redistribute loads around split surface plies, leading to splitting along the entire gauge length. As temperature rose and the strength of the resin fell, the load that could be transferred was reduced. If splitting occurred in one location it was less likely that the loads would be redistributed to adjacent surface plies because the stiffness and strength of the resin was too low to redistribute effectively this load. In contrast the T650/F584 and T650/PR500 were manufactured from a woven fabric. At elevated temperatures and in the wet condition the reduced matrix stiffness and strength allowed for easier scissoring of the fabric (where the angle between the 0° and 90° fibre tows decreased). In this situation the softer the matrix then the more extensive the deformation.

The failure features were a function of both temperature and moisture content. For example Figure 3-5 shows that for T650/F584 the 50 °C ETW strength was approximately the same as that for the 105 °C ETD condition and for T650/PR500 the 80 °C ETW test gave approximately the same strength as the 105 °C ETD test. The failure appearance of the two T650/F584 examples (Figure 3-7) were reasonably similar, but not so the T650/PR500 (Figure 3-8). These changes make it more difficult to justify substituting ETW test with ETW tests.

4.5 Open hole compression

The approximately linear σ-ε plots shown in Figure 3-9 were expected. The load in compression tests with more than 10 % or so of fibres oriented in the loading direction is supported by those fibres. The initial mechanical response of the composite at different temperatures and moisture contents will be very similar because the environment does not affect the fibres. The elastic modulus of each material remained approximately constant for all tests (45-50 GPa for AS4/3501-6 and 40-45 GPa for T650/F584 and T650/PR500). Stiffness is controlled largely by the waviness of the load bearing fibres. The AS4/3501-6 laminates were stiffer because they were fabricated from unidirectional tape, whereas the T650 fibres were in the form of a plain woven fabric with fibres that undulated about the 0° direction.

Failure in compression is caused by microbuckling of the load bearing fibres. The load at which buckling occurred is controlled by fibre waviness, matrix stiffness and matrix yield strength in the presence of fibres. Thus, as the resins softened and weakened due to increasing temperature and moisture content, then compression strength fell.

The trends in strain-to-failure for the materials followed closely those for strength because of the approximately linear σ-ε behaviour.

Figure 3-11 showed that strength fell with increasing temperature and moisture content, with no apparently consistent relation between ETW and ETD strength. The knockdown appeared to be linearly expanding for AS4/3501-6, non-linear expanding for T650/F584 and fixed for the T650/PR500. Clearly accurate prediction of ETW properties on the basis

of ETD data requires models to account for more than just the depression in T_g. Establishing such models was beyond the scope of this program.

Fractography showed that all coupons failed by microbuckling in the ligament between the edge of the hole and the nearest coupon edge. In addition there was no difference in the appearance of each material regardless of temperature and moisture content. This indicates that the failure mechanism did not change. Any failure model would need only to establish the appropriate parameters to predict the onset of unstable microbuckling. As stated in the previous paragraph, this was outside to scope of this program.

Figure 3-11 was compared with the equivalent figure in reference [5]. The OHC strength of T300/914 and IM7/977-2 was significantly higher. Recalculating the strength of AS4/3501-6, T650/F584 and T650/PR500 using net section stress, rather than gross section stress, increased strength by approximately 17 % and largely addressed this discrepancy. As with the ILS and ±45° tension results, the ETW knockdown was substantially larger in Figure 3-11 (10 to 30 %) than reference [5] (less than 5 %). The former is consistent with the literature and suggests that the T300/914 and IM7/977-2 coupons were not fully moisturised during testing.

Figure 3-12 supports the concerns regarding moisture loss that were made in Section 2.2, and the measures taken to ameliorate it. It was found that the moisture content of AS4/3501-6 and T650/F584 coupons tested at 120 °C was approximately 0.2 wt % lower than at 25 °C. This demonstrates the very high diffusion rates at elevated temperature and that without the measures taken in this work the moisture loss may well have been higher.

The relatively rapid loss of moisture, remembering that the OHC coupons were only in the ETW environment for five minutes and CAI coupons for twelve minutes, also highlights that assuming a uniform distribution of moisture through a real structure (the end-of-life condition), and going to significant effort to maintain the full equilibrium moisture level during testing, will be very conservative. It is unlikely that a military aircraft will experience both high loads and the maximum operating temperature simultaneously. High loads are expected during combat manoeuvres, however this typically occurs well after take off, perhaps after a high speed transit where composite materials have had an opportunity to warm and dry. MOL conditions are expected when the aircraft is left on the ground in the sun or during high-speed flight. In both of these cases the applied loads are relatively low.

Results for the T300J/DA508 coupons must be treated with caution. The modulus increased by 10 % from 25 °C to 50 °C then remained constant for the remaining tests. The drop in OHC strength with increasing temperature was very low, at 120 °C it was still approximately 95 % of the 25 °C strength. Commensurate with a linear σ-ε behaviour, the trends in strain-to-failure followed those of strength and remained close to the 25 °C value for all tests. This was in contrast to the results for the other materials and tests shown in this report and reference [5], where modulus remained approximately constant and strength fell substantially with elevated temperature.

A likely explanation for the strength retention was that the T300J/DA508 coupons were overheated during the lower temperature tests. These coupons were tested in order from 120 °C then 105 °C then 80 °C and finally 50 °C, with only a few minutes break between tests at each temperature. While the environment within the chamber may have fallen rapidly and equilibrated at the lower test temperature, it is possible that the relatively massive anti-buckling guides retained much of their heat. Thus the 120 °C test result could be considered accurate while the lower temperature values may be considered as artificially depressed. This hypothesis is supported by the observation that the average net strength of T300J/DA508 was 327 MPa at 120 °C. Comparable with the equivalent values for T300/914 and IM7/977-2 of 395 and 332 MPa respectively [5]. However the strength of T300J/DA508 at lower temperatures was substantially below the equivalent strengths of these materials.

This explanation does not however account for the results of the 25 °C tests on T300J/DA508. The tests at this temperature were conducted on the following day, by which time the temperature of the test fixtures had certainly fallen to ambient laboratory temperature. No satisfactory explanation was found for the relatively low modulus and strength measured for T300J/DA508 at 25 °C.

4.6 Compression after impact

The impact damage area data from Appendix E was averaged and is shown in Table 6. It shows that the area on AS4/3501-6 coupons was substantially larger and more variable than that in T650/F584 and T650/PR500 coupons. A number of factors contribute to this difference, two of which are presented briefly. The first is the flatness of the fracture face. The inter-ply regions are very smooth, straight and flat in tape laminates. In fabrics this region is undulating within each fabric ply and even more so between adjacent plies because of fibre nesting. The second major factor is that the wavy fibres in fabrics can accommodate more straightening without transmitting loads through to regions remote from the impact site, through mechanisms such as plastic tow straightening [17].

Table 6 also shows that the area and variability of dry coupons tended to be larger than the wet material. T650/PR500 did not follow this trend but the difference was small. This variability indicated that absorbed moisture influenced the extent of impact damage in a more complex way than merely plasticising the resin. This supports further this assertion made in Section 4.5.

Table 6: Summary of impact damage area data from Appendix E

Material	Dry		Wet	
	Damage area (mm^2)	Coefficient of variance (%)	Damage area (mm^2)	Coefficient of variance (%)
AS4/3501-6	2559	30.9	1515	30.7
T650/F584	724	8.8	643	7.4
T650/PR500	560	12.0	602	10.4

As with the OHC tests, the shape of the σ-ε plots were dictated by the load bearing 0° fibres and failure was initiated when the matrix yielded and allowed microbuckling of the load bearing fibres. The modulus of each material was relatively constant for all tests and the strain-to-failure followed the same trends as the strength.

The behaviour of AS4/3501-6, as shown in Figure 3-22, was unlike that of this material in the ILS, ±45° tension and OHC tests. The CAI strength of the dry material showed very little drop with temperature, 134 MPa @ 25 °C and 129 MPa @ 120 °C. The magnitude of the test results appear reasonable because the CAI strain-to-failure was approximately 3000 με, which is close to that used as the design allowable for this material. It is unlikely that this effect was caused by variable damage area because the average damage area actually increased marginally from 25 to 105 °C.

Evidence that this data was valid, and not caused by poor experimental technique, was gained from the CAI results presented in reference [5]. The CAI strength of dry IM7/977-2 impacted with 31 J was 200 MPa @ 25 °C and 190 MPa @ 120 °C, a fall that was comparable to the AS4/3501-6. Possibly the CAI strength is so low at 25 °C that even reducing resin stiffness and strength has little effect on CAI behaviour.

The ETW CAI strength of AS4/3501-6 was mostly higher than the ETD CAI strength. This was most likely due to the much larger damage area on wet coupons. Average area was 2559 mm^2 for dry and 1515 mm^2 for wet coupons. The effects of this reduced damage area may be quantified by assuming the impact damage acted as an open hole. Models that predict the strength of composite laminates in the presence of open holes, such as Whitney and Nuismer's point and average stress criteria, could be used to predict the strength of the ETW coupons with the same damage area as the ETD coupons. Such analysis is beyond the scope of this program.

Behaviour of T650/F584 and T650/PR500 was consistent with that observed in the ILS, ±45° tension and OHC tests. CAI strength fell with increasing temperature and moisture content. There was a relatively large difference in the ETW knockdown for T650/F584 and a very small knockdown for T650/PR500. The ETW knockdown varied and certainly could not be predicted on the basis of ETD strength and T_g alone.

Figure 3-23 shows that the moisture losses measured in the CAI coupons were similar to those from the OHC testing. The AS4/3501-6 and T650/F584 each lost 0.2 wt % moisture. In contrast with the OHC tests even the T650/PR500 CAI coupons lost 0.1 wt % moisture at 120 °C. In all cases the moisture loss was an approximately linear function of test temperature. It was surprising that the large exposed face and extended soak time in the dry air did not increase substantially the amount of moisture lost from the CAI coupons at higher temperatures.

As with the OHC coupons, failure occurred by microbuckling. Although the appearance of the microbuckles was different on AS4/3501-6 (Figure 3-24) and T650/PR500 (Figure 3-25), moisture or temperature did not affect the failure morphology of each material. Thus changing failure features would not be a reason to prevent ETD tests being used to simulate ETW tests for these materials.

In contrast the T650/F584 showed distinct differences between the ETD and ETW coupons The ETW surface was dull and powdery, and there was easily pull-out of fibres when cutting. This suggests that the moisture had reduced substantially the bond between the resin and fibre. While this did not appear to change the failure mechanism, which was still fibre microbuckling in both the ETD and ETW cases, the changed behaviour would need to be accounted for if ETW testing were to be substituted by ETD testing.

The dull appearance of wet T650/F584 CAI coupons was not observed to anywhere near the same extent on the ILS, ±45° tension and OHC coupons. The most likely explanation for this difference is that the fibre/resin bond was weakened equally on those coupons, however the shock loading from the impact strike caused extensive fibre/resin disbonding in the CAI coupons. This facilitated easier cracking of the resin during testing.

5. Conclusions

The effect of temperature and moisture on the resin dominated properties of three aerospace grade composites was determined. It was found that there was no simple relation between properties in the ETD and ETW condition.

Apart from the general trend of strength falling with increasing temperature and moisture content there was no consistent relation between the ETW and ETD behaviour. Both the ratio of ETD/ETW strength and the temperature difference required for equivalent ETD and ETW strengths depended on the material and type of test. The most consistent case was the T650/PR500, where the ETW strength was ≈0.9 of the ETD strength for most test types.

The analysis described in this paper has shown conclusively that the relationship between ETD and ETW strength depended on material and test type. ETW strength of the materials tested in this work could not be predicted on the basis of ETD strength and T_g alone. It is possible that ETW behaviour can be predicted but this would require additional parameters, the identification of which were beyond the scope of this program.

6. Acknowledgements

This was a large program and it would not have been possible to complete the work without the assistance of many others. The author is very grateful to the following for their contribution to the indicated area:

Program set-up Roger Vodicka, Alan Baker, Richard Chester

French Counterparts	Christine Deschemin (CEAT), Thiery Ansart (CEAT)
Specimen manufacture	Peter Haggart, Marilyn Anderson, Mick Crossthwaite, Ken Houghton (Cooperative Research Centre for Advanced Composite Structures, CRC-ACS) and John van den Berg.
Testing	Sharlene Vella and Brett Nelson (University of New South Wales), Anthony Walley, Soon Aik Gan, Bruce Crosbie, David Parslow
C-scanning	Chris Howe
Fractography	Eva Kowal, Noel Goldsmith, Robert Pell and Peter Mazeika

References

1 Federal Aviation Administration, "Composite aircraft structure", Advisory Circular No: 20-107A, U.S. Department of Transportation, April 1984, 11 pp.

2 Department of Defense, "Composite materials handbook", MIL-HDBK-17F, Volume 1, Polymer matrix composites, Guidelines for characterization of structural materials, Document Automation and Production Service (DAPS), Bldg 4D, (DODSSP/ASSIST), 700 Robbins Ave, Philadelphia, PA, 19111-5094, 17 June 2002, 585 pp.

3 T.A. Collings, R.J. Harvey, A.W. Dalziel, "The use of elevated temperature in the structural testing of FRP components for simulating the effects of hot and wet environmental exposure", Composites, 24(8), 1993, pp. 625-634.

4 Department of Defence, "New certification procedures for composite materials", Technical Arrangement between Minister for Defence of Australia and the Minister of Defence of the French Republic TA 1/99, 12 February, 1999, 9 pp.

5 Deschemin, C., "New certification procedures for composite materials (TA 1/99), Work Package 1 : Study of the equivalence of hot/dry and hot/wet testing", S – 99/5148000/P2/A, Centre d'Essais Aéronatique de Toulouse (CEAT), 47 rue Saint-Jean, BP 23 – 31131, Balma, Cedex, France, 13 May 2003, 29 pp.

6 Callus, P., "Fatigue and Fracture Laboratory: SACMA SRM 2R 94 compression after impact (CAI) tests", Work Instruction AVD-SMTC-W212 Issue 2, Defence Science and Technology Organisation, Platforms Sciences Laboratory, Air Vehicles Division, Structures and Materials Test Centre, PO Box 4331, Melbourne, Victoria, 3001, Australia, 30 November 2004, 27 pp.

7 3M Product data, Scotchply PR500 Epoxy Resin, Issue No. 2, 1 April, 1990.

8 American Society for Testing and Materials, "Standard test method for short-beam shear strength of polymer matrix composite materials and their laminates", ASTM D 2344/D 2344M-00, ASTM, PO Box C700, West Conshohocken, PA, 19428-2959, USA, June 2000, 8 pp.

9 American Society for Testing and Materials, "Standard test method for in-plane shear response of polymer matrix composite materials by tensile test of a ±45° laminate", ASTM D 3518/D 3518M-94, ASTM, PO Box C700, West Conshohocken, PA, 19428-2959, USA, January 1995, 7 pp.

10 Suppliers of Advanced Composite Materials Association, "SACMA Recommended test method, Open-hole compression properties of oriented fiber-resin composites", Recommended Method SRM 3R-94, 1994, 10 pp.
11 Callus, P., "Fatigue and Fracture Laboratory: SACMA SRM 3R 94 open hole compression (OHC) tests", Work Instruction AVD-ASTL-W211 Issue 3, Defence Science and Technology Organisation, Platforms Sciences Laboratory, Air Vehicles Division, Structures and Materials Test Centre, PO Box 4331, Melbourne, Victoria, 3001, Australia, 11 August 2003, 35 pp.
12 Suppliers of Advanced Composite Materials Association, "SACMA Recommended test method, Compression after impact properties of oriented fiber-resin composites", Recommended Method SRM 2R-94, 1994, 11 pp.
13 Callus, P., "Fatigue and Fracture Laboratory: Operation of the drop weight impact test system", Work Instruction AVD-SMTC-W210 Issue 4, Defence Science and Technology Organisation, Platforms Sciences Laboratory, Air Vehicles Division, Structures and Materials Test Centre, PO Box 4331, Melbourne, Victoria, 3001, Australia, 30 November 2004, 17 pp.
14 3M Product data, Scotchply PR500 Epoxy Resin, Issue No. 2, 1 April, 1990.
15 OM K. Joshi, "The effect of moisture on the shear properties of carbon fibre composites", Composites, 14(3), July 1983, pp 196-200.
16 C.C. Chamis, R.F. Lark and J.H. Sinclair, "Integrated theory for predicting the hygrothermomechanical response of advanced structural composites", Advanced Composite Materials-Environmental Effects, ASTM STP 658, J. R. Vinson, Ed., American Society for Testing and Materials, 1978, pp. 160-192.
17 Cox, B.N., Dadkhah, M.S. and Morris, W.L., 'On the tensile failure of 3D woven composites', Composites: Part A, Volume 27A, Number 6, 1996, pp. 447-458.

Appendix A: Glass transition temperature data

The T_g (max tan δ) for the triplicate specimens that were tested is shown in Table A.1.

Table A.1: T_g for individual coupons

Material	Condition	T_g (°C) of indicated coupon			
		1	2	3	Average
AS4/3501-6	Dry	208.87	209.74	208.40	209.00
	Wet	153.10	154.07	159.37	155.51
T650/F584	Dry	183.41	183.74	182.73	183.29
	Wet	149.39	148.41	156.81	151.54
T650/PR500	Dry	199.07	199.06	191.91	196.68
	Wet	198.08	187.45	188.07	191.20

Appendix B: Interlaminar shear data

The dimensions, maximum load, absolute and normalised ILSS data are shown in Table B.1 to Table B.3.

Table B.1: Summary of ILS data for AS4/3501-6

Temp (°C)	Dry							Wet						
	Specn	Width (mm)	Thick. (mm)	Vf (%)	Pmax (kN)	ILSS (MPa)	Normalised	Specn	Width (mm)	Thick. (mm)	Vf (%)	Pmax (kN)	ILSS (MPa)	Normalised
25	25-1-2	6.350	2.340	57.6	2.101	106.0	0.983	A1	9.91	2.52	53.5	2.760	82.9	0.769
25	25-2	6.365	2.415	55.8	2.311	113.0	1.048	A2	9.90	2.50	53.9	2.350	71.2	0.660
25	25-3	6.370	2.405	56.1	2.056	101.0	0.936	A3	9.93	2.52	53.5	2.650	79.4	0.736
25	25-4	6.360	2.385	56.5	2.112	104.0	0.964	A4	9.92	2.52	53.5	2.700	81.0	0.751
25	25-5	6.350	2.375	56.8	2.246	112.0	1.038	A5	9.98	2.53	53.3	2.850	84.7	0.785
25	25-6	6.355	2.405	56.1	2.274	112.0	1.038	-	-	-	-	-	-	-
25	25-7	6.355	2.470	54.6	2.243	107.0	0.992	-	-	-	-	-	-	-
50	50-1	6.365	2.390	56.4	1.959	96.6	0.896	A6	9.94	2.52	53.5	2.120	63.5	0.589
50	50-2	6.370	2.310	58.4	1.809	92.2	0.855	A7	9.91	2.50	53.9	2.310	69.9	0.648
50	50-3	6.355	2.315	58.2	1.869	95.3	0.884	A8	9.92	2.50	53.9	2.000	60.5	0.561
50	50-4	6.350	2.350	57.4	2.061	104.0	0.964	A9	9.96	2.50	53.9	2.340	70.5	0.653
50	50-5	6.360	2.325	58.0	1.836	93.1	0.863	A10	9.92	2.48	54.4	1.940	59.1	0.548
50	50-6	6.370	2.340	57.6	1.918	96.5	0.895	-	-	-	-	-	-	-
50	50-7	6.400	2.415	55.8	2.215	107.0	0.992	-	-	-	-	-	-	-
50	50-8	6.370	2.330	57.9	1.933	97.7	0.906	-	-	-	-	-	-	-
80	80-1	6.350	2.410	55.9	1.826	89.5	0.830	A11	9.93	2.46	54.8	1.720	52.8	0.490
80	80-2	6.360	2.335	57.7	1.574	79.5	0.737	A12	9.91	2.59	52.1	1.960	57.3	0.531
80	80-3	6.365	2.310	58.4	1.747	89.1	0.826	A13	9.72	2.51	53.7	1.840	56.6	0.524
80	80-4	6.355	2.440	55.3	1.896	91.7	0.850	A14	9.78	2.52	53.5	1.870	56.9	0.528
80	80-5	6.365	2.335	57.7	1.653	83.4	0.773	A15	9.84	2.59	52.1	1.920	56.5	0.524
80	80-6	6.355	2.340	57.6	1.824	92.0	0.853	-	-	-	-	-	-	-
80	80-7	6.360	2.400	56.2	1.885	92.6	0.859	-	-	-	-	-	-	-
80	80-8	6.365	2.420	55.7	1.738	84.6	0.784	-	-	-	-	-	-	-
105	105-1	6.360	2.385	56.5	1.612	79.7	0.739	A16	9.75	2.52	53.5	1.460	44.6	0.413
105	105-2	6.360	2.390	56.4	1.669	82.4	0.764	A17	9.76	2.61	51.7	1.450	42.7	0.396
105	105-3	6.370	2.400	56.2	1.710	83.9	0.778	A18	9.83	2.54	53.1	1.480	44.5	0.412
105	105-4	6.360	2.430	55.5	1.793	87.0	0.807	A19	9.91	2.52	53.5	1.420	42.6	0.395
105	105-5	6.320	2.420	55.7	1.784	87.5	0.811	A20	9.94	2.47	54.6	1.400	42.8	0.397
120	120-1	6.350	2.330	57.9	1.441	73.0	0.677	A21	9.60	2.59	52.1	1.300	39.2	0.364
120	120-2	6.360	2.450	55.0	1.444	69.5	0.644	A22	9.82	2.53	53.3	-	-	-
120	120-3	6.360	2.440	55.3	1.567	75.7	0.702	A23	9.96	2.61	51.7	-	-	-
120	120-4	6.350	2.320	58.1	1.612	82.1	0.761	A24	10.01	2.52	53.5	-	-	-
120	120-5	6.360	2.325	58.0	1.667	84.6	0.784	A25	9.86	2.54	53.1	-	-	-
120	120-6	6.360	2.455	54.9	1.661	79.8	0.740	-	-	-	-	-	-	-
120	120-7	6.355	2.400	56.2	1.580	77.7	0.720	-	-	-	-	-	-	-
120	120-8	6.355	2.400	56.2	1.475	72.5	0.672	-	-	-	-	-	-	-
Average														
25		6.358	2.399	56.2	2.192	107.9	1.000		9.93	2.52	53.5	2.662	79.8	0.740
50		6.368	2.347	57.5	1.950	97.8	0.907		9.93	2.50	53.9	2.142	64.7	0.600
80		6.359	2.374	56.8	1.768	87.8	0.814		9.84	2.53	53.2	1.862	56.0	0.519
105		6.354	2.405	56.1	1.714	84.1	0.780		9.84	2.53	53.3	1.442	43.4	0.403
120		6.356	2.390	56.4	1.556	76.9	0.713		9.85	2.56	52.7	1.300	39.2	0.364
Standard Deviation														
25		0.008	0.040	0.9	0.099	4.6	0.043		0.03	0.01	0.23	0.190	5.2	0.048
50		0.015	0.037	0.9	0.133	5.2	0.048		0.02	0.01	0.31	0.179	5.3	0.049
80		0.006	0.049	1.2	0.113	4.8	0.044		0.09	0.06	1.18	0.092	1.8	0.017
105		0.019	0.019	0.5	0.077	3.3	0.030		0.09	0.05	1.06	0.032	1.0	0.009
120		0.004	0.058	1.4	0.092	5.2	0.048		0.16	0.04	0.81	#####	#####	#####
Coefficient of Variance (%)														
25		0.1	1.7	1.7	4.5	4.3	4.3		0.3	0.4	0.4	7.1	6.5	6.5
50		0.2	1.6	1.6	6.8	5.3	5.3		0.2	0.6	0.6	8.4	8.1	8.1
80		0.1	2.1	2.1	6.4	5.4	5.4		0.9	2.2	2.2	4.9	3.2	3.2
105		0.3	0.8	0.8	4.5	3.9	3.9		0.9	2.0	2.0	2.2	2.3	2.3
120		0.1	2.4	2.4	5.9	6.7	6.7		1.6	1.5	1.5	#####	#####	#####

Table B.2: Summary of ILS data for T650/F584

Temp (°C)	Dry							Wet						
	Specn	Width (mm)	Thick. (mm)	Vf (%)	Pmax (kN)	ILSS (MPa)	Normalised	Specn	Width (mm)	Thick. (mm)	Vf (%)	Pmax (kN)	ILSS (MPa)	Normalised
25	W1	9.86	2.52	51.9	2.850	86.0	1.039	D1	9.97	2.51	52.1	2.370	71.0	0.858
25	W2	9.97	2.43	53.8	2.630	81.4	0.983	D2	9.91	2.51	52.1	2.460	74.2	0.896
25	W3	10.05	2.47	53.0	2.610	78.9	0.952	D3	9.97	2.51	52.1	2.410	72.2	0.872
25	W4	9.96	2.52	51.9	2.780	83.1	1.003	D4	9.96	2.40	54.5	2.310	72.5	0.875
25	W5	9.93	2.57	50.9	2.880	84.6	1.022	D5	9.98	2.57	50.9	2.440	71.3	0.862
50	W6	9.93	2.55	51.3	2.700	80.0	0.966	D6	9.98	2.57	50.9	2.310	67.5	0.816
50	W7	9.94	2.41	54.3	2.320	72.6	0.877	D7	9.94	2.52	51.9	2.250	67.4	0.814
50	W8	9.97	2.50	52.3	2.440	73.4	0.887	D8	9.95	2.56	51.1	2.220	65.4	0.789
50	W9	9.94	2.55	51.3	2.760	81.7	0.986	D9	10.00	2.46	53.2	2.100	64.0	0.773
50	W10	9.77	2.50	52.3	2.480	76.2	0.920	D10	9.88	2.43	53.8	2.050	64.0	0.773
80	W11	10.02	2.51	52.1	2.340	69.8	0.843	D11	9.92	2.52	51.9	1.780	53.4	0.645
80	W12	10.00	2.52	51.9	2.360	70.2	0.848	D12	9.96	2.59	50.5	1.650	48.0	0.579
80	W13	9.95	2.51	52.1	2.280	68.5	0.827	D13	9.93	2.58	50.7	1.750	51.2	0.619
80	W14	9.81	2.50	52.3	2.330	71.3	0.861	D14	9.96	2.55	51.3	1.780	52.6	0.635
80	W15	9.98	2.45	53.4	2.200	67.5	0.815	D15	9.96	2.44	53.6	1.700	52.5	0.634
105	W16	9.97	2.49	52.5	1.990	60.1	0.726	D16	10.00	2.54	51.5	1.280	37.8	0.456
105	W17	9.94	2.53	51.7	2.030	60.5	0.731	D17	9.99	2.58	50.7	1.280	37.2	0.450
105	W18	9.89	2.54	51.5	2.000	59.7	0.721	D18	9.99	2.52	51.9	1.240	36.9	0.446
105	W19	9.83	2.47	53.0	1.900	58.7	0.709	D19	9.97	2.58	50.7	1.170	34.1	0.412
105	W20	9.86	2.45	53.4	1.900	59.0	0.712	D20	10.00	2.58	50.7	1.320	38.4	0.463
120	W21	10.04	2.42	54.1	1.670	51.6	0.623	D21	9.89	2.52	51.9	1.160	34.9	0.422
120	W22	9.89	2.54	51.5	1.860	55.5	0.671	D22	10.00	2.58	50.7	-	-	-
120	W23	9.96	2.57	50.9	1.820	53.3	0.644	D23	9.96	2.54	51.5	-	-	-
120	W24	9.89	2.57	50.9	1.800	53.1	0.641	D24	9.96	2.54	51.5	-	-	-
120	W25	9.98	2.49	52.5	1.770	53.4	0.645	D25	9.91	2.54	51.5	-	-	-
Average														
25		9.95	2.50	52.3	2.750	82.8	1.000		9.96	2.50	52.4	2.398	72.3	0.873
50		9.91	2.50	52.3	2.540	76.8	0.927		9.95	2.51	52.2	2.186	65.7	0.793
80		9.95	2.50	52.4	2.302	69.4	0.839		9.95	2.54	51.6	1.732	51.5	0.622
105		9.90	2.50	52.4	1.964	59.6	0.720		9.99	2.56	51.1	1.258	36.9	0.446
120		9.95	2.52	52.0	1.784	53.4	0.645		9.94	2.54	51.4	1.160	34.9	0.422
Standard Deviation														
25		0.07	0.05	1.1	0.124	2.8	0.034		0.03	0.06	1.3	0.060	1.2	0.015
50		0.08	0.06	1.2	0.184	4.0	0.048		0.05	0.06	1.3	0.108	1.7	0.021
80		0.08	0.03	0.6	0.064	1.5	0.018		0.02	0.06	1.2	0.056	2.1	0.026
105		0.06	0.04	0.8	0.060	0.8	0.009		0.01	0.03	0.6	0.057	1.6	0.020
120		0.06	0.06	1.3	0.072	1.4	0.017		0.04	0.02	0.4	#####	#####	#####
Coefficient of Variance (%)														
25		0.7	2.1	2.1	4.5	3.4	3.4		0.3	2.5	2.5	2.5	1.7	1.7
50		0.8	2.3	2.3	7.3	5.2	5.2		0.5	2.4	2.5	4.9	2.6	2.6
80		0.8	1.1	1.1	2.8	2.1	2.1		0.2	2.4	2.4	3.3	4.1	4.1
105		0.6	1.5	1.5	3.1	1.3	1.3		0.1	1.1	1.1	4.5	4.5	4.5
120		0.6	2.5	2.6	4.0	2.7	2.7		0.4	0.9	0.9	#####	#####	#####

Table B.3: Summary of ILS data for T650/PR500

Temp (°C)	Dry							Wet						
	Specn	Width (mm)	Thick. (mm)	Vf (%)	Pmax (kN)	ILSS (MPa)	Normalised	Specn	Width (mm)	Thick. (mm)	Vf (%)	Pmax (kN)	ILSS (MPa)	Normalised
25	P1	9.94	2.52	51.1	2.400	71.9	0.990	25-1	10.40	2.37	54.4	2.050	62.4	0.859
25	P2	9.78	2.47	52.2	2.330	72.3	0.996	25-2	9.90	2.48	51.9	2.200	67.2	0.926
25	P3	10.00	2.48	51.9	2.400	72.6	1.000	25-3	10.16	2.38	54.1	2.000	62.0	0.854
25	P4	9.78	2.43	53.0	2.350	74.2	1.021	25-4	9.99	2.46	52.4	2.050	62.6	0.862
25	P5	9.94	2.46	52.4	2.350	72.1	0.993	25-5	10.26	2.42	53.2	2.300	69.5	0.957
50	P6	9.92	2.42	53.2	2.290	71.5	0.985	50-1	10.24	2.36	54.6	2.050	63.6	0.876
50	P7	9.90	2.51	51.3	2.300	69.4	0.956	50-2	10.21	2.38	54.1	2.050	63.3	0.871
50	P8	9.98	2.49	51.7	2.360	71.2	0.981	50-3	9.98	2.43	53.0	2.000	61.9	0.852
50	P9	9.80	2.42	53.2	2.140	67.7	0.932	50-4	10.23	2.39	53.9	2.150	66.0	0.908
50	P10	9.81	2.43	53.0	2.250	70.8	0.975	50-5	9.92	2.47	52.2	2.050	62.7	0.864
80	P11	10.02	2.45	52.6	2.070	63.2	0.871	80-1	10.25	2.40	53.7	2.000	61.0	0.840
80	P12	9.96	2.42	53.2	2.030	63.2	0.870	80-2	10.25	2.40	53.7	1.900	57.9	0.798
80	P13	9.94	2.51	51.3	2.160	64.9	0.894	80-3	10.16	2.38	54.1	1.900	58.9	0.812
80	P14	10.02	2.43	53.0	2.010	61.9	0.853	80-4	9.86	2.47	52.2	1.900	58.5	0.806
80	P15	9.97	2.49	51.7	2.110	63.7	0.878	80-5	10.19	2.40	53.7	1.950	59.8	0.824
105	P16	9.70	2.46	52.4	1.850	58.1	0.801	105-1	10.26	2.38	54.1	1.775	54.5	0.751
105	P17	9.85	2.49	51.7	1.890	57.8	0.796	105-2	10.15	2.43	53.0	1.695	51.5	0.710
105	P18	9.90	2.51	51.3	1.950	58.9	0.811	105-3	10.39	2.41	53.4	1.650	49.4	0.681
105	P19	9.82	2.44	52.8	1.850	57.9	0.798	105-4	10.12	2.41	53.4	1.650	50.7	0.699
105	P20	9.98	2.43	53.0	1.800	55.7	0.767	105-5	10.08	2.44	52.8	1.625	49.6	0.682
120	P21	9.96	2.42	53.2	1.810	56.3	0.776	120-1	10.13	2.44	52.8	1.490	45.2	0.623
120	P22	9.73	2.43	53.0	1.720	54.6	0.751	120-2	10.22	2.37	54.4	1.400	43.4	0.597
120	P23	9.94	2.51	51.3	1.810	54.4	0.749	120-3	10.24	2.50	51.5	1.510	44.2	0.609
120	P24	9.98	2.49	51.7	1.780	53.7	0.740	120-4	10.26	2.39	53.9	1.410	43.1	0.594
120	P25	9.92	2.43	53.0	1.700	52.9	0.728	120-5	10.01	2.42	53.2	1.415	43.8	0.603
Average														
25		9.89	2.47	52.1	2.4	72.6	1.000		10.14	2.42	53.2	2.120	64.7	0.892
50		9.88	2.45	52.5	2.3	70.1	0.966		10.12	2.41	53.6	2.060	63.5	0.874
80		9.98	2.46	52.4	2.1	63.4	0.873		10.14	2.41	53.5	1.930	59.2	0.816
105		9.85	2.47	52.2	1.9	57.7	0.794		10.20	2.41	53.4	1.679	51.2	0.705
120		9.91	2.46	52.5	1.8	54.4	0.749		10.17	2.42	53.2	1.445	43.9	0.605
Standard Deviation														
25		0.10	0.03	0.69	0.032	0.9	0.013		0.20	0.05	1.1	0.125	3.4	0.047
50		0.08	0.04	0.91	0.082	1.6	0.022		0.15	0.04	1.0	0.055	1.5	0.021
80		0.04	0.04	0.82	0.061	1.1	0.015		0.16	0.03	0.8	0.045	1.2	0.016
105		0.10	0.03	0.71	0.056	1.2	0.016		0.13	0.02	0.5	0.059	2.1	0.029
120		0.10	0.04	0.87	0.051	1.3	0.017		0.10	0.05	1.1	0.051	0.8	0.011
Coefficient of Variance (%)														
25		1.0	1.3	1.3	1.4	1.3	1.3		2.0	2.0	2.0	5.9	5.2	5.2
50		0.8	1.7	1.7	3.6	2.3	2.3		1.5	1.8	1.8	2.7	2.4	2.4
80		0.4	1.6	1.6	2.9	1.7	1.7		1.6	1.4	1.4	2.3	2.0	2.0
105		1.1	1.4	1.4	3.0	2.1	2.1		1.2	1.0	1.0	3.5	4.1	4.1
120		1.0	1.7	1.7	2.9	2.3	2.3		1.0	2.1	2.1	3.5	1.9	1.9

Appendix C: ±45° tension data

The dimensions, maximum load, absolute and normalised ±45° tension data are shown in Table C.1 to Table C.3.

Table C.1: Summary of ±45° tension data for AS4/3501-6

Temp (°C)	Dry							Wet						
	Specn	Ave Width (mm)	Ave Thick. (mm)	Vf (vol. %)	Pmax (kN)	±45° Strength (MPa)	Normalised	Specn	Ave Width (mm)	Ave Thick. (mm)	Vf (vol. %)	Pmax (kN)	±45° Strength (MPa)	Normalised
25	25-1	24.95	2.502	53.9	14.600	116.9	1.004	A1	25.13	2.373	56.8	13.818	115.8	0.994
25	25-2	25.07	2.457	54.9	13.900	112.8	0.968	A2	25.17	2.417	55.8	13.906	114.3	0.981
25	25-3	24.96	2.497	54.0	15.200	122.1	1.048	A3	25.24	2.403	56.1	14.854	122.5	1.052
25	25-4	25.08	2.487	54.2	14.000	112.3	0.964	A4	25.12	2.407	56.0	14.092	116.5	1.000
25	25-5	25.05	2.517	53.6	14.900	118.3	1.016	-	-	-	-	-	-	-
50	50-1	25.07	2.468	54.6	14.000	113.4	0.974	W1	25.17	2.360	57.1	12.764	107.4	0.922
50	50-2	25.02	2.492	54.1	14.200	113.8	0.977	W2	25.16	2.557	52.7	13.096	101.8	0.874
50	50-3	25.12	2.497	54.0	13.900	110.9	0.952	W3	25.04	2.323	58.0	13.076	112.4	0.965
50	50-4	25.05	2.508	53.8	14.500	115.0	0.988	W4	25.12	2.423	55.6	12.988	106.7	0.916
50	50-5	25.09	2.470	54.6	14.400	116.6	1.001	-	-	-	-	-	-	-
80	80-1	25.15	2.533	53.2	13.700	107.8	0.925	W5	25.22	2.420	55.7	10.898	89.2	0.766
80	80-2	25.07	2.462	54.8	13.900	112.3	0.964	W6	25.24	2.380	56.7	10.850	90.4	0.776
80	80-3	25.04	2.497	54.0	13.900	110.9	0.952	W7	25.25	2.320	58.1	10.596	90.3	0.775
80	80-4	25.12	2.455	54.9	13.700	111.0	0.953	W8	25.15	2.340	57.6	10.528	89.6	0.769
80	80-5	24.99	2.507	53.8	13.500	107.9	0.926	-	-	-	-	-	-	-
105	105-1	25.05	2.455	54.9	13.000	105.7	0.908	W9	25.24	2.353	57.3	8.640	72.8	0.625
105	105-2	25.09	2.502	53.9	13.500	107.9	0.926	W10	25.00	2.383	56.6	8.300	69.7	0.598
105	105-3	25.03	2.500	53.9	13.400	107.3	0.921	W11	25.08	2.360	57.1	8.590	72.6	0.623
105	105-4	25.06	2.483	54.3	13.200	106.3	0.913	W12	25.02	2.343	57.5	8.470	72.2	0.620
105	105-5	25.04	2.505	53.8	13.500	107.8	0.925	-	-	-	-	-	-	-
120	120-1	25.07	2.487	54.2	12.600	101.3	0.870	W13	25.14	2.350	57.4	7.042	59.6	0.512
120	120-2	25.00	2.467	54.7	13.100	105.9	0.909	W14	25.11	2.383	56.6	7.138	59.6	0.512
120	120-3	25.08	2.468	54.6	12.900	104.4	0.896	W15	25.01	2.307	58.4	7.618	66.0	0.567
120	120-4	25.08	2.482	54.3	13.100	105.1	0.902	W16	25.12	2.347	57.4	7.530	63.9	0.549
120	120-5	25.04	2.452	55.0	12.900	105.2	0.903	-	-	-	-	-	-	-
Average														
25		25.02	2.492	54.1	14.520	116.5	1.000		25.17	2.400	56.2	14.168	117.3	1.007
50		25.07	2.487	54.2	14.200	113.9	0.978		25.12	2.416	55.9	12.981	107.1	0.919
80		25.07	2.491	54.1	13.740	110.0	0.944		25.22	2.365	57.0	10.718	89.9	0.772
105		25.05	2.489	54.2	13.320	107.0	0.919		25.09	2.360	57.1	8.500	71.8	0.617
120		25.05	2.471	54.6	12.920	104.4	0.896		25.09	2.347	57.5	7.332	62.3	0.535
Standard Deviation														
25		0.06	0.022	0.5	0.563	4.1	0.035		0.05	0.019	0.4	0.472	3.6	0.031
50		0.04	0.017	0.4	0.255	2.1	0.018		0.06	0.103	2.3	0.152	4.3	0.037
80		0.06	0.033	0.7	0.167	2.0	0.018		0.05	0.044	1.1	0.183	0.6	0.005
105		0.02	0.021	0.5	0.217	0.9	0.008		0.11	0.017	0.4	0.151	1.4	0.012
120		0.04	0.014	0.3	0.205	1.8	0.015		0.06	0.031	0.8	0.284	3.2	0.028
Coefficient of Variance (%)														
25		0.2	0.9	0.9	3.9	3.5	3.5		0.2	0.8	0.8	3.3	3.1	3.1
50		0.1	0.7	0.7	1.8	1.8	1.8		0.2	4.3	4.2	1.2	4.1	4.1
80		0.2	1.3	1.3	1.2	1.9	1.9		0.2	1.9	1.9	1.7	0.6	0.6
105		0.1	0.8	0.8	1.6	0.9	0.9		0.4	0.7	0.7	1.8	2.0	2.0
120		0.1	0.6	0.6	1.6	1.7	1.7		0.2	1.3	1.3	3.9	5.1	5.1

Table C.2: Summary of ±45° tension data for T650/F584

Temp (°C)	Dry							Wet						
	Specn	Ave Width (mm)	Ave Thick. (mm)	Vf (vol. %)	Pmax (kN)	±45° Strength (MPa)	Normalised	Specn	Ave Width (mm)	Ave Thick. (mm)	Vf (vol. %)	Pmax (kN)	±45° Strength (MPa)	Normalised
25	X3	25.04	2.663	49.1	16.202	121.5	0.984	X26	25.08	2.760	47.4	14.404	107.9	0.874
25	X4	24.77	2.613	50.1	15.948	123.2	0.998	X28	24.96	2.660	49.2	14.190	106.8	0.865
25	X8	24.91	2.587	50.6	15.684	121.7	0.986	Y2	24.94	2.717	48.2	14.130	104.3	0.844
25	X20	25.02	2.607	50.2	14.864	113.9	0.923	Y5	25.03	2.610	50.1	13.252	101.4	0.821
25	X25	24.72	2.310	56.6	15.654	137.0	1.110	Y6	25.09	2.627	49.8	13.458	102.1	0.827
50	X1	24.77	2.647	49.4	15.380	117.3	0.950	Y23	25.09	2.633	49.7	12.002	90.8	0.736
50	X10	25.02	2.620	49.9	12.519	95.5	0.773	Y22	25.08	2.640	49.6	11.700	88.3	0.716
50	X15	25.09	2.650	49.4	12.519	94.1	0.763	Y21	25.13	2.677	48.9	11.328	84.2	0.682
50	X17	24.99	2.617	50.0	12.519	95.5	0.773	Y20	25.10	2.703	48.4	11.456	84.4	0.684
50	X24	25.12	2.680	48.8	12.519	93.0	0.753	Y19	25.01	2.703	48.4	11.690	86.5	0.700
80	X2	24.93	2.663	49.1	13.838	104.2	0.844	Y14	24.97	2.670	49.0	9.844	73.8	0.598
80	X11	25.03	2.627	49.8	14.296	108.7	0.881	Y15	25.18	2.630	49.8	9.648	72.8	0.590
80	X18	25.02	2.653	49.3	13.486	101.6	0.823	Y16	25.07	2.657	49.2	9.776	73.4	0.594
80	X19	24.98	2.630	49.8	13.438	102.3	0.828	Y17	25.05	2.713	48.2	9.482	69.8	0.565
80	X23	25.16	2.063	63.4	13.096	100.0	0.810	Y18	24.99	2.730	47.9	9.268	67.9	0.550
105	X9	25.08	2.643	49.5	11.778	88.8	0.720	Y13	25.12	2.657	49.2	7.198	53.9	0.437
105	X12	25.06	2.640	49.6	12.958	97.9	0.793	Y12	25.03	2.673	49.0	7.216	53.9	0.437
105	X16	25.02	2.623	49.9	12.548	95.6	0.774	Y11	25.09	2.663	49.1	7.266	54.4	0.440
105	X21	24.99	2.667	49.1	11.290	84.7	0.686	Y10	25.08	2.637	49.6	7.256	54.9	0.444
105	X22	25.06	2.650	49.4	11.348	85.4	0.692	Y9	25.13	2.670	49.0	7.402	55.2	0.447
120	X5	24.94	2.630	49.8	9.970	76.0	0.616	Y8	25.03	2.677	48.9	7.402	55.2	0.447
120	X6	25.01	2.670	49.0	9.590	71.8	0.582	Y7	25.10	2.703	48.4	7.208	53.1	0.430
120	X7	24.96	2.613	50.1	9.932	76.1	0.617	Y4	25.13	2.720	48.1	7.294	53.3	0.432
120	X13	24.99	2.573	50.9	11.846	92.1	0.746	Y1	25.29	2.677	48.9	7.294	53.9	0.436
120	X14	25.35	2.567	51.0	11.640	90.6	0.734	X27	25.14	2.693	48.6	7.460	55.1	0.446
Average														
25		24.9	2.556	51.3	15.670	123.5	1.000		25.02	2.675	48.9	13.887	104.5	0.846
50		25.0	2.643	49.5	13.091	99.1	0.803		25.08	2.671	49.0	11.635	86.8	0.703
80		25.0	2.527	52.3	13.631	103.3	0.837		25.05	2.680	48.8	9.604	71.5	0.579
105		25.0	2.645	49.5	11.984	90.5	0.733		25.09	2.660	49.2	7.268	54.4	0.441
120		25.1	2.611	50.1	10.596	81.3	0.659		25.14	2.694	48.6	7.332	54.1	0.438
Standard Deviation														
25		0.14	0.140	3.0	0.503	8.4	0.068		0.07	0.063	1.1	0.501	2.9	0.023
50		0.14	0.026	0.5	1.279	10.2	0.083		0.04	0.033	0.6	0.259	2.8	0.023
80		0.09	0.260	6.2	0.455	3.4	0.027		0.08	0.041	0.7	0.233	2.6	0.021
105		0.04	0.016	0.3	0.741	6.0	0.048		0.04	0.014	0.3	0.080	0.6	0.005
120		0.17	0.043	0.8	1.060	9.3	0.076		0.10	0.018	0.3	0.099	1.0	0.008
Coefficient of Variance (%)														
25		0.6	5.5	5.9	3.2	6.8	6.8		0.3	2.3	2.3	3.6	2.7	2.7
50		0.6	1.0	1.0	9.8	10.3	10.3		0.2	1.3	1.3	2.2	3.2	3.2
80		0.3	10.3	11.9	3.3	3.3	3.3		0.3	1.5	1.5	2.4	3.6	3.6
105		0.1	0.6	0.6	6.2	6.6	6.6		0.2	0.5	0.5	1.1	1.0	1.0
120		0.7	1.6	1.6	10.0	11.5	11.5		0.4	0.7	0.7	1.4	1.8	1.8

Table C.3: Summary of ±45° tension data for T650/PR500

Temp (°C)	Dry							Wet						
	Specn	Ave Width (mm)	Ave Thick. (mm)	Vf (vol. %)	Pmax (kN)	±45° Strength (MPa)	Normalised	Specn	Ave Width (mm)	Ave Thick. (mm)	Vf (vol. %)	Pmax (kN)	±45° Strength (MPa)	Normalised
25	1A	25.06	2.383	54.1	16.064	134.5	0.940	1B	24.96	2.317	55.6	15.312	132.4	0.925
25	2F	25.10	2.460	52.4	16.718	135.4	0.946	1C	25.08	2.323	55.5	15.156	130.1	0.909
25	7A	25.04	2.450	52.6	19.620	159.9	1.117	1D	25.00	2.377	54.2	15.156	127.5	0.891
25	8E	25.13	2.447	52.6	17.548	142.7	0.997	2A	25.09	2.477	52.0	16.064	129.3	0.903
25	-	-	-	-	-	-	-	2B	25.05	2.413	53.4	15.996	132.3	0.924
50	3A	25.01	2.410	53.4	14.268	118.4	0.827	2C	25.14	2.427	53.1	14.200	116.4	0.813
50	3B	25.03	2.347	54.9	15.068	128.2	0.896	2E	25.00	2.367	54.4	14.014	118.3	0.827
50	5C	25.06	2.520	51.1	14.532	115.1	0.804	3E	25.09	2.433	52.9	14.278	116.9	0.817
50	6C	25.05	2.423	53.2	14.864	122.4	0.855	3F	25.27	2.337	55.1	14.170	120.0	0.838
50	-	-	-	-	-	-	-	4B	24.98	2.473	52.1	14.454	117.0	0.817
80	1E	25.01	2.350	54.8	12.558	106.8	0.747	4E	25.01	2.353	54.7	11.534	98.0	0.685
80	1F	25.01	2.390	53.9	12.304	102.9	0.719	5A	25.05	2.497	51.6	11.954	95.6	0.668
80	2D	24.96	2.417	53.3	13.106	108.7	0.759	5D	25.03	2.423	53.2	11.514	94.9	0.663
80	8F	25.05	2.430	53.0	13.984	114.8	0.802	5E	25.00	2.493	51.7	11.318	90.8	0.634
80	-	-	-	-	-	-	-	6A	24.98	2.427	53.1	11.456	94.5	0.660
105	4D	24.99	2.480	51.9	10.742	120.2	0.840	6B	25.08	2.380	54.1	9.590	80.3	0.561
105	5F	25.10	2.413	53.4	11.446	94.5	0.660	6D	24.98	2.467	52.2	9.296	75.4	0.527
105	6F	25.13	2.503	51.5	11.250	89.4	0.625	6E	25.04	2.407	53.5	9.542	79.2	0.553
105	7B	25.09	2.473	52.1	13.584	109.5	0.765	7C	25.10	2.433	52.9	12.324	100.4	0.702
105	-	-	-	-	-	-	-	7D	25.02	2.440	52.8	12.256	100.9	0.705
120	3C	25.02	2.330	55.3	8.868	76.1	0.532	7F	25.05	2.417	53.3	-	-	
120	3D	24.98	2.373	54.3	8.672	73.1	0.511	8A	25.09	2.450	52.6	10.556	85.9	0.600
120	5B	25.03	2.413	53.4	9.072	75.1	0.525	8B	24.95	2.500	51.5	9.600	77.8	0.544
120	7E	25.14	2.467	52.2	11.826	95.4	0.667	8C	25.03	2.520	51.1	10.498	83.2	0.581
120	-	-	-		-	-	-	8D	25.02	2.517	51.2	9.726	77.2	0.539
Average														
25		25.08	2.435	52.9	17.488	143.12	1.000		25.04	2.381	54.1	15.537	130.3	0.911
50		25.04	2.425	53.2	14.683	121.0	0.846		25.10	2.407	53.5	14.223	117.7	0.823
80		25.01	2.397	53.8	12.988	108.3	0.757		25.01	2.439	52.8	11.555	94.8	0.662
105		25.08	2.467	52.2	11.756	103.4	0.722		25.04	2.425	53.1	10.602	87.2	0.610
120		25.04	2.396	53.8	9.610	79.9	0.558		25.03	2.481	51.9	10.095	81.0	0.566
Standard Deviation														
25		0.03	0.035	0.8	1.546	11.8	0.082		0.06	0.067	1.5	0.455	2.1	0.015
50		0.02	0.072	1.6	0.354	5.7	0.040		0.12	0.055	1.2	0.161	1.5	0.010
80		0.04	0.035	0.8	0.744	5.0	0.035		0.03	0.059	1.3	0.238	2.6	0.018
105		0.06	0.038	0.8	1.255	14.1	0.098		0.05	0.033	0.7	1.546	12.4	0.086
120		0.07	0.058	1.3	1.487	10.4	0.073		0.05	0.045	1.0	0.502	4.2	0.029
Coefficient of Variance (%)														
25		0.1	1.4	1.5	8.8	8.2	8.2		0.2	2.8	2.8	2.9	1.6	1.6
50		0.1	2.9	2.9	2.4	4.7	4.7		0.5	2.3	2.3	1.1	1.2	1.2
80		0.1	1.5	1.5	5.7	4.6	4.6		0.1	2.4	2.5	2.1	2.7	2.7
105		0.2	1.6	1.6	10.7	13.6	13.6		0.2	1.4	1.4	14.6	14.2	14.2
120		0.3	2.4	2.4	15.5	13.0	13.0		0.2	1.8	1.8	5.0	5.2	5.2

Appendix D: Open hole compression data

The dimensions, maximum load, absolute and normalised OHC data are shown in Table D.1 to Table D.7.

Table D.1: Summary of OHC data for dry AS4/3501-6

Temp (°C)	Specn	Ave Width (mm)	Ave Thickness (mm)	Vf (vol. %)	Pmax (kN)	Modulus		Failure strain		Strength	
						(GPa)	Normalised	(με)	Normalised	(MPa)	Normalised
25	A03	38.04	2.410	55.9	29.7	48.9	0.967	6808	1.052	324	1.024
25	A04	38.04	2.382	56.6	29.2	47.8	0.945	6981	1.079	322	1.018
25	C01	37.64	2.109	63.9	26.0	55.2	1.092	6146	0.950	327	1.034
25	C03	38.19	2.261	59.6	27.1	51.4	1.017	6215	0.961	314	0.992
25	C08	38.16	2.409	56.0	27.1	49.5	0.979	6198	0.958	295	0.932
50	A05	38.16	2.423	55.6	29.3	49.8	0.985	6644	1.027	317	1.002
50	A08	38.20	2.385	56.5	28.4	46.1	0.912	6460	0.999	312	0.986
50	C02	37.93	2.218	60.8	26.1	50.8	1.005	6137	0.949	310	0.980
50	C06	38.22	2.327	57.9	25.0	50.1	0.991	6254	0.967	281	0.888
50	C07	38.08	2.361	57.1	27.4	48.4	0.957	6400	0.989	304	0.961
80	A13	38.12	2.375	56.8	25.1	46.7	0.924	5894	0.911	278	0.879
80	A14	38.21	2.357	57.2	26.6	48.6	0.961	6206	0.959	295	0.932
80	A15	38.19	2.385	56.5	26.7	49.4	0.977	6090	0.941	293	0.926
80	A16	38.21	2.374	56.8	25.9	49.1	0.971	6033	0.933	285	0.901
80	A17	38.16	2.346	57.5	23.9	49.9	0.987	5492	0.849	267	0.844
105	A18	38.20	2.392	56.4	23.6	48.1	0.951	5722	0.884	258	0.815
105	A19	38.10	2.384	56.6	24.0	48.4	0.957	5634	0.871	264	0.834
105	A20	38.17	2.386	56.5	24.2	49.2	0.973	5554	0.858	266	0.841
105	A21	38.12	2.339	57.6	22.9	49.5	0.979	5355	0.828	257	0.812
105	C12	37.93	2.354	57.3	24.0	49.0	0.969	5611	0.867	269	0.850
120	C13	38.12	2.394	56.3	21.4	46.5	0.920	5060	0.782	234	0.740
120	NA1	38.06	2.231	60.4	22.4	50.9	1.007	5297	0.819	263	0.831
120	NA3	38.02	2.208	61.1	22.6	51.0	1.009	5424	0.838	269	0.850
120	NA4	38.00	2.291	58.9	21.7	48.0	0.949	5235	0.809	249	0.787
120	NA5	38.02	2.263	59.6	22.1	49.0	0.969	5325	0.823	257	0.812
Average											
25		38.014	2.314	58.4	27.8	50.6	1.000	6470	1.000	316	1.000
50		38.118	2.343	57.6	27.2	49.0	0.970	6379	0.986	305	0.963
80		38.178	2.367	57.0	25.6	48.7	0.964	5943	0.919	284	0.896
105		38.104	2.371	56.9	23.7	48.8	0.966	5575	0.862	263	0.831
120		38.044	2.277	59.3	22.0	49.1	0.971	5268	0.814	254	0.804
Standard Deviation											
25		0.220	0.130	3.4	1.6	2.9	0.057	393	0.061	13	0.041
50		0.118	0.078	2.0	1.7	1.9	0.037	195	0.030	14	0.045
80		0.038	0.016	0.4	1.2	1.2	0.024	276	0.043	11	0.036
105		0.105	0.023	0.6	0.5	0.6	0.011	137	0.021	5	0.016
120		0.048	0.072	1.8	0.5	1.9	0.038	135	0.021	14	0.043
Coefficient of Variance (%)											
25		0.6	5.6	5.9	5.6	5.7	5.7	6.1	6.1	4.1	4.1
50		0.3	3.3	3.4	6.3	3.8	3.8	3.1	3.1	4.6	4.6
80		0.1	0.7	0.7	4.5	2.5	2.5	4.6	4.6	4.0	4.0
105		0.3	1.0	1.0	2.2	1.2	1.2	2.5	2.5	2.0	2.0
120		0.1	3.2	3.1	2.2	3.9	3.9	2.6	2.6	5.3	5.3

Table D.2: Summary of OHC data for wet AS4/3501-6

Temp (°C)	Specn	Ave Width (mm)	Ave Thickness (mm)	Vf (vol. %)	Pmax (kN)	Modulus		Failure strain		Strength		Moisture (wt %)
						(GPa)	Normalised	(με)	Normalised	(MPa)	Normalised	
25	B08	38.20	2.328	57.9	25.0	49.6	0.981	5695	0.880	281	0.888	-
25	B09	38.13	2.327	57.9	26.2	49.7	0.983	6072	0.939	296	0.936	-
25	B11	38.22	2.295	58.8	27.1	50.3	0.995	6231	0.963	309	0.977	1.41
25	B12	38.21	2.322	58.1	24.9	50.2	0.993	5709	0.882	280	0.885	-
25	B13	38.17	2.312	58.3	25.9	51.4	1.017	5959	0.921	293	0.926	1.44
50	B10	38.21	2.273	59.3	23.7	49.7	0.983	5528	0.854	273	0.863	-
50	C18	38.19	2.395	56.3	23.0	44.7	0.884	5481	0.847	252	0.796	-
50	C19	38.08	2.368	56.9	22.5	46.4	0.918	5354	0.828	249	0.787	-
50	C20	38.12	2.397	56.3	23.1	49.7	0.983	5213	0.806	253	0.800	-
50	C21	38.17	2.359	57.2	21.7	49.6	0.981	4912	0.759	241	0.762	-
80	B02	38.21	2.425	55.6	20.2	47.4	0.938	4684	0.724	218	0.689	-
80	B03	38.18	2.399	56.2	20.2	48.5	0.959	4639	0.717	221	0.698	-
80	B04	38.23	2.355	57.3	20.3	48.1	0.951	4792	0.741	226	0.714	-
80	B05	38.20	2.364	57.0	20.8	49.8	0.985	4728	0.731	230	0.727	-
80	B06	38.20	2.341	57.6	20.3	48.4	0.957	4734	0.732	227	0.717	-
105	B07	38.02	2.322	58.1	18.1	47.8	0.945	4374	0.676	205	0.648	1.27
105	B14	38.20	2.349	57.4	17.7	45.5	0.900	4409	0.681	197	0.623	1.27
105	B15	38.16	2.415	55.8	18.0	47.3	0.936	4334	0.670	195	0.616	-
105	B16	38.22	2.392	56.4	18.1	47.1	0.932	4303	0.665	198	0.626	-
105	B17	38.22	2.391	56.4	18.4	45.4	0.898	4506	0.696	201	0.635	1.25
120	B18	38.18	2.367	57.0	15.1	40.0	0.791	4268	0.660	167	0.528	-
120	B19	38.13	2.371	56.9	15.0	42.5	0.841	3939	0.609	166	0.525	1.27
120	B20	38.19	2.387	56.5	15.9	42.5	0.841	4139	0.640	175	0.553	1.24
120	B21	38.22	2.346	57.5	15.0	39.9	0.789	4134	0.639	167	0.528	-
120	C14	38.15	2.400	56.2	14.7	33.4	0.661	4539	0.702	161	0.509	-
Average												
25		38.19	2.317	58.2	25.8	50.2	0.994	5933	0.917	292	0.922	1.43
50		38.15	2.358	57.2	22.8	48.0	0.950	5298	0.819	254	0.802	#DIV/0!
80		38.20	2.377	56.7	20.4	48.4	0.958	4715	0.729	224	0.709	#DIV/0!
105		38.16	2.374	56.8	18.1	46.6	0.922	4385	0.678	199	0.630	1.26
120		38.17	2.374	56.8	15.1	39.7	0.784	4204	0.650	167	0.528	1.26
Standard Deviation												
25		0.036	0.014	0.3	0.9	0.7	0.014	232	0.036	12	0.038	0.02
50		0.053	0.051	1.3	0.7	2.3	0.046	248	0.038	12	0.037	#DIV/0!
80		0.018	0.034	0.8	0.3	0.9	0.017	57	0.009	5	0.015	#DIV/0!
105		0.084	0.037	0.9	0.3	1.1	0.022	79	0.012	4	0.012	0.01
120		0.035	0.021	0.5	0.5	3.7	0.074	221	0.034	5	0.016	0.02
Coefficient of Variance (%)												
25		0.1	0.6	0.6	3.5	1.4	1.4	3.9	3.9	4.1	4.1	1.2
50		0.1	2.1	2.2	3.3	4.9	4.9	4.7	4.7	4.7	4.7	#DIV/0!
80		0.0	1.4	1.4	1.2	1.8	1.8	1.2	1.2	2.2	2.2	#DIV/0!
105		0.2	1.6	1.6	1.4	2.4	2.4	1.8	1.8	2.0	2.0	0.7
120		0.1	0.9	0.9	3.0	9.4	9.4	5.3	5.3	3.0	3.0	1.9

Table D.3: Summary of OHC data for dry T650/F584

Temp (°C)	Specn	Ave Width (mm)	Ave Thickness (mm)	Vf (vol. %)	Pmax (kN)	Modulus		Failure strain		Strength	
						(GPa)	Normalised	(με)	Normalised	(MPa)	Normalised
25	A02	37.89	2.716	48.2	27.8	43.3	0.980	6465	0.996	270	0.973
25	A05	37.85	2.647	49.4	27.8	45.0	1.019	6416	0.988	278	1.002
25	A06	38.18	2.671	49.0	28.2	43.8	0.991	6554	1.009	277	0.999
25	A08	37.88	2.622	49.9	27.8	44.2	1.000	6499	1.001	280	1.009
25	A12	38.04	2.628	49.8	28.2	44.6	1.010	6535	1.006	282	1.017
50	A04	38.15	2.618	50.0	26.5	44.5	1.007	6086	0.937	265	0.955
50	A09	38.06	2.670	49.0	27.5	43.5	0.985	6361	0.980	271	0.977
50	A17	38.22	2.649	49.4	28.8	44.6	1.010	6615	1.019	284	1.024
50	A19	38.22	2.673	49.0	26.7	44.3	1.003	6122	0.943	261	0.941
50	A21	37.94	2.680	48.8	27.7	43.3	0.980	6430	0.990	273	0.984
80	A03	38.06	2.674	48.9	25.7	44.3	1.003	5978	0.921	253	0.912
80	A07	38.01	2.638	49.6	24.2	43.3	0.980	5709	0.879	241	0.869
80	A11	38.14	2.689	48.7	24.8	42.7	0.967	5851	0.901	242	0.872
80	A13	38.16	2.662	49.2	23.7	43.2	0.978	5554	0.855	234	0.844
80	A14	38.21	2.689	48.7	26.1	43.2	0.978	6049	0.932	254	0.916
105	A15	38.19	2.676	48.9	23.0	42.2	0.955	5443	0.838	225	0.811
105	A18	38.20	2.645	49.5	24.1	43.3	0.980	5685	0.875	238	0.858
105	A20	37.99	2.700	48.5	22.8	42.6	0.964	5417	0.834	222	0.800
105	C08	38.15	2.658	49.2	23.6	43.0	0.973	5604	0.863	233	0.840
105	C09	38.18	2.647	49.4	23.8	44.2	1.000	5584	0.860	235	0.847
120	C10	38.16	2.658	49.2	21.2	42.6	0.964	5277	0.813	209	0.753
120	C11	38.14	2.654	49.3	21.0	42.4	0.960	5109	0.787	208	0.750
120	C12	38.12	2.639	49.6	20.8	42.7	0.967	5049	0.778	207	0.746
120	C13	38.16	2.634	49.7	21.0	43.3	0.980	5026	0.774	209	0.753
120	C14	38.22	2.665	49.1	20.6	42.3	0.957	4985	0.768	202	0.728
Average											
25		37.968	2.657	49.3	28.0	44.2	1.000	6494	1.000	277	1.000
50		38.118	2.658	49.2	27.4	44.0	0.997	6323	0.974	271	0.976
80		38.116	2.670	49.0	24.9	43.3	0.981	5828	0.898	245	0.882
105		38.142	2.665	49.1	23.5	43.1	0.975	5547	0.854	231	0.831
120		38.160	2.650	49.4	20.9	42.7	0.966	5089	0.784	207	0.746
Standard Deviation											
25		0.140	0.038	0.7	0.2	0.7	0.015	55	0.009	5	0.016
50		0.119	0.025	0.5	0.9	0.6	0.014	221	0.034	9	0.032
80		0.080	0.021	0.4	1.0	0.6	0.013	201	0.031	9	0.031
105		0.087	0.023	0.4	0.5	0.8	0.017	113	0.017	7	0.025
120		0.037	0.013	0.2	0.2	0.4	0.009	114	0.018	3	0.011
Coefficient of Variance (%)											
25		0.4	1.4	1.4	0.8	1.5	1.5	0.9	0.9	1.6	1.6
50		0.3	0.9	1.0	3.3	1.4	1.4	3.5	3.5	3.2	3.2
80		0.2	0.8	0.8	4.0	1.4	1.4	3.4	3.4	3.5	3.5
105		0.2	0.9	0.9	2.3	1.8	1.8	2.0	2.0	3.0	3.0
120		0.1	0.5	0.5	1.1	0.9	0.9	2.2	2.2	1.4	1.4

Table D.4: Summary of OHC data for wet T650/F584

Temp (°C)	Specn	Ave Width (mm)	Ave Thickness (mm)	Vf (vol. %)	Pmax (kN)	Modulus		Failure strain		Strength		Moisture (wt %)
						(GPa)	Normalised	(με)	Normalised	(MPa)	Normalised	
25	B01	38.24	2.546	48.2	24.1	46.7	1.057	5510	0.849	247	0.890	1.22
25	B02	38.25	2.702	49.4	25.1	43.7	0.989	5777	0.890	243	0.876	-
25	B03	38.16	2.683	49.0	24.2	45.6	1.032	5414	0.834	237	0.854	1.29
25	B04	38.27	2.644	49.9	24.9	42.4	0.960	5985	0.922	246	0.887	-
25	B05	38.09	2.635	49.8	23.4	45.8	1.037	5351	0.824	233	0.840	
50	B11	38.23	2.632	50.0	23.4	44.2	1.000	5422	0.835	233	0.840	-
50	B12	38.24	2.624	49.0	23.2	44.3	1.003	5365	0.826	231	0.833	1.17
50	B13	38.14	2.642	49.4	24.6	40.4	0.914	5828	0.897	244	0.880	-
50	B14	38.18	2.659	49.0	23.8	39.4	0.892	5598	0.862	234	0.844	1.16
50	B15	38.21	2.667	48.8	24.4	40.8	0.923	5749	0.885	240	0.865	1.18
80	B06	38.18	2.699	48.9	20.4	43.3	0.980	4728	0.728	198	0.714	-
80	B07	38.20	2.681	49.6	21.0	42.8	0.969	4981	0.767	205	0.739	-
80	B08	38.16	2.652	48.7	20.2	40.7	0.921	4952	0.763	200	0.721	-
80	B09	38.17	2.641	49.2	19.5	43.4	0.982	4635	0.714	194	0.699	-
80	B10	38.16	2.650	48.7	20.4	42.0	0.951	4902	0.755	202	0.728	-
105	B16	38.19	2.675	48.9	15.9	40.6	0.919	4011	0.618	156	0.562	1.10
105	B17	38.19	2.658	49.5	17.0	39.9	0.903	4289	0.660	167	0.602	-
105	B18	38.19	2.656	48.5	17.7	42.7	0.967	4263	0.656	174	0.627	1.08
105	B19	38.16	2.681	49.2	17.1	40.4	0.914	4385	0.675	167	0.602	1.07
105	B20	38.13	2.708	49.4	17.2	39.5	0.894	4413	0.680	166	0.598	-
120	B21	37.96	2.681	49.2	13.6	36.1	0.817	3895	0.600	133	0.479	1.07
120	C02	38.20	2.665	49.3	13.3	36.5	0.826	3793	0.584	130	0.469	1.08
120	C04	38.23	2.656	49.6	12.5	32.8	0.742	4771	0.735	123	0.443	-
120	C06	38.19	2.669	49.7	13.9	28.7	0.650	4232	0.652	136	0.490	-
120	C07	38.20	2.673	49.1	13.1	33.5	0.758	4478	0.690	129	0.465	-
Average												
25		38.20	2.642	49.3	24.3	44.8	1.015	5607	0.864	241	0.870	1.25
50		38.20	2.645	49.2	23.9	41.8	0.947	5592	0.861	236	0.852	1.17
80		38.17	2.665	49.0	20.3	42.4	0.961	4840	0.745	200	0.720	#DIV/0!
105		38.17	2.676	49.1	17.0	40.6	0.919	4272	0.658	166	0.598	1.08
120		38.16	2.669	49.4	13.3	33.5	0.759	4234	0.652	130	0.469	1.07
Standard Deviation												
25		0.075	0.060	0.7	0.7	1.7	0.040	266	0.041	6	0.022	0.05
50		0.041	0.018	0.5	0.6	2.3	0.052	201	0.031	5	0.020	0.01
80		0.017	0.024	0.4	0.5	1.1	0.025	151	0.023	4	0.015	#DIV/0!
105		0.027	0.021	0.4	0.7	1.2	0.028	159	0.024	6	0.023	0.02
120		0.111	0.009	0.2	0.5	3.1	0.071	405	0.062	5	0.018	0.01
Coefficient of Variance (%)												
25		0.2	2.3	1.4	2.8	3.9	3.9	4.8	4.8	2.5	2.5	3.8
50		0.1	0.7	1.0	2.6	5.4	5.4	3.6	3.6	2.3	2.3	0.8
80		0.0	0.9	0.8	2.7	2.6	2.6	3.1	3.1	2.1	2.1	#DIV/0!
105		0.1	0.8	0.9	3.9	3.1	3.1	3.7	3.7	3.9	3.9	1.5
120		0.3	0.3	0.5	4.0	9.3	9.3	9.6	9.6	3.7	3.7	0.8

Table D.5: Summary of OHC data for dry T650/PR500

Temp (°C)	Specn	Ave Width (mm)	Ave Thickness (mm)	Vf (vol. %)	Pmax (kN)	Modulus		Failure strain		Strength	
						(GPa)	Normalised	(με)	Normalised	(MPa)	Normalised
25	000205	37.95	2.301	56.0	26.7	47.0	1.038	6435	0.974	305	1.021
25	000215	37.87	2.304	55.9	27.5	43.1	0.952	6906	1.046	315	1.055
25	000216	37.92	2.314	55.7	26.8	48.9	1.080	6428	0.973	305	1.021
25	001101	38.00	2.555	50.4	27.4	42.3	0.934	6713	1.016	282	0.944
25	001102	37.94	2.494	51.6	27.0	45.1	0.996	6542	0.990	286	0.958
50	000202	37.98	2.265	56.9	25.9	44.5	0.983	6455	0.977	301	1.008
50	000211	38.09	2.487	51.8	26.6	41.5	0.917	6582	0.997	281	0.941
50	000512	38.14	2.481	51.9	26.2	45.8	1.011	6295	0.953	277	0.928
50	000520	38.03	2.268	56.8	26.9	50.1	1.106	6460	0.978	312	1.045
50	000522	38.14	2.357	54.7	26.3	50.1	1.106	6086	0.921	293	0.981
80	000213	38.10	2.320	55.5	25.1	49.8	1.100	5936	0.899	285	0.954
80	000219	37.96	2.334	55.2	22.3	49.8	1.100	5284	0.800	252	0.844
80	000501	38.14	2.219	58.1	23.2	45.9	1.014	5903	0.894	274	0.918
80	001103	37.94	2.453	52.5	22.8	44.1	0.974	5593	0.847	245	0.820
80	001104	38.12	2.390	53.9	24.1	47.6	1.051	5768	0.873	264	0.884
105	000502	38.05	2.163	59.6	20.6	47.3	1.045	5167	0.782	250	0.837
105	000503	38.05	2.178	59.1	22.0	51.2	1.131	5332	0.807	265	0.887
105	000504	38.16	2.203	58.5	20.8	50.9	1.124	4984	0.755	247	0.827
105	001105	38.05	2.337	55.1	20.9	46.6	1.029	5079	0.769	235	0.787
105	001106	38.01	2.333	55.2	22.1	44.7	0.987	5498	0.832	249	0.834
120	000508	38.07	2.285	56.4	21.5	46.7	1.031	5309	0.804	248	0.831
120	000515	38.14	2.247	57.3	20.6	49.5	1.093	4937	0.747	240	0.804
120	000519	38.12	2.285	56.4	20.5	48.1	1.062	5000	0.757	236	0.790
120	001107	38.05	2.335	55.2	20.7	47.8	1.056	4985	0.755	233	0.780
120	001108	38.03	2.326	55.4	20.9	47.1	1.040	5094	0.771	237	0.794
Average											
25		37.936	2.394	53.9	27.1	45.3	1.000	6605	1.000	299	1.000
50		38.076	2.372	54.4	26.4	46.4	1.025	6376	0.965	293	0.981
80		38.052	2.343	55.0	23.5	47.4	1.048	5697	0.863	264	0.884
105		38.064	2.243	57.5	21.3	48.1	1.063	5212	0.789	249	0.835
120		38.082	2.296	56.1	20.8	47.8	1.057	5065	0.767	239	0.800
Standard Deviation											
25		0.047	0.122	2.7	0.4	2.7	0.060	204	0.031	14	0.047
50		0.070	0.109	2.5	0.4	3.7	0.082	191	0.029	14	0.048
80		0.094	0.087	2.1	1.1	2.5	0.055	267	0.040	16	0.054
105		0.056	0.085	2.2	0.7	2.8	0.062	205	0.031	11	0.036
120		0.047	0.036	0.9	0.4	1.1	0.024	148	0.022	6	0.019
Coefficient of Variance (%)											
25		0.1	5.1	5.0	1.3	6.0	6.0	3.1	3.1	4.7	4.7
50		0.2	4.6	4.6	1.5	8.0	8.0	3.0	3.0	4.9	4.9
80		0.2	3.7	3.7	4.7	5.2	5.2	4.7	4.7	6.1	6.1
105		0.1	3.8	3.8	3.3	5.9	5.9	3.9	3.9	4.3	4.3
120		0.1	1.5	1.6	1.9	2.3	2.3	2.9	2.9	2.4	2.4

Table D.6: Summary of OHC data for wet T650/PR500

Temp (°C)	Specn	Ave Width (mm)	Ave Thickness (mm)	Vf (vol. %)	Pmax (kN)	Modulus		Failure strain		Strength		Moisture (wt %)
						(GPa)	Normalised	(με)	Normalised	(MPa)	Normalised	
25	000201	38.04	2.297	56.1	25.8	48.2	1.064	6139	0.929	295	0.988	-
25	000203	38.01	2.292	56.2	27.6	41.3	0.912	6840	1.036	317	1.062	-
25	000505	37.94	2.222	58.0	22.3	52.1	1.151	5208	0.789	265	0.887	-
25	000507	37.90	2.242	57.5	24.7	54.3	1.199	5704	0.864	290	0.971	-
25	000516	38.01	2.267	56.8	24.9	50.5	1.115	5888	0.891	289	0.968	-
50	000204	38.14	2.301	56.0	27.5	48.9	1.080	6445	0.976	314	1.052	-
50	000206	38.09	2.312	55.7	23.1	39.7	0.877	5867	0.888	262	0.877	0.53
50	000207	38.14	2.323	55.5	22.7	53.2	1.175	5043	0.764	256	0.857	0.53
50	000506	38.16	2.238	57.6	22.0	47.5	1.049	5443	0.824	257	0.861	-
50	000510	38.12	2.385	54.0	23.5	49.8	1.100	5481	0.830	259	0.867	0.54
80	000208	38.13	2.365	54.5	22.5	48.6	1.073	5229	0.792	249	0.834	0.52
80	000209	38.05	2.405	53.6	23.0	40.1	0.886	5757	0.872	252	0.844	-
80	000210	37.92	2.461	52.3	22.4	41.1	0.908	5580	0.845	240	0.804	0.55
80	000212	38.03	2.543	50.7	24.2	40.2	0.888	5988	0.907	250	0.837	0.56
80	000214	38.19	2.296	56.1	23.0	50.1	1.106	5442	0.824	263	0.881	-
105	000217	38.07	2.341	55.0	19.9	44.8	0.989	5020	0.760	224	0.750	0.50
105	000218	38.15	2.351	54.8	21.7	45.2	0.998	5284	0.800	242	0.810	-
105	000220	38.11	2.337	55.1	19.7	42.5	0.939	4993	0.756	221	0.740	0.52
105	000221	38.14	2.371	54.3	20.4	48.2	1.064	4774	0.723	226	0.757	-
105	000222	38.23	2.425	53.1	21.5	43.8	0.967	5331	0.807	232	0.777	0.53
120	000223	38.11	2.454	52.5	19.2	38.3	0.846	4931	0.747	206	0.690	-
120	000224	37.96	2.490	51.7	19.6	40.0	0.883	5163	0.782	207	0.693	-
120	000509	38.15	2.329	55.3	20.1	50.0	1.104	4817	0.729	227	0.760	0.54
120	000511	38.12	2.442	52.7	20.4	46.5	1.027	4916	0.744	219	0.733	0.59
120	000514	38.12	2.248	57.3	20.8	46.5	1.027	5188	0.785	243	0.814	0.50
Average												
25		37.98	2.264	56.9	25.1	49.3	1.088	5956	0.902	291	0.975	#DIV/0!
50		38.13	2.312	55.7	23.8	47.8	1.056	5656	0.856	270	0.903	0.54
80		38.06	2.414	53.4	23.0	44.0	0.972	5599	0.848	251	0.840	0.55
105		38.14	2.365	54.5	20.6	44.9	0.992	5080	0.769	229	0.767	0.52
120		38.09	2.393	53.9	20.0	44.3	0.977	5003	0.757	220	0.738	0.54
Standard Deviation												
25		0.058	0.032	0.8	1.9	5.0	0.110	601	0.091	19	0.062	#DIV/0!
50		0.026	0.053	1.3	2.2	5.0	0.110	529	0.080	25	0.083	0.00
80		0.103	0.094	2.1	0.7	4.9	0.108	291	0.044	8	0.028	0.02
105		0.059	0.036	0.8	0.9	2.1	0.047	229	0.035	8	0.028	0.01
120		0.075	0.101	2.3	0.6	4.9	0.109	164	0.025	15	0.051	0.05
Coefficient of Variance (%)												
25		0.2	1.4	1.4	7.7	10.1	10.1	10.1	10.1	6.4	6.4	#DIV/0!
50		0.1	2.3	2.3	9.1	10.5	10.5	9.4	9.4	9.2	9.2	0.9
80		0.3	3.9	3.9	3.1	11.2	11.2	5.2	5.2	3.3	3.3	3.9
105		0.2	1.5	1.5	4.4	4.7	4.7	4.5	4.5	3.6	3.6	2.8
120		0.2	4.2	4.3	3.2	11.1	11.1	3.3	3.3	7.0	7.0	8.9

Table D.7: Summary of OHC data from T300J/DA508

Temp (°C)	Specn	Ave Width (mm)	Ave Thickness (mm)	Pmax (kN)	Modulus		Failure strain		Strength	
					(GPa)	Normalised	(με)	Normalised	(MPa)	Normalised
25	10	38.12	2.005	23.1	44.8	0.991	6354	1.049	302	1.041
25	09	38.10	2.049	21.7	45.6	1.009	5761	0.951	278	0.959
50	08	38.11	2.036	22.6	50.2	1.111	5797	0.957	291	1.003
50	07	38.12	2.025	21.9	51.5	1.139	5666	0.935	284	0.979
80	06	38.09	2.044	22.0	50.1	1.108	5748	0.949	283	0.976
80	05	38.09	2.044	22.6	49.7	1.100	5821	0.961	290	1.000
105	04	38.12	2.046	21.4	51.3	1.135	5492	0.907	275	0.948
105	03	38.14	2.024	21.1	48.5	1.073	5726	0.945	273	0.941
120	02	38.12	2.010	20.8	47.1	1.042	5766	0.952	271	0.934
120	01	38.11	1.997	20.9	49.3	1.091	5592	0.923	274	0.945
Average										
25		38.11	2.027	22.4	45.20	1.000	6058	1.000	290	1.000
50		38.12	2.031	22.3	50.9	1.125	5732	0.946	288	0.991
80		38.09	2.044	22.3	49.9	1.104	5785	0.955	287	0.988
105		38.13	2.035	21.3	49.9	1.104	5609	0.926	274	0.945
120		38.12	2.004	20.9	48.2	1.066	5679	0.938	273	0.940
Standard Deviation										
25		0.0	0.031	1.0	0.6	0.013	419	0.069	17	0.059
50		0.0	0.008	0.5	0.9	0.020	93	0.015	5	0.017
80		0.0	0.000	0.4	0.3	0.006	52	0.009	5	0.017
105		0.0	0.016	0.2	2.0	0.044	165	0.027	1	0.005
120		0.0	0.009	0.1	1.6	0.034	123	0.020	2	0.007
Coefficient of Variance (%)										
25		0.0	1.5	4.4	1.3	1.3	6.9	6.9	5.9	5.9
50		0.0	0.4	2.2	1.8	1.8	1.6	1.6	1.7	1.7
80		0.0	0.0	1.9	0.6	0.6	0.9	0.9	1.7	1.7
105		0.0	0.8	1.0	4.0	4.0	2.9	2.9	0.5	0.5
120		0.0	0.5	0.3	3.2	3.2	2.2	2.2	0.8	0.8

Appendix E: Compression after impact data

The coupon dimensions, maximum load, absolute and normalised CAI data are shown in Table E.1 to Table E.6.

Table E.1: Summary of CAI data for dry AS4/3501-6

Temp (°C)	Specn	Ave Width (mm)	Ave Thickness (mm)	Vf (vol.%)	Impact energy		Dam.A (mm^2)	Pmax (kN)	Modulus		Failure strain		Strength	
					Incident	Rebound			(GPa)	Normalised	(με)	Normalised	(MPa)	Normalised
25	B01	99.94	4.616	58.4	30.89	3.92	2358	62.0	47.0	1.039	2870	0.971	135	1.009
25	B06	99.88	4.672	57.7	31.28	5.59	2842	63.0	42.5	0.940	3144	1.064	135	1.009
25	B11	100.01	4.650	58.0	31.18	5.84	3243	61.9	45.5	1.006	2933	0.993	133	0.994
25	B16	100.01	4.650	58.0	31.28	5.20	3349	61.2	45.9	1.015	2871	0.972	132	0.987
50	B02	99.98	4.672	57.7	31.28	4.11	1792	63.3	45.7	1.011	2959	1.002	136	1.017
50	B07	99.92	4.691	57.5	31.48	6.19	3090	62.6	43.4	0.960	3044	1.030	134	1.002
50	B12	99.98	4.680	57.6	31.38	3.91	1486	66.0	45.2	0.999	3120	1.056	141	1.054
50	B17	100.03	4.687	57.5	31.48	5.66	3726	58.8	44.3	0.980	2823	0.955	126	0.942
80	B03	99.92	4.670	57.7	31.38	3.66	1344	63.6	-	-	-	-	136	1.017
80	B08	99.90	4.670	57.7	31.48	5.48	3137	60.5	43.6	0.964	2951	0.999	130	0.972
80	B13	100.02	4.642	58.1	31.18	5.87	2476	64.4	46.6	1.030	2984	1.010	139	1.039
80	B18	99.89	4.684	57.6	31.58	4.52	1722	62.5	43.7	0.966	3041	1.029	134	1.002
105	B04	99.94	4.713	57.2	31.68	6.34	3443	61.7	44.1	0.975	3050	1.032	131	0.979
105	B09	99.98	4.690	57.5	31.68	5.32	2877	62.8	45.1	0.997	3064	1.037	134	1.002
105	B14	100.02	4.679	57.6	31.38	5.15	1616	64.9	44.6	0.986	3190	1.080	139	1.039
105	B19	100.04	4.671	57.7	31.28	5.09	1580	63.2	-	-	-	-	135	1.009
105	B21	99.88	4.682	57.6	31.48	4.39	2429	63.0	-	-	-	-	135	1.009
120	B05	99.95	4.680	57.6	31.38	5.31	1804	60.5	45.0	0.995	2938	0.994	129	0.964
120	B10	100.05	4.686	57.5	31.38	6.15	3243	60.4	45.2	0.999	2923	0.989	129	0.964
120	B15	99.98	4.680	57.6	31.38	5.70	3443	57.6	-	-	-	-	123	0.920
120	B20	100.08	4.587	58.8	30.70	4.82	3137	60.3	45.0	0.995	2943	0.996	131	0.979
120	B22	99.96	4.624	58.3	30.99	4.14	2158	60.4	45.3	1.002	3039	1.029	131	0.979
Average														
25		99.96	4.647	58.0	31.16	5.14	2948	62.0	45.2	1.000	2955	1.000	134	1.000
50		99.98	4.683	57.6	31.41	4.97	2524	62.7	44.7	0.987	2987	1.011	134	1.004
80		99.93	4.667	57.8	31.41	4.88	2170	62.8	44.6	0.987	2992	1.013	135	1.007
105		99.97	4.687	57.5	31.50	5.26	2389	63.1	44.6	0.986	3101	1.050	135	1.008
120		100.00	4.651	58.0	31.17	5.22	2757	59.8	45.1	0.998	2961	1.002	129	0.961
Standard Deviation														
25		0.06	0.023	0.3	0.18	0.85	450	0.7	1.9	0.043	130	0.044	2	0.011
50		0.05	0.008	0.1	0.09	1.13	1061	3.0	1.0	0.022	127	0.043	6	0.047
80		0.06	0.018	0.2	0.17	0.99	798	1.7	1.7	0.038	46	0.015	4	0.028
105		0.06	0.016	0.2	0.18	0.70	807	1.2	0.5	0.011	77	0.026	3	0.021
120		0.06	0.044	0.6	0.31	0.78	728	1.3	0.1	0.003	53	0.018	3	0.025
Coefficient of Variance (%)														
25		0.1	0.5	0.5	0.6	16.6	15.3	1.2	4.3	4.3	4.4	4.4	1.1	1.1
50		0.0	0.2	0.2	0.3	22.8	42.1	4.7	2.3	2.3	4.3	4.3	4.6	4.6
80		0.1	0.4	0.4	0.5	20.3	36.8	2.7	3.8	3.8	1.5	1.5	2.8	2.8
105		0.1	0.3	0.3	0.6	13.3	33.8	1.8	1.1	1.1	2.5	2.5	2.1	2.1
120		0.1	0.9	1.0	1.0	14.9	26.4	2.1	0.3	0.3	1.8	1.8	2.6	2.6

Table E.2: Summary of CAI data for wet AS4/3501-6

Temp (°C)	Specn	Ave Width (mm)	Ave Thickness (mm)	Vf (vol.%)	Impact energy		Dam.A (mm^2)	Pmax (kN)	Modulus		Failure strain		Strength		Moisture (wt %)
					Incident	Rebound			(GPa)	Normalised	(με)	Normalised	(MPa)	Normalised	
25	A01	99.94	4.741	56.9	31.78	6.76	2075	65.2	45.2	0.999	3078	1.042	138	1.032	1.42
25	A06	99.97	4.768	56.6	31.98	6.14	1462	69.8	44.4	0.982	3279	1.110	146	1.092	1.44
25	A11	100.00	4.776	56.5	32.08	6.24	708	72.3	44.4	0.982	3408	1.153	151	1.129	1.43
25	A16	100.02	4.730	57.0	31.48	5.46	1486	69.2	45.4	1.004	3240	1.097	146	1.092	1.45
50	A02	99.91	4.780	56.4	32.19	7.23	1179	67.6	44.5	0.984	3172	1.074	142	1.062	1.64
50	A07	100.05	4.756	56.7	31.78	6.60	1757	64.6	43.2	0.955	3123	1.057	136	1.017	1.63
50	A12	99.99	4.684	57.6	31.68	5.74	778	68.1	-	-	-	-	145	1.084	1.65
50	A17	100.01	4.709	57.3	31.48	6.03	1557	63.4	44.4	0.982	3018	1.021	135	1.009	1.67
80	A03	99.96	4.780	56.4	32.08	6.31	825	66.7	43.4	0.960	3301	1.117	140	1.047	1.41
80	A08	99.93	4.720	57.1	31.58	5.89	1675	64.1	45.0	0.995	3172	1.074	136	1.017	1.41
80	A13	99.04	4.727	57.0	31.48	7.01	1333	60.2	45.4	1.004	2952	0.999	129	0.964	1.43
80	A18	99.97	4.744	56.8	31.78	6.20	1910	63.1	44.6	0.986	3051	1.033	133	0.994	1.44
105	A04	99.89	4.752	56.7	31.98	6.14	1250	61.4	44.3	0.980	3032	1.026	129	0.964	1.33
105	A09	99.84	4.777	56.5	31.98	7.35	1533	62.3	43.6	0.964	3073	1.040	131	0.979	1.33
105	A14	100.00	4.706	57.3	31.58		1085	64.5	45.0	0.995	3213	1.087	137	1.024	1.21
105	A19	99.97	4.675	57.7	31.38		943	64.0	45.2	0.999	3112	1.053	137	1.024	1.37
105	-	-	-	-	-	-	-	-	-	-	-	-	-	-	-
120	A05	99.88	4.733	57.0	31.88	5.55	2962	51.7	41.7	0.922	2720	0.921	109	0.815	1.39
120	A10	100.01	4.761	56.6	31.88	6.30	1934	59.1	42.6	0.942	3020	1.022	124	0.927	1.40
120	A15	99.99	4.730	57.0	31.78	6.06	2123	57.9	42.9	0.949	2972	1.006	123	0.920	1.44
120	A21	99.86	4.754	56.7	31.78	5.89	1792	54.2	42.9	0.949	2758	0.933	114	0.852	1.44
120	A22	99.88	4.705	57.3	31.68	6.63	1439	54.0	42.7	0.944	2793	0.945	115	0.860	-
Average															
25		99.98	4.754	56.7	31.77	6.36	1433	69.1	44.9	0.992	3251	1.100	145	1.086	1.44
50		99.99	4.732	57.0	31.78	6.40	1318	65.9	44.0	0.974	3104	1.051	140	1.043	1.64
80		99.73	4.743	56.9	31.73	6.35	1436	63.5	44.6	0.986	3119	1.056	135	1.006	1.42
105		99.93	4.728	57.0	31.73	6.74	1203	63.1	44.5	0.985	3108	1.052	134	0.998	1.31
120		99.92	4.737	56.9	31.80	6.09	2050	55.4	42.6	0.941	2853	0.966	117	0.875	1.42
Standard Deviation															
25		0.035	0.022	0.3	0.27	0.54	561	2.948	0.5	0.012	136	0.046	5	0.040	0.01
50		0.059	0.044	0.5	0.30	0.66	432	2.285	0.7	0.016	79	0.027	5	0.036	0.02
80		0.457	0.027	0.3	0.27	0.47	471	2.686	0.9	0.019	151	0.051	5	0.035	0.02
105		0.073	0.046	0.6	0.30	0.85	253	1.448	0.7	0.016	78	0.026	4	0.031	0.07
120		0.070	0.022	0.3	0.08	0.41	568	3.043	0.5	0.011	135	0.046	6	0.048	0.03
Coefficient of Variance (%)															
25		0.0	0.5	0.5	0.8	8.4	39.1	4.3	1.2	1.2	4.2	4.2	3.7	3.7	0.8
50		0.1	0.9	0.9	0.9	10.3	32.8	3.5	1.6	1.6	2.5	2.5	3.4	3.4	1.0
80		0.5	0.6	0.6	0.8	7.4	32.8	4.2	1.9	1.9	4.8	4.8	3.5	3.5	1.2
105		0.1	1.0	1.0	0.9	12.7	21.1	2.3	1.6	1.6	2.5	2.5	3.1	3.1	5.2
120		0.1	0.5	0.5	0.3	6.7	27.7	5.5	1.2	1.2	4.7	4.7	5.4	5.4	1.9

Table E.3: Summary of CAI data for dry T650/F584

Temp (°C)	Specn	Ave Width (mm)	Ave Thickness (mm)	Vf (vol.%)	Impact energy		Dam.A (mm^2)	Pmax (kN)	Modulus		Failure strain		Strength	
					Incident	Rebound			(GPa)	Normalised	(με)	Normalised	(MPa)	Normalised
25	A01	100.19	5.288	49.5	35.508	13.073	767	114.8	39.9	0.983	5533	0.996	217	0.970
25	A06	100.20	5.248	49.9	-	-	660	120.5	41.3	1.017	5607	1.009	229	1.024
25	A11	100.20	5.236	50.0	35.153	12.463	802	119.7	-	-	-	-	228	1.020
25	A16	99.93	5.251	49.8	34.231	14.153	708	118.5	41.6	1.025	5519	0.993	226	1.011
25	A21	100.08	5.284	49.5	35.389	13.194	660	115.2	39.6	0.975	5564	1.001	218	0.975
50	A02	99.68	5.300	49.4	35.508	-	719	113.9	40.2	0.990	5451	0.981	216	0.966
50	A07	100.09	5.244	49.9	35.153	13.013	861	116.6	40.3	0.993	5572	1.003	222	0.993
50	A12	100.00	5.280	49.6	35.270	12.160	684	114.2	41.0	0.907	5363	0.965	216	0.966
50	A17	100.08	5.254	49.8	35.271	13.855	814	119.2	42.0	1.034	5467	0.984	227	1.015
50	A22	100.15	5.296	49.4	35.628	-	637	113.9	39.9	0.983	5437	0.979	215	0.962
50	-	-	-	-	-	-	-	-	-	-	-	-	-	-
80	A03	100.09	5.271	49.6	35.389	13.378	731	111.1	40.1	0.988	5357	0.964	211	0.944
80	A08	100.08	5.224	50.1	34.919	14.885	731	112.7	40.3	0.993	5341	0.961	216	0.966
80	A13	99.68	5.297	49.4	35.508	13.630	802	110.4	-	-	-	-	209	0.935
80	A18	99.91	5.249	49.9	35.271	13.409	708	111.9	41.1	1.012	5321	0.958	213	0.953
80	O09	100.02	5.221	50.1	35.036	11.815	684	106.0	41.0	1.010	5070	0.913	203	0.908
80	-	-	-	-	-	-	-	-	-	-	-	-	-	-
105	A04	100.12	5.240	49.9	35.036	13.316	755	109.6	41.1	1.012	5215	0.939	209	0.935
105	A09	100.08	5.236	50.0	35.153	13.073	767	111.3	40.9	1.007	5338	0.961	212	0.948
105	A14	99.71	5.282	49.5	35.389	13.888	684	106.9	40.5	0.998	5110	0.920	203	0.908
105	A19	100.07	5.249	49.9	35.271	13.630	731	107.2	40.8	1.005	5130	0.923	204	0.912
105	O10	100.02	5.223	50.1	35.153	11.893	672	104.8	40.5	0.998	5090	0.916	201	0.899
105	-	-	-	-	-	-	-	-	-	-	-	-	-	-
120	A05	100.09	5.223	50.1	35.036	-	755	108.4	41.1	1.012	5201	0.936	207	0.926
120	A10	100.16	5.250	49.8	35.271	13.662	719	107.8	40.2	0.990	5267	0.948	205	0.917
120	A15	99.96	5.264	49.7	34.573	13.630	825	108.5	40.5	0.998	5243	0.944	206	0.921
120	A20	99.97	5.280	49.6	35.508	13.472	649	108.7	40.1	0.988	5312	0.956	206	0.921
120	O11	99.90	5.223	50.1	34.919	12.983	684	97.2	40.1	0.988	4781	0.861	186	0.832
120	O14	99.09	5.243	49.9	35.153	13.921	613	108.6	40.7	1.002	5280	0.950	209	0.935
Average														
25		100.12	5.261	49.7	35.07	13.22	719	117.7	40.6	1.000	5556	1.000	224	1.000
50		100.00	5.275	49.6	35.37	13.01	743	115.6	40.7	0.981	5458	0.982	219	0.980
80		99.96	5.252	49.8	35.22	13.42	731	110.4	40.6	1.001	5272	0.949	210	0.941
105		100.00	5.246	49.9	35.20	13.16	722	108.0	40.8	1.004	5177	0.932	206	0.920
120		99.86	5.247	49.9	35.08	13.53	708	106.5	40.5	0.996	5181	0.932	203	0.909
Standard Deviation														
25		0.12	0.023	0.2	0.58	0.70	64	2.6	1.0	0.025	39	0.007	6	0.025
50		0.19	0.025	0.2	0.20	0.85	92	2.3	0.8	0.046	75	0.014	5	0.023
80		0.17	0.032	0.3	0.24	1.09	44	2.6	0.5	0.012	136	0.024	5	0.022
105		0.17	0.022	0.2	0.13	0.77	42	2.5	0.3	0.006	102	0.018	5	0.020
120		0.39	0.023	0.2	0.32	0.35	76	4.6	0.4	0.010	199	0.036	9	0.038
Coefficient of Variance (%)														
25		0.1	0.4	0.4	1.6	5.3	8.8	2.2	2.5	2.5	0.7	0.7	2.5	2.5
50		0.2	0.5	0.5	0.6	6.5	12.4	2.0	2.1	4.7	1.4	1.4	2.4	2.4
80		0.2	0.6	0.6	0.7	8.1	6.0	2.4	1.2	1.2	2.6	2.6	2.3	2.3
105		0.2	0.4	0.4	0.4	5.9	5.8	2.3	0.6	0.6	2.0	2.0	2.2	2.2
120		0.4	0.4	0.4	0.9	2.6	10.8	4.3	1.0	1.0	3.8	3.8	4.2	4.2

Table E.4: Summary of CAI data for wet T650/F584

Temp (°C)	Specn	Ave Width (mm)	Ave Thickness (mm)	Vf (vol.%)	Impact energy		Dam.A (mm^2)	Pmax (kN)	Modulus		Failure strain		Strength		Moisture (wt %)
					Incident	Rebound			(GPa)	Normalised	(με)	Normalised	(MPa)	Normalised	
25	B01	100.15	5.361	48.8	35.271	13.316	660	101.9	38.0	0.936	5084	0.915	190	0.850	1.15
25	B06	100.21	5.309	49.3	35.508	13.441	637	101.3	39.1	0.963	4978	0.896	190	0.850	1.13
25	B11	100.21	5.356	48.9	35.869	12.463	672	100.3	37.7	0.929	5011	0.902	187	0.836	1.13
25	B17	100.10	5.297	49.4	35.271	13.694	613	104.9	39.6	0.975	5104	0.919	198	0.886	1.14
25	B22	100.17	5.378	48.7	35.991	11.867	613	101.4	37.9	0.933	4988	0.898	188	0.841	1.17
50	B02	100.09	5.351	48.9	35.991	12.749	637	95.3	37.4	0.921	4809	0.866	178	0.796	1.26
50	B07	100.25	5.302	49.4	35.508	13.347	708	93.5	39.0	0.961	4589	0.826	176	0.787	1.24
50	B12	100.16	5.310	49.3	35.748	13.503	684	98.5	38.8	0.956	4872	0.877	185	0.827	1.27
50	B18	100.23	5.295	49.4	35.508	12.187	731	90.4	38.5	0.948	4629	0.833	170	0.760	1.09
50	O01	100.03	5.307	49.3	35.628	12.520	590	89.8	38.6	0.951	4442	0.800	169	0.756	1.24
50	O05	100.01	5.292	49.5	35.628	11.867	601	91.9	38.1	0.938	4632	0.834	174	0.778	-
80	B03	100.09	5.341	49.0	35.869	13.073	684	85.4	37.3	0.919	4535	0.816	160	0.716	1.09
80	B08	100.22	5.292	49.5	35.508	14.153	625	87.2	37.9	0.933	4587	0.826	164	0.733	1.07
80	B13	100.15	5.297	49.4	35.389	12.352	684	86.5	37.7	0.929	4607	0.829	163	0.729	1.09
80	B19	100.07	5.305	49.3	35.389	12.297	738	84.6	38.0	0.936	4412	0.794	159	0.711	-
80	O02	99.97	5.309	49.3	35.389	12.633	637	84.5	37.8	0.931	4439	0.799	159	0.711	1.09
80	O06	99.95	5.305	49.3	35.628	12.269	566	87.2	37.5	0.924	4634	0.834	165	0.738	1.09
105	B04	100.07	5.307	49.3	35.508	13.888	625	80.8	37.9	0.933	4258	0.766	152	0.680	1.02
105	B09	100.14	5.304	49.3	35.748	12.983	578	80.2	37.9	0.933	4201	0.756	151	0.675	1.00
105	B14	100.12	5.309	49.3	35.628	13.378	708	81.0	37.7	0.929	4218	0.759	153	0.684	1.01
105	B20	99.96	5.336	49.0	35.869	13.224	585	80.6	37.2	0.916	4300	0.774	151	0.675	-
105	O03	100.03	5.319	49.2	35.628	12.269	637	76.0	37.2	0.916	4117	0.741	143	0.640	1.00
105	O07	99.98	5.257	49.8	35.389	11.919	616	73.8	37.4	0.921	3913	0.704	141	0.631	0.99
120	B05	100.12	5.307	49.3	35.748	12.052	637	68.5	34.4	0.847	3887	0.700	129	0.577	1.04
120	B10	100.13	5.328	49.1	35.869	13.503	672	70.4	34.6	0.852	4041	0.727	132	0.590	1.03
120	B16	100.04	5.290	49.5	35.389	12.954	696	70.1	35.6	0.877	3864	0.695	133	0.595	1.04
120	B21	100.08	5.342	49.0	35.748	13.043	649	72.8	34.7	0.855	4140	0.745	136	0.608	-
120	O04	100.02	5.313	49.3	35.628	12.520	566	69.5	34.7	0.855	3954	0.712	131	0.586	1.05
120	O08	99.99	5.251	49.8	35.153	11.999	592	66.9	35.1	0.865	3775	0.679	127	0.568	1.03
Average															
25		100.17	5.340	49.0	35.58	12.96	639	102.0	38.5	0.947	5033	0.906	191	0.852	1.15
50		100.13	5.310	49.3	35.67	12.70	658	93.2	38.4	0.946	4662	0.839	175	0.784	1.22
80		100.08	5.308	49.3	35.53	12.80	656	85.9	37.7	0.929	4536	0.816	162	0.723	1.08
105		100.05	5.305	49.3	35.63	12.94	625	78.7	37.6	0.925	4168	0.750	149	0.664	1.00
120		100.06	5.305	49.3	35.59	12.68	635	69.7	34.9	0.858	3944	0.710	131	0.587	1.04
Standard Deviation															
25		0.046	0.035	0.3	0.33	0.76	27	1.743	0.8	0.021	57	0.010	4	0.019	0.02
50		0.101	0.021	0.2	0.18	0.64	58	3.276	0.6	0.014	156	0.028	6	0.026	0.07
80		0.103	0.017	0.2	0.19	0.73	60	1.236	0.3	0.006	92	0.017	3	0.012	0.01
105		0.073	0.026	0.2	0.17	0.73	47	3.061	0.3	0.008	139	0.025	5	0.023	0.01
120		0.056	0.032	0.3	0.27	0.59	49	1.979	0.4	0.011	131	0.024	3	0.014	0.01
Coefficient of Variance (%)															
25		0.0	0.7	0.7	0.9	5.9	4.2	1.7	2.2	2.2	1.1	1.1	2.3	2.3	1.4
50		0.1	0.4	0.4	0.5	5.0	8.8	3.5	1.5	1.5	3.3	3.3	3.3	3.3	6.0
80		0.1	0.3	0.3	0.5	5.7	9.1	1.4	0.7	0.7	2.0	2.0	1.6	1.6	0.9
105		0.1	0.5	0.5	0.5	5.6	7.5	3.9	0.9	0.9	3.3	3.3	3.5	3.5	1.1
120		0.1	0.6	0.6	0.8	4.7	7.7	2.8	1.2	1.2	3.3	3.3	2.4	2.4	0.6

Table E.5: Summary of CAI data for dry T650/PR500

Temp (°C)	Specn	Ave Width (mm)	Ave Thickness (mm)	Vf (vol.%)	Impact energy		Dam.A (mm^2)	Pmax (kN)	Modulus		Failure strain		Strength	
					Incident	Rebound			(GPa)	Normalised	(με)	Normalised	(MPa)	Normalised
25	000209	100.05	5.024	51.3	33.79	12.46	637	123.0	41.9	1.056	5980	0.977	245	1.031
25	000214	100.24	5.066	50.9	34.01	14.78	613	126.8	42.0	1.059	6086	0.994	250	1.052
25	000408	100.26	5.250	49.1	35.15	12.66	601	123.3	39.2	0.988	6096	0.996	234	0.985
25	000413	100.15	5.435	47.4	36.24	15.48	601	132.5	38.8	0.978	6458	1.055	244	1.027
25	000502	100.25	5.567	46.3	37.37	-	585	125.5	37.5	0.945	6094	0.996	224	0.942
25	000507	100.29	5.505	46.8	36.73	15.91	526	126.2	38.6	0.973	6011	0.982	229	0.964
50	000210	100.12	5.031	51.2	33.79	13.76	531	118.5	41.0	1.034	5875	0.960	235	0.989
50	000215	100.26	5.102	50.5	34.23	13.26	649	120.3	41.2	1.039	5838	0.954	235	0.989
50	000409	100.27	5.426	47.5	36.48	13.76	519	116.4	39.1	0.986	5609	0.916	214	0.900
50	000414	100.15	5.313	48.5	35.63	13.89	528	122.4	39.6	0.998	5956	0.973	230	0.968
50	000503	100.30	5.549	46.4	37.24	14.99	436	128.6	-	-	-	-	231	0.972
50	000508	100.14	5.440	47.4	36.36	14.02	566	120.0	38.7	0.976	5760	0.941	220	0.926
80	000211	100.08	5.047	51.0	34.01	14.43	613	117.7	41.1	1.036	5832	0.953	233	0.980
80	000216	100.09	5.221	49.3	35.04	14.43	542	119.3	39.7	1.001	5888	0.962	228	0.959
80	000410	100.12	5.261	49.0	35.51	14.57	460	112.4	39.2	0.988	5569	0.910	213	0.896
80	000415	100.33	5.253	49.0	35.15	14.81	660	120.0	39.2	0.988	5834	0.953	228	0.959
80	000504	100.21	5.456	47.2	36.48	14.67	448	122.8	38.6	0.973	5992	0.979	225	0.947
80	000509	100.19	5.679	45.4	37.89	14.96	495	120.5	36.8	0.928	5885	0.961	212	0.892
105	000212	100.16	5.181	49.7	34.80	15.14	613	117.0	36.5	0.920	5924	0.968	226	0.951
105	000406	100.21	5.293	48.7	35.51	15.18	601	117.3	39.6	0.998	5665	0.926	221	0.930
105	000411	100.21	5.226	49.3	35.15	14.60	519	113.0	40.0	1.008	5516	0.901	216	0.909
105	000416	100.26	5.247	49.1	35.27	14.92	613	119.4	39.8	1.003	5786	0.945	227	0.955
105	000505	100.13	5.706	45.2	38.29	14.96	425	117.0	36.6	0.923	5733	0.937	205	0.863
105	000510	100.22	5.520	46.7	36.99	15.33	519	112.3	37.9	0.955	5419	0.885	203	0.854
120	000213	100.22	5.031	51.2	33.79	13.63	554	109.1	42.2	1.064	5234	0.855	216	0.909
120	000407	100.13	5.265	48.9	35.27	14.92	566	113.2	39.8	1.003	5534	0.904	215	0.905
120	000412	100.25	5.250	49.1	35.27	14.71	642	115.5	39.8	1.003	5624	0.919	219	0.921
120	000501	100.18	5.724	45.0	38.43	15.37	684	114.6	35.9	0.905	5664	0.925	200	0.842
120	000506	100.19	5.552	46.4	37.11	15.63	507	110.0	37.2	0.938	5443	0.889	198	0.833
120	000511	100.23	5.482	47.0	36.61	14.29	547	112.2	37.9	0.955	5478	0.895	204	0.858
Average														
25		100.21	5.308	48.6	35.55	14.26	594	126.2	39.7	1.000	6121	1.000	238	1.000
50		100.21	5.310	48.6	35.62	13.95	538	121.0	39.9	1.006	5808	0.949	228	0.957
80		100.17	5.320	48.5	35.68	14.64	537	118.8	39.1	0.986	5833	0.953	223	0.939
105		100.20	5.362	48.1	36.00	15.02	548	116.0	38.4	0.968	5674	0.927	216	0.910
120		100.20	5.384	47.9	36.08	14.76	583	112.4	38.8	0.978	5496	0.898	209	0.878
Standard Deviation														
25		0.090	0.230	2.1	1.47	1.60	37	3.4	1.9	0.047	172	0.028	10	0.043
50		0.078	0.204	1.9	1.36	0.58	69	4.2	1.1	0.028	132	0.021	9	0.036
80		0.094	0.219	2.0	1.35	0.21	86	3.5	1.4	0.036	142	0.023	9	0.036
105		0.046	0.206	1.8	1.35	0.25	75	2.8	1.6	0.041	184	0.030	10	0.044
120		0.043	0.249	2.2	1.64	0.73	66	2.5	2.3	0.057	154	0.025	9	0.038
Coefficient of Variance (%)														
25		0.1	4.3	4.4	4.1	11.2	6.3	2.7	4.7	4.7	2.8	2.8	4.3	4.3
50		0.1	3.8	3.9	3.8	4.1	12.8	3.5	2.8	2.8	2.3	2.3	3.8	3.8
80		0.1	4.1	4.0	3.8	1.5	16.0	3.0	3.6	3.6	2.4	2.4	3.9	3.9
105		0.0	3.8	3.7	3.8	1.7	13.7	2.4	4.2	4.2	3.2	3.2	4.8	4.8
120		0.0	4.6	4.6	4.5	4.9	11.3	2.2	5.8	5.8	2.8	2.8	4.3	4.3

Table E.6: Summary of CAI data for wet T650/PR500

Temp (°C)	Specn	Ave Width (mm)	Ave Thickness (mm)	Vf (vol.%)	Impact energy		Dam.A (mm^2)	Pmax (kN)	Modulus		Failure strain		Strength		Moisture (wt %)
					Incident	Rebound			(GPa)	Normalised	(με)	Normalised	(MPa)	Normalised	
25	000201	100.17	5.051	51.0	33.564	13.441	590	113.4	40.6	1.024	5643	0.922	224	0.942	0.61
25	000207	100.12	5.062	50.9	33.895	14.153	540	109.1	41.6	1.049	5267	0.861	215	0.905	0.61
25	000304	100.25	5.204	49.5	34.803	14.706	601	119.2	39.7	1.001	5913	0.966	228	0.959	0.63
25	000309	100.29	5.249	49.1	35.036	14.742	568	120.1	40.1	1.011	5840	0.954	228	0.959	0.65
25	000401	100.32	5.489	46.9	36.608	15.479	630	117.1	38.0	0.958	5781	0.944	213	0.896	0.67
25	-	-	-	-	-	-	-	-	-	-	-	-	-	-	-
50	000203	100.18	5.125	50.3	34.345	13.535	587	118.5	40.7	1.026	5836	0.953	231	0.972	0.75
50	000208	100.14	5.189	49.6	34.803	14.921	642	108.7	40.4	1.018	5316	0.869	209	0.879	0.74
50	000305	100.32	5.278	48.8	35.508	14.600	764	113.8	39.7	1.001	5562	0.909	215	0.905	0.75
50	000310	100.33	5.095	50.6	34.119	15.252	564	110.3	40.8	1.029	5420	0.886	216	0.909	0.75
50	000402	100.28	5.368	48.0	35.748	14.885	689	114.4	38.5	0.971	5667	0.926	212	0.892	0.77
50	-	-	-	-	-	-	-	-	-	-	-	-	-	-	-
80	000204	99.92	5.202	49.5	34.803	14.600	493	111.9	40.9	1.031	5351	0.874	215	0.905	0.61
80	000301	100.13	5.386	47.8	36.113	15.594	476	115.9	38.8	0.978	5644	0.922	215	0.905	0.63
80	000306	99.99	5.143	50.1	34.458	-	597	109.3	40.4	1.018	5399	0.882	213	0.896	0.61
80	000311	100.28	5.067	50.8	34.007	13.888	604	100.8	41.7	1.051	4867	0.795	198	0.833	0.59
80	000316	100.21	5.196	49.6	34.687	13.855	578	107.4	40.1	1.011	5253	0.858	206	0.867	-
80	000403	100.31	5.332	48.3	35.628	14.020	590	109.6	38.7	0.976	5368	0.877	205	0.863	0.62
105	000205	100.17	5.044	51.1	33.785	12.836	481	102.6	41.9	1.056	4949	0.809	203	0.854	0.57
105	000302	100.30	5.259	49.0	35.153	13.566	505	104.0	39.0	0.983	5169	0.844	197	0.829	0.59
105	000307	100.01	5.106	50.5	34.231	14.289	587	101.8	40.6	1.024	5014	0.819	199	0.837	0.58
105	000312	100.12	5.157	50.0	34.345	14.671	679	107.5	39.5	0.996	5301	0.866	208	0.875	-
105	000314	100.19	5.177	49.8	34.573	15.215	573	105.4	39.9	1.006	5142	0.840	203	0.854	0.58
105	000404	100.32	5.273	48.9	35.271	13.823	521	103.6	38.1	0.961	5228	0.854	196	0.825	0.60
120	000206	100.17	5.031	51.2	33.785	14.706	557	92.6	41.9	1.056	4439	0.725	184	0.774	0.57
120	000303	100.32	5.220	49.4	34.919	14.289	762	102.5	39.1	0.986	5089	0.831	196	0.825	0.59
120	000308	100.28	5.152	50.0	34.573	13.888	710	99.1	40.1	1.011	4828	0.789	192	0.808	0.58
120	000313	100.23	5.283	48.8	35.271	13.598	642	99.0	38.7	0.976	4878	0.797	187	0.787	-
120	000315	100.25	5.140	50.1	34.458	14.153	639	99.0	39.8	1.003	4887	0.798	192	0.808	0.58
120	000405	100.31	5.431	47.4	36.113	14.323	689	99.0	38.0	0.958	4920	0.804	182	0.766	0.62
Average															
25		100.23	5.211	49.5	34.78	14.50	586	115.8	40.0	1.008	5689	0.929	222	0.932	0.64
50		100.25	5.211	49.5	34.90	14.64	649	113.1	40.0	1.009	5560	0.908	217	0.911	0.75
80		100.14	5.221	49.4	34.95	14.39	556	109.2	40.1	1.011	5314	0.868	209	0.878	0.61
105		100.19	5.169	49.8	34.56	14.07	558	104.2	39.8	1.004	5134	0.839	201	0.846	0.58
120		100.26	5.210	49.5	34.85	14.16	666	98.5	39.6	0.998	4840	0.791	189	0.795	0.59
Standard Deviation															
25		0.083	0.178	1.7	1.19	0.76	34	4.538	1.3	0.033	256	0.042	7	0.030	0.03
50		0.085	0.112	1.1	0.71	0.66	81	3.825	1.0	0.024	204	0.033	9	0.036	0.01
80		0.158	0.119	1.1	0.78	0.74	56	5.023	1.2	0.030	255	0.042	7	0.029	0.01
105		0.115	0.088	0.9	0.57	0.84	72	2.051	1.3	0.033	132	0.022	5	0.019	0.01
120		0.056	0.138	1.3	0.79	0.38	71	3.222	1.4	0.034	216	0.035	5	0.023	0.02
Coefficient of Variance (%)															
25		0.1	3.4	3.3	3.4	5.2	5.8	3.9	3.3	3.3	4.5	4.5	3.2	3.2	4.2
50		0.1	2.2	2.1	2.0	4.5	12.4	3.4	2.4	2.4	3.7	3.7	3.9	3.9	1.5
80		0.2	2.3	2.3	2.2	5.1	10.1	4.6	2.9	2.9	4.8	4.8	3.3	3.3	2.3
105		0.1	1.7	1.7	1.6	6.0	12.9	2.0	3.3	3.3	2.6	2.6	2.2	2.2	2.1
120		0.1	2.6	2.6	2.3	2.7	10.6	3.3	3.4	3.4	4.5	4.5	2.9	2.9	3.3

DISTRIBUTION LIST

France-Australia Technical Arrangement TA 1/99 – Work Package 1: Study of the equivalence of hot/dry and hot/wet testing

Paul J. Callus

AUSTRALIA

DEFENCE ORGANISATION	**No. of copies**
Task Sponsor	
DGTA	1 Printed
S&T Program	
Chief Defence Scientist	1
Deputy Chief Defence Scientist Policy	1
AS Science Corporate Management	1
Director General Science Policy Development	1
Counsellor Defence Science, London	Doc Data Sheet
Counsellor Defence Science, Washington	Doc Data Sheet
Scientific Adviser to MRDC, Thailand	Doc Data Sheet
Scientific Adviser Joint	1
Navy Scientific Adviser	1
Scientific Adviser – Army	1
Force Scientific Adviser	1
Scientific Adviser to the DMO	1
Deputy Chief Defence Scientist Information and Deputy Chief Defence Scientist Systems	
Platforms Sciences Laboratory	
Deputy Chief Defence Scientist Aerospace	Doc Data Sht & Exec Summ
Chief of Air Vehicles Division	Doc Data Sht & Dist List
Research Leader	1
Head	1
Task Manager	1
Paul J. Callus	1 Printed
DSTO Library and Archives	
Library Fishermans Bend	1
Capability Development Group	
Director General Maritime Development	Doc Data Sheet
Director General Land Development	1
Director General Capability and Plans	Doc Data Sheet
Assistant Secretary Investment Analysis	Doc Data Sheet
Director Capability Plans and Programming	Doc Data Sheet

Director General Australian Defence Simulation Office	Doc Data Sheet
Chief Information Officer Group	
Director General Australian Defence Simulation Office	Doc Data Sheet
AS Information Strategy and Futures	Doc Data Sheet
Director General Information Services	Doc Data Sheet
Strategy Group	
Director General Military Strategy	Doc Data Sheet
Assistant Secretary Governance and Counter-Proliferation	Doc Data Sheet
Navy	
Maritime Operational Analysis Centre, Building 89/90 Garden Island Sydney NSW Deputy Director (Operations) Deputy Director (Analysis)	Doc Data Sht & Dist List
Director General Navy Capability, Performance and Plans, Navy Headquarters	Doc Data Sheet
Director General Navy Strategic Policy and Futures, Navy Headquarters	Doc Data Sheet
Air Force	
SO (Science) - Headquarters Air Combat Group, RAAF Base, Williamtown NSW 2314	Doc Data Sht & Exec Summ
AS14	1 Printed
AS14A	1 Printed
Army	
ABCA National Standardisation Officer Land Warfare Development Sector, Puckapunyal	e-mailed Doc Data Sheet
SO (Science) - Land Headquarters (LHQ), Victoria Barracks NSW	Doc Data & Exec Summary
SO (Science), Deployable Joint Force Headquarters (DJFHQ) (L), Enoggera QLD	Doc Data Sheet
Joint Operations Command	
Director General Joint Operations	Doc Data Sheet
Chief of Staff Headquarters Joint Operations Command	Doc Data Sheet
Commandant ADF Warfare Centre	Doc Data Sheet
Director General Strategic Logistics	Doc Data Sheet
COS Australian Defence College	Doc Data Sheet
Intelligence and Security Group	
AS Concepts, Capability and Resources	1
DGSTA , DIO	1 Printed
Director Advanced Capabilities	Doc Data Sheet
Manager, Information Centre, Defence Intelligence Organisation	1
Defence Materiel Organisation	
Deputy CEO	Doc Data Sheet

Head Aerospace Systems Division	Doc Data Sheet
Head Maritime Systems Division	Doc Data Sheet
Program Manager Air Warfare Destroyer	Doc Data Sheet
CDR Joint Logistics Command	Doc Data Sheet

OTHER ORGANISATIONS

National Library of Australia	1
NASA (Canberra)	1

UNIVERSITIES AND COLLEGES

Australian Defence Force Academy

Library	1
Head of Aerospace and Mechanical Engineering	1
Serials Section (M list), Deakin University Library, Geelong, VIC	1
Hargrave Library, Monash University	Doc Data Sheet

OUTSIDE AUSTRALIA

INTERNATIONAL DEFENCE INFORMATION CENTRES

US Defense Technical Information Center	1
UK Dstl Knowledge Services	1
Canada Defence Research Directorate R&D Knowledge & Information Management (DRDKIM)	1
NZ Defence Information Centre	1

ABSTRACTING AND INFORMATION ORGANISATIONS

Library, Chemical Abstracts Reference Service	1
Engineering Societies Library, US	1
Materials Information, Cambridge Scientific Abstracts, US	1
Documents Librarian, The Center for Research Libraries, US	1

INFORMATION EXCHANGE AGREEMENT PARTNERS

National Aerospace Laboratory, Japan	1
National Aerospace Laboratory, Netherlands	1

CEAT (France)

C. Deschemin	1 Printed
SPARES	6 Printed

Total number of copies: 43 Printed: 12 PDF: 31

DEFENCE SCIENCE AND TECHNOLOGY ORGANISATION
DOCUMENT CONTROL DATA

1. PRIVACY MARKING/CAVEAT (OF DOCUMENT)

2. TITLE

France-Australia Technical Arrangement TA 1/99 – Work Package 1: Study of the Equivalence of Hot/Dry and Hot/Wet Testing

3. SECURITY CLASSIFICATION (FOR UNCLASSIFIED REPORTS THAT ARE LIMITED RELEASE USE (L) NEXT TO DOCUMENT CLASSIFICATION)

Document	(U)
Title	(U)
Abstract	(U)

4. AUTHOR(S)

Paul J. Callus

5. CORPORATE AUTHOR

DSTO Defence Science and Technology Organisation
506 Lorimer St
Fishermans Bend Victoria 3207 Australia

6a. DSTO NUMBER	6b. AR NUMBER	6c. TYPE OF REPORT	7. DOCUMENT DATE
DSTO-TR-1708	AR-013-374	Technical Report	April 2005

8. FILE NUMBER	9. TASK NUMBER	10. TASK SPONSOR	11. NO. OF PAGES	12. NO. OF REFERENCES
2005/1004380/1	AIR 03/188	DGTA	74	17

13. URL on the World Wide Web

http://www.dsto.defence.gov.au/corporate/reports/DSTO-TR-1708.pdf

14. RELEASE AUTHORITY

Chief, Air Vehicles Division

15. SECONDARY RELEASE STATEMENT OF THIS DOCUMENT

Approved for public release

OVERSEAS ENQUIRIES OUTSIDE STATED LIMITATIONS SHOULD BE REFERRED THROUGH DOCUMENT EXCHANGE, PO BOX 1500, EDINBURGH, SA 5111

16. DELIBERATE ANNOUNCEMENT

No limitations

17. CITATION IN OTHER DOCUMENTS Yes

18. DSTO RESEARCH LIBRARY THESAURUS

Polymer matrix composites; Elevated temperature wet; Elevated temperature dry; Aircraft structures

19. ABSTRACT

Substantial savings could be made in the airworthiness certification of composite aircraft structure if the strength of polymer matrix composites in the elevated temperature wet (ETW) condition could be predicted from parameters that are easier to measure such as strength in the elevated temperature dry (ETD) condition and the glass transition temperature (T_g). The feasibility of this approach was tested by measuring the strength of AS4/3501-6 unidirectional prepreg tape, T650/F584 plain weave prepreg fabric and T650/PR500 plain weave fabric consolidated by resin transfer moulding, in the dry and 70°C/85 % relative humidity equilibrated condition, from 25 to 120 °C using interlaminar shear, ±45° tension, open hole compression and compression after impact tests. Apart from a decrease in strength with increasing temperature and moisture content there was no consistent relation between ETD and ETW strength. It was therefore not possible to predict ETW strength for these materials and tests on the basis of ETD strength and T_g only.